



ADDIS ABABA UNIVERSITY

Addis Ababa Institute of Technology

School of Graduate Studies

**Impact of Drawdown Speed on Slope Stability of Tendaho Dam Under Static
and Pseudo Static Earthquake Loading Condition**

A Thesis Submitted to the School of Graduate Studies of Addis Ababa University in Partial
Fulfillment for the Requirements of the Degree of Master of Science in Civil and Environmental
Engineering (Major in Hydraulic Engineering)

BY:
Ashebir Tesfaye Debelo

Advisor: Dr.–Ing. Asie Kemal

Addis Ababa, Ethiopia

September; 2018

Addis Ababa Institute of Technology

School of Graduate Studies
School of civil and environmental engineering

**Impact of Drawdown Speed on Slope Stability of Tendaho Dam Under Static
and Pseudo Static Earthquake Loading Condition**

This is to certify that the thesis prepared by Ashebir Tesfaye Debelo, entitled “Impact of Drawdown Speed on Slope Stability of Tendaho Dam Under Static and Pseudo Static Earthquake Loading Condition” and submitted in partial fulfillment of the requirements for the degree of Master of Science in Civil Engineering under Hydraulic Engineering compiles with the regulations of the university and meets the accepted standards with respect to originality and quality.

BY:

Ashebir Tesfaye Debelo

Approved by board of examiners

Dr.–Ing. Asie Kemal
(Advisor)

signature

Dr.–Henok Fikre
(external examiner)

signature

Dr.–Yilma Silashi
(internal examiner)

signature

Dr.–Agizaw Niguse
(Chairman, Civil and
Environmental Engineering Department)

signature

Certification

I, the undersigned, certify that I read and hear and recommend for acceptance by Addis Ababa Institute of Technology a thesis entitled “**Impact of Drawdown Speed on Slope Stability of Tendaho Dam Under Static and Pseudo Static Earthquake Loading Condition**” in partial fulfillment of the requirements for the degree of Master of Science in Civil Engineering (Major Hydraulic Engineering).

Dr.-Ing. Asie Kemal Jabir
(advisor)

DECLARATION AND COPY RIGHT

I, Ashebir Tesfaye Debelo, declare that this thesis is my own original work and that it has not been presented and will not be presented to any other University for similar or any other degree award.

Signature _____

This thesis is a copyright material protected under the Berne convention, the copyright Act, 1999 and other international and national enactments in that behalf, on intellectual property. It may not be reproduced by any means in full or in part, except for short extracts in fair dealing, for research or private study, critical scholarly review or discourse with an acknowledgement, without written permission of the Directorate of Postgraduate Studies, on behalf of both the Author and Addis Ababa University

Ashiber Tesfaye
Ashitesfu@yahoo.com
+251926096314
September, 201

Abstract:

Dams are hydraulic structures used to store, control, divert water impounding it behind the upstream side of dam in a reservoir for different purposes, like hydropower generation, water supply, irrigation, navigation and transportation, etc. Although dams have many advantages, the risk that may happen due to the failure still exists.

One of the most dangerous conditions causing failure of earthen dams' upstream slope is speed of drawdown condition when the countervailing upstream water pressure has disappeared with fastest speed; it causes a danger to the upstream slope.

In this work Tendaho earthen dam, low permeability construction material, which is located on the highly seismically active zone, Eastern Ethiopia Rift Valley was studied. The overall objective of the study was assessing the impact of drawdown speed on Slope Stability of Tendaho dam under static and pseudo static earthquake loading Condition by using different methods. Traditional limit equilibrium methods and a finite element software, GeoStudio 2007 and 2012 computer program were utilized in the slope stability analysis. Seep/w, Slope/w and Sigma/w GeoStudio sub program were used to analysis and develop pore pressure curve and factor of safety curve for purpose of reservoir water level operation monitoring.

The developed factor of safety curve shows that safety of upstream slope of the dam decrease during drawdown condition and seismic load effect. The upstream slope of Tendaho dam is stable during different drawdown speed and reservoir water level fall from FRL to MDDL. But, the worst case scenario occurs when reservoir water falls below 387m from FRL (408m) within recommended values of evacuation periods. In addition, during earthquake force was applied to the model the critical drawdown level and evacuation period is 394m and 40 days, respectively. It is also found that drawdown situation of Tendaho dam under reservoir operation have not affect on upstream slope of the dam and emergency drawdown is not required till now. However, assessing the dam slope stability under different drawdown speed and earthquake loading condition is important to avoid the upstream slope sliding during drawdown condition in the future.

Keywords: Earthen Dam, Finite Element Method, Limit Equilibrium Method, Factor of Safety, Earthquake Force, Slope Stability, Drawdown Speed

Acknowledgments

I would like to express my sincere gratitude to my supervisor **Dr.-Ing. Asie Kemal** for giving me Invaluable guidance, advice, criticism, encouragements and for his continuous support from the inception of this work to the end.

I would also like to thank **Ethiopia road authority (ERA)** for their financial support. I am also grateful to the Ethiopian construction design and supervision works corporation (ECDSWC), **water and energy design and supervision sector**, for providing me data free of charge.

I am further grateful the Ethiopian construction design and supervision works corporation, **head work design team** and **material laboratory analysis staff**, for their technical advices and moral support.

At last but not least, I would like to extend my deepest gratitude to kuraz sugar development project, lot-2 site project consultant and contractor staffs, for their motivation provided, encouragement, appreciable support in work area and true friendship.

I would also like to express deep felt gratitude to my family members and all my best friends for their continuous support.

Above all, my sincere thanks go to the Almighty God for all my successful works. This day, God what you have done for me is really beyond what I can imagine and I have dreamt. Indeed, thanks for everything you have been doing for me.

Table of Contents

Abstract:	
Acknowledgments.....	v
List of figures.....	viii
List of Tables	x
List of Abbreviations	xi
1 INTRODUCTION	1
1.1 Background.....	1
1.2 Statement of Problem.....	2
1.3 Research Questions	3
1.4 Objective of the Study	3
1.4.1 General Objective	3
1.4.2 Specific Objective.....	3
2. LITERATURE REVIEW	4
2.1 General.....	4
2.2 Review on Major Causes of Dam Failure and Their Statistics	4
2.1.1 Types of Dams	4
2.1.2 Major Causes of Dam Failure and Their Statistics	5
2.3 Embankment Dam’s Failure Mechanisms and Design Practices.....	6
2.4 History of Dam in Ethiopia.....	9
2.5 Classical Design Practices and Standards for Slope Stability.....	9
2.5.1 Total and Effective Shear Strength	10
2.5.2 Slope Stability and Factor of Safety against Sliding.....	13
2.6 Methods of Slope Stability Analysis in GeoStudio Software	16
2.6.1 Limit Equilibrium Method.....	16
2.6.2 Finite Element Modeling	18
2.6.3 Slip Surface Shapes.....	18
2.7 Slope/w	21
2.8 Rapid Drawdown	25
2.9 Pore Water Pressure.....	25
2.10 Seismic dam Slope Analysis.....	26
2.10.1 Pseudo static Method	27

2.10.2 Dynamic finite element method	28
2.11 Empirical review	31
3. MATERIALS AND METHODS	35
3.1 Description of Study Area	35
3.1.1 Location	35
3.1.2 Climate	36
3.1.3 Geology of the Dam Area	36
3.2 Material Sources and Properties	36
3.3 Data Collection	40
3.3.1 Primary Data	41
3.3.2 Secondary Data	42
3.4 Modeling and Data Analyzing Tools	42
3.4.1 Limit Equilibrium Modeling and Analyzing Method	43
3.4.2 Steady State Seepage	46
3.4.3 Slope/W	47
3.4.4 Finite Element Modeling and Analyzing Method	47
3.4.5 Pseudo Static Seismic Parameters determination	50
4 RESULTS AND DISCUSSIONS	54
4.1 General	54
4.2 Dam Geometry Modeling Result	55
4.3 Long-Term Steady-State Conditions	55
4.4 Limit Equilibrium Method of Analysis	56
4.5 Finite Element Method of Analysis	57
4.6 Discussions of major results	59
4.7 Under Operation Drawdown Situation of Tendaho Dam	68
4.8 Reservoir Evacuation Rating Curve	69
5. CONCLUSION AND RECOMMENDATIONS	71
5.1 Conclusion	71
5.2 Recommendations	72
6. REFERENCES	74
7. APPENDICES	77

List of figures

Figure 2 -1. Porewater pressures and vertical geostatic stress assuming static groundwater	13
Figure 2-3. Embankment sliding and stability analysis using method of slices formulation	14
Figure 2-4. Slope stability analysis using analytical method	17
Figure 2.5 Slice discretization and slice forces in a sliding mass	19
Figure 2-6 Conditions for a simple circular slip surface	21
Figure 2-7 situation for a typical composite slip surface	22
Figure 2.8 Forces acting on a slice through a sliding mass with a circular slip surface	24
Figure 2.9 Inertial forces and earthquake movement direction	29
Figure 2.10 Inertial forces due to earthquake movement	30
Figure 2.11 Mandali dam	33
Figure 2.12. Typical section of Al-Wand dam with the material details.	34
Figure 2.13. The minimum factor of safety and slip surface in Al-Wand dam	35
Figure 2.14 Values of a factor of safety during rapid drawdown for a period of reservoir emptying of 1 day in Al-Wand dam	35
Figure 2.15 dam cross section for rapid drawdown analysis.	36
Figure 2.16 A) Comparison of pore pressure B) Comparison of FoS	36
Figure 3-1 Location map of study area	37
Figure 3.2 geological section along tendaho dam axis	38
Figure 3.3 Geometry and scheme of zoning of Tendaho Dam	40
Figure 3.4: Material site	41
Figure 3-5 Primary data collection at Tendaho dam site	43
Figure 3-6 summery of modeling and analyzing approaches	45
Figure 4.1 material and geometry of tendaho dam	57
Figure 4.2 Long-term steady-state conditions at FRL	58
Figure 4.3 Reservoir elevation with time during drawdown	58
Figure 4.4 Seep Conditions and drawdown after 20 days	59
Figure 4.5 Fluid-pressure boundary condition representing the reservoir weight	60
Figure 4.6 Fluid boundary functions representing the reservoir drawdown	60
Figure 4.7 Fluid boundary functions and hydraulic boundary function representing changing pore-pressures contour after 20 days' drawdown	61

Figure 4.8 Comparison of pore pressures at Point coordinate (84, 0) in u/s from the two types of analyses, various evacuation period and water level fall from FRL to MDDL	62
Figure 4.9 Comparison of pore pressures at Point in u/s (84, 0) from the two types of analyses, 27 days' evacuation and water level fall from FRL to MDDL	63
Figure 4.10 Comparison of factors of safety from the three types of analyses, 20 days' evacuation periods and water level fall from FRL to MDDL	64
Figure 4.11 Comparison of factors of safety from the three types of analyses, 27 days' evacuation and water level fall from FRL to MDDL	64
Figure 4.12 Comparison of factors of safety from two types of analyses, three types of evacuation periods constant water level fall from 408m to 387m (21m)..	65
Figure 4.13 Comparison of factors of safety for effect of earthquake is considered, two evacuation periods constant water level fall from 408m to 394m (13m).	66
Figure 4.14 Couple analysis capability deformation analysis, represents y-total stress contour variation and seep Conditions after 20 days start of the drawdown	67
Figure 4.15 Couple analysis capability deformation analysis, at drawdown from FRL to MDDL with various evacuation days	67
Figure 4.16 Comparison of factors of safety for two types of analyses, drawdown under reservoir operation	70
Figure 4.17 Comparison of evacuation rating curve for drawdown from FRL to MDDL.	71
Figure 4.18 Comparison of evacuation rating curve for drawdown from FRL to 387m.	71

List of Tables

Table 2.1: Types of dams and register statistics	5
Table 2.2: Statistics on causes of dam failure	6
Table 2.3: Common causes of dam and appurtenant structures failure	8
Table 2.4: Deterministic effective stress stability analysis F_s , s min.	17
Table 2.5: Various Load Cases and Minimum Required Factor of Safety for FRL Condition	18
Table 2.6: Rate of seismic hazard	31
Table 3.1 Main Material laboratory test result of tendaho dam.....	42
Table 3.2 material properties from liquefaction analysis of Tendaho earth-fill dam	42
Table 3-3 Equations of Statics Satisfied	46
Table 3-4 Interslice force characteristics and relationships	47
Table 4.1- Minimum Desired Values of Factors of Safety for Various Loading Conditions.....	56
Table 4.2 Summary of minimum factor safety at different drawdown.....	68

List of Abbreviations

ETCOLD Ethiopian Committee of on Large Dams

FEM Finite Element Method

ICOLD International Committee of Large Dams

USACE United States Army Corps of Engineer

D/S Down Stream

FoS Factor of Safety

RBL River Bed Level

FRL full reservoir level

EQ Earth quake

USACE: United States Army Corps of Engineers

USBR: United States Bureau of Reclamation

U/S Upstream

α_h Horizontal Seismic Coefficient

α_v Vertical Seismic Coefficient

LEM limit equilibrium Method

MMC Million Metric Cubes

MoWIE Ministry of Water, Irrigation and Electricity

MWL Maximum Water Level

ECDSWC Ethiopia construction design and supervision works corporation

ECWC Ethiopia construction works corporation

1 INTRODUCTION

1.1 Background

Dams are hydraulic structures used to store, control, divert water impounding it behind the upstream side of dam in a reservoir for different purposes, like hydropower generation, water supply, irrigation, navigation and transportation, etc. Although dams have many advantages, the risk that may happen due to the failure still exists. Dams can have a risk to downstream communities and properties if not designed, operated and maintained properly. All dams, regardless of their design or construction, have increased forces applied to them during extreme events which increase the potential risk of failure (Ahmad Asnaashari, 2014).

According to ICOLD, the various causes leading to the failure of earth dams can be grouped in to the three classes (Hydraulic failures, Seepage failures, Structural failures) (ICOLD, 2000). Slope stability failure is one of Structural failures of dam and it may be happen during rapid drawdown for upstream slope and steady seepage condition for downstream slope. For this reason, slope stability analysis during different drawdown speed is an important consideration in the design of embankment dams [Tran, 2008]. The case study dam, tendaho earthen dam, yet, there is no any study conducted on the effects of drawdown speed under static and earthquake loading condition.

However, engineering design of an earth dam is an important subject from the safety and economy of construction cost point of view. Evaluation of safety of a given design involves intensive computation. Despite the progress in soft computing and development of software for analysis of design safety, their utilization in practical applications appears to be limited. Perhaps accessibility, cost considerations, understanding and user-friendliness can be some of the causes for the problem. Under the current practices, the concentration is directed more at ensuring safety, and the economic requirements are often given low or no consideration during the design of the dams. The concept of finding an optimal design itself seems to be a genuine idea for many designer engineers in practice (Murthy et al., 2013).

This master thesis focus on Tendaho earthfill dam upstream slope safety assessment under different drawdown speed and loading condition by employing Limit Equilibrium Method computer program Slope/W and the Finite Element Method computer program SIGMA/W with Slope/W frame work. For both methods GeoStudio 2007 and 2012 computer program were used

to determine pore pressure and develop factor of safety versus evacuation period. Limit equilibrium methods is traditional utilized in the slope stability analysis and the accommodation of saturated and unsaturated pore-water pressures is considered (Fredlund and Feng, 2011).

Tendaho dam and irrigation development project for sugar cane plantation is one of the Mega-projects undertaken by Ministry of Water, Irrigation and Electricity to irrigate gross land of 60,000Ha of sugar cane and is targeted to produce 500,000 tons of sugar annually. A Zoned earthen dam was constructed across Awash River at Tendaho to store $1.86 \times 10^9 \text{m}^3$ of water at its FSL for sugar cane irrigation found at downstream of the dam [WWDSE, 2007]. This large stored volume of water makes Tendaho dam to be categorized as a large earth-fill dam. Hence, it often poses a higher hazard potential than any other embankment dams built in the country, given the extreme storage volumes and downstream population and properties.

Consequently, the assessment of impact of drawdown speed on slope stability of Tendaho dam under static and earthquake loading Condition is very important for monitoring safe performance upstream slope of the dam under all operational conditions.

1.2 Statement of Problem

Ethiopia is building a number of earth and rock fill dams. Even though dams are valuable resources, they become more expensive to repair if problems are not solved on time. A minor problem can turn into a major reconstruction project or even result in a complete dam failure. However, most dams are constructed to serve at least the design period. For this reason, dam slope stability assessment under different drawdown speed and earthquake loading condition is very important. Since, under different drawdown speed a slope is partially or totally submerged, the pore pressure inside slope will change as the water level changes, which will influence slope stability. Although dams are constructed with great attention to carefully survey, design, and constructed such as Gouhou dam in China, Baldwin Hills Dam in Los Angeles, Teton Dam in USBR have been failed and result serious accidents in the world (USACE, 2006).

Therefore, all embankment dams in service should be systematically evaluated for their safe performance under all operational conditions. Besides, from the total number of dams the failed dam percentage for earth and rock-fill is 70% more than gravity dams (Bulletin 99, 1995).

Hence, assessing the dam slope stability under different drawdown speed within seismic loading condition is important to serve the designed period and in order to decrease potential hazard. Slope stability of embankment dam also influenced by the properties of material from which dam is constructed. Permeability of the earth fill dam is low relative to rock fill dam and dissipation of pore water pressure is less for earth dam with low permeability. Thus, in this study tendaho earth fill dam, low permeability construction material, which is located on the highly seismically active zone, Eastern ethiopia Rift Valley, in which a sudden earthquake might happen is studied and operation plan of its stored water is evaluated with slope safety. Also, the situation of tendaho dam upstream slope under reservoir operation drawdown condition is evaluated. Since, reservoir water was dried in year 2008 E.C due to Awash River inflow is declined and it affects u/s slope of the dam.

1.3 Research Questions

After completion of this study, the following main questions are answered:

1. What is the situation of Tendaho dam upstream slope under reservoir operation drawdown condition?
2. Could evacuation period curve have developed for existing embankment dam?
3. How long will it take to evacuate embankment dam within safe upstream slope?

1.4 Objective of the Study

1.4.1 General Objective

The overall objective of this study is to assess the impact of drawdown speed on slope stability of Tendaho dam under static and pseudo static earthquake loading condition by using different methods.

1.4.2 Specific Objective

- ❖ To determine the fastest evacuation period of stored water
- ❖ To determine the pore water pressure developed due to various drawdown speed
- ❖ To estimate slope stability under various drawdown speed and loading condition by using LEM and FEM
- ❖ To determine upstream slope stability of Tandaho under operation condition

2. LITERATURE REVIEW

2.1 General

In this chapter different literatures works including recent scientific journals, articles, guidelines and books related to embankment dam slope stability modeling and analyzing under different drawdown speed and loading condition, factor of safety estimation methods, were reviewed widely according to the recent and updated different federal agencies dam slope stability assessment guidelines, standards, criterion and personal studies of other researchers in this study area.

2.2 Review on Major Causes of Dam Failure and Their Statistics

2.1.1 Types of Dams

Dams are numerous in type classified usually in terms of materials used for their construction and their form. Common types are homogeneous or zoned earthfills; rockfills with earth core or concrete face; and concrete dams that depend on gravity, arch, or buttress resistance. Some dams are composites of various materials, including earthfill, rockfill, masonry, and concrete. A few have timber, asphaltic, or synthetic members.

Topography, geology and availability of construction materials and technology are primary factors in weighing the comparative merits of dam types.

Novak et al. (2003) give an initial broad classification of dams into two generic groups based on the principal construction material employed (Novak et al., 2003).

1. *Embankment dams*: are constructed of earthfill and/or rockfill; upstream and downstream face slopes are similar and of moderate angles, giving wide section and high construction volume relative to height.

2. *Concrete dams*: are constructed of mass concrete; face slopes are dissimilar, generally steep downstream and near vertical upstream, and dams have relatively slender profile. This group can be considered to include also older dams of appropriate structural type constructed in masonry (Novak et al., 2003).

Novak et al. (2003) also identifies the principal types within the two generic groups (see Table 2.1). The dam for the case study in this thesis is a zoned earth fill dam.

Table 2.1: Types of dams and register statistics (ICOLD, 1988a, in Novak et al., 2003).

Group	Type	Percent from total number of Constructed large dams
Embankment dams	earth fill Rock fill	82.9
Concrete dams (including masonry)	gravity	11.3
	Arch	4.4
	Buttress	1.0
	multiple arch	0.4
Total large dams ² (ICOLD, 1988a)	36235	

2 Large dams are defined by ICOLD as dams exceeding 15 m in height or, storage volume in excess of 10^6 m^3 or a flood discharge capacity of over $2000 \text{ m}^3 \text{ s}^{-1}$. Based on this definition the case study dam in this thesis is categorized as a large dam with its height of 54.5 m and storage capacity of $1.86 \cdot 10^9 \text{ m}^3$.

2.1.2 Major Causes of Dam Failure and Their Statistics

There are varying statistics on causes of dam failure, for example statistics given by International Commission on Large Dams (ICOLD), US Army Corps of Engineers (USACE) and Novak et al. (2003) are given in Table 2.2. Many attempts have been made at compiling and assessing statistics on dam failure. Main attempts on worldwide scale have been made by International Commission on Large Dams (ICOLD) in 1974, 1983 and 1995. ICOLD (1995) states that foundation problems are the most common causes of failure in concrete dams, with internal erosion and foundation shear strength each contributing for 21%. In case of earth and rockfill dams, the most common cause of failure is overtopping (31% as primary cause and 18% as secondary cause) followed by internal erosion in the body of the dam (15% as primary cause 13% as secondary cause), and in the foundation (12% as primary cause and 5% as secondary) (ICOLD, 1995).

Table 2.2: Statistics on causes of dam failure (Novak et al., 2003).

Source	Overtopping	Foundation defects *	Internal erosion **	Others
USACE (2006)	34%	30%	20%	6%
Novak et al. (2003)	30-35%	No data	30-35 %	
ICOLD (1995)	31% primary cause 18 % secondary cause	No data	27% primary cause 18 % secondary	

* Slope instability, differential settlement, high uplift pressure, foundation seepage

** Piping and seepage

2.3 Embankment Dam's Failure Mechanisms and Design Practices

It is comprehensible that the degree of importance of different causes of dam failure varies with dam type. Dam design principles and considerations evolved with the identification of major causes of dam failure and the progressive understanding of their mechanisms. In addition, knowledge on causes of dam failure is crucial for dam safety evaluation, dam monitoring and rehabilitation decisions. The following paragraphs provide a summary on the major causes of dam failure and their mechanisms (Novak et al. ,2003).

Earthfill embankments may be damaged by distortions at critical points. Differential settlement may be severe at steep abutments and at structural interfaces where effective compaction is difficult to obtain. At these locations, deformation of the fill may open dangerous paths of seepage. For this reason, there have been many failures along outlet conduits. Although properly constructed embankments are able to accommodate substantial movement, they have relatively poor resistance to overflow; so their freeboard and associated spillway capacity must be determined conservatively (Novak et al. ,2003).

In contrast, most concrete dams can withstand overtopping for at least several hours. The key to their safety may be the resistance of the foundation to impact of the spill. Essential criteria governing the structural competence of concrete dams are the margin of safety against overall structural stability (this includes safety against rotation and tipping of the dam; and translation and sliding of the dam body and natural rock foundation) in relation to all probable conditions of loading including empty reservoir condition. Moreover, there should not be over stress and material failure in the dam concrete and the rock foundation.

Arc dams can carry large loads, but their integrity depends inherently on strength of the abutments. Failure may be caused by rock deteriorations or by shearing under water pressures. Weakening of arch support also may be triggered by foundation erosion. Gravity dams are noted for durability because of their large masses, they can survive considerable weathering and site deficiencies. However, sometimes some have failed where foundation elements were susceptible to sliding. A few buttressed dams also have shown this tendency (Novak et al., 2003).

Novak et al. (2003) identifies the following principal defect mechanisms and failure modes for embankment dams:

1. Overtopping leading to washout: spillway and outlet capacity must be sufficient to prevent overtopping. Also there should be sufficient freeboard to prevent overtopping by wave action. The freeboard must also include an allowance for the predicted long-term settlement of the embankment, foundation compressibility and sedimentation. Overtopping has risk of serious erosion and possible washout of embankment.
2. Internal erosion and piping with migration of fines from core and foundation: regression of 'pipe' and formation of internal cavities, may initiate by internal cracking or by seepage along culvert perimeter. Seepage within and under the embankment must be controlled to prevent concealed internal erosion and migration of materials. Hydraulic gradients, seepage pressures and seepage velocities within and under the dams must, therefore, be contained at levels acceptable for the materials concerned. Care must be taken to ensure that outlet or other facilities constructed through the dam do not permit unobstructed passage of seepage water along their perimeters with risk of soil migration and piping.
3. Embankment and foundation settlement (deformation and internal cracking): care must be taken with soft compressible foundations and proper compaction has to be done during construction of dams.
4. Instability: the embankment, including its foundation, must be stable under construction and under all conditions of reservoir operation. Instability might occur when downstream slope too high and/or too steep in relation to shear strength of the shoulder material or when there is rapid drawdown of water level or because of failure of downstream foundation due to overstress of soft, weak horizons. Face slopes must,

therefore, be sufficiently flat to ensure that internal and foundation stress remains within acceptable limits under different conditions of loading (Novak et al. ,2003). In this regard, the following loading and critical conditions must be analyzed:

- a. End of construction (both slopes critical);
- b. Steady state, reservoir full (downstream slope critical);
- c. Rapid drawdown (upstream slope critical);
- d. Seismic loading condition additional to 1, 2 and 3, if appropriate to the location

Major failure modes of different types of dams and appurtenant structures are often known and they shall be included in risk analysis of dams. For instance, Table 2.3 provides the common categories of failure modes for the different types of dams and appurtenant structures.

Table 2.3: Common causes of dam and appurtenant structures failure (Negede Abete dissertation, 2009).

Earthfill dams	Rockfill dams	Concrete Dams	Spillways
<ul style="list-style-type: none"> • seepage and piping (foundation and dam body), • slop instability (sliding), • breach due to overtopping, • upstream face erosion due to waves, • cracking, • settlement 	<ul style="list-style-type: none"> • leakage, • eroding and cracking of upstream concrete face/membra e, • settlement and translation, • piping through the core zone, • cracking of the core zone, • loss of freeboard due to excessive settlement, • slope instability (sliding). 	<ul style="list-style-type: none"> • Leakage through foundation, • overtopping and downstream foundation erosion, • translation and sliding of the dam body and natural rock foundation, • cracking, weathering, concrete deterioration. 	<ul style="list-style-type: none"> • deficient capacity (hydrologic underestimation of peak flood) • hydraulic (failure to accommodate high energy condition), • structural (deterioration of flow surface, inadequate structural capacity, deficiencies in surface tolerance to preclude cavitation), • cavitation and abrasion, • excessive uplift pressure, • gate malfunctioning, • Inadequate capacity of downstream and approach channel.

In the following section 2.5 the widely adopted (deterministic) design practices and standards with regard to the two failure mechanisms are presented.

2.4 History of Dam in Ethiopia

Dam construction in Ethiopia started in the late thirties. The first modern dam is Aba Samuel dam, constructed on the Akaki River, tributary of the Awash River and was commissioned in 1939. Now a day in Ethiopia the demands for irrigation is arising through the development and expansion of organized agriculture, to satisfy this demand many embankment dams are constructed and most of which are used for this purpose. Currently, there are more than 50 small and large dams in operation. Though previously the country was mainly involved in small-scale irrigation projects, that do not need sophisticated studies and techniques; recently there are large-scale irrigation projects such as Tendaho, Ribb, ArjoDedessa, Kesem (ETCOLD, 2014).

However, no dam can be considered one hundred percent safe as there will never be a complete understanding of the uncertainties associated with natural and manmade destructive forces, material behavior and construction processes. A dam, which is safe at the time of completion, does not automatically remain safe. A few dam owners may believe that a dam, which was safe at the time of its completion, will always remain safe. Life-span of a dam is as long as it is safe, i.e. as long as proper monitoring can be guaranteed (ETCOLD, 2014).

Hence, assessing the impact of drawdown speed on slope stability with different loading condition is an important consideration in the design of large embankment dams like Tendaho dam.

2.5 Classical Design Practices and Standards for Slope Stability

In earth fill construction it is necessary to consider the load-bearing characteristics of the compacted fill and also the behavior of the soil as construction proceeds. Problems related to the response of soils to specific loading conditions are generally grouped into two: problems of deformation and problems of stability. The problem of deformation deals with settlement and consolidation. A soil mass may undergo deformation as a result of changes in external loading called settlement, and/or due to own weight of a compressible soil and changes in drainage conditions called consolidation. A limited amount of deformation occurs with no net volume change, and is thus comparable with elasto-plastic behavior of many non-particulate materials.

The most significant soil deformation, however, usually involve volume changes arising from alterations in the geometric configuration of the soil particles assemblage, e.g. loosely packed

arrangement of soil particles will on loading adopt a more compact and denser structure. Such change occurs almost immediately on load application where the soil structure is relatively coarse, as with sands. In saturated clay soils, however, volume changes and settlement due to external loading will take place slowly through complex hydrodynamic process known as consolidation. Problems of settlement and deformation analysis are not part of the case study in this thesis and therefore no further discussion is given on this topic.

Problems of stability concern the equilibrium between forces and moments and the mobilized soil strength. When the forces and moments arising from loading (or from the removal of support as in a trench excavation), exceed the shear resistance which the soil can mobilize, failure will occur. Such a failure is generally manifested by progressive and, in the final phase, large and relatively rapid mass displacements (Novak et al., 2003).

Therefore, stability problems involve concepts of soil shear strength and stress-strain response. The strength and stress aspects related are discussed in the following topic.

2.5.1 Total and Effective Shear Strength

Stability depends on the balance between the resistance to shearing which can be mobilized, i.e. the shearing strength of the soil, and the shearing stress resulting from the principal loads. The shear strength of a soil is defined as the maximum resistance to shearing stress which can be mobilized, when this is exceeded failure occurs, usually along identifiable failure surfaces. Soil shear strength is commonly quantified through two component parameters:

Apparent cohesion (c): essentially arising from the complex electrical forces binding clay-size particles together;

Apparent Angle of shear resistance (ϕ): developed by interparticle frictional resistance and particle interlocking.

The shear strength (the maximum resistance to shearing) of a soil at a point on a particular plane can be expressed using the Mohr-Coulomb failure criteria as a linear function of the normal stress (σ) at that same point:

$$\tau = c + \sigma \cdot \tan \phi$$

2-1

Where τ (kN/m^2) is shear strength at failure, σ (kN/m^2) is normal stress, c (kN/m^2) is apparent cohesion and ϕ (degrees) apparent angle of shear resistance.

A soil in embankments may constitute a two- or three-phase system comprising solid soil matrix and fluid, either air or water or both. Provided that water is present in the soil pores as a continuous liquid phase, Bernoulli's laws apply. That do mean hydrostatic pressures (pore water pressures) exists and it varies with the moisture content and boundary conditions, and most importantly stress characteristics are also influenced with the level of this pressure. Silty soils and clays frequently employed in embankment fills are generally non-saturated when first compacted, i.e. some pore space is filled with compressible pore air. But, as reservoir is filled with water and the seepage front advances through the embankment the fill will progress to saturated state. In dam engineering much of soil mechanics practice is prescribed assuming this ultimate saturation condition. Therefore, stress and strength at a point in a body of the earth fill is determined from the combined effects of the solid soil matrix and the pore water. This is illustrated in Figure 2-2 (a) and (b) shows a vertical section through a soil mass generating a vertical total stress (σ) and static pore water pressure (u_n) on the horizontal plane X-X at depth z .

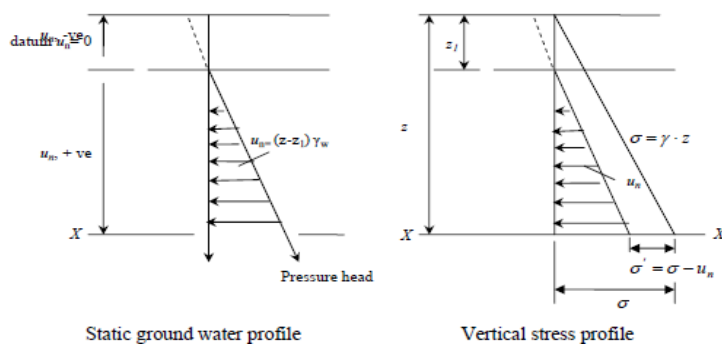


Figure 2.1. Porewater pressures and vertical geostatic stress assuming static groundwater (after Novak et al., 2003).

Positive porewater pressure below the water table decreases interparticle contact pressure and thus it decreases intergranular (effective) stress (σ'), transmitted through the soil particles. Effective stress (σ') is less than the total stress (σ) by an amount equivalent to the pore water pressure u_n as given in Eq. (2-2).

2.5.2 Slope Stability and Factor of Safety against Sliding

When a soil structure such as dam slope and foundation fails, there is a distinct movement of body of soil relative to another body of soil. The zone between these two bodies is a failure zone, which can be approximated by a curve without thickness. This curve is usually assumed to be a circle (see Figure 2-3). Stability analysis based on such an assumption is called slip circle method. This method takes stability analysis as a two-dimensional limit-equilibrium problem, which can be solved based on consideration of static equilibrium of potentially unstable ‘active’ mass of soil overlaying a circular conjectural failure surface. It can be solved by analytical or graphical methods. In both methods essentially the analysis applies the same principles of equilibrium though the techniques are different. In the graphical method the total sum of forces is considered; there is equilibrium (no sliding failure) if this sum equals zero. In the analytical methods the overturning moment is compared with resisting moment. For that purpose, the slice method is applied (see Figure 2-3 and Figure 2-4). There is equilibrium if the overturning and resisting moments are equal. The analytical methods are more convenient for use in probabilistic design and risk analysis as they lend themselves to applications using computer program. In Figure 2-3 and Figure 2-4 the elements needed for application of analytical slope stability analysis method are given.

When using analytic slope stability analysis methods in risk analysis the overturning resisting moment equations have to be formulated as a reliability equation. In reliability terms the overturning moment can be taken as load and the resisting moment as resistance. The system fails only when the latter is less than the former. Based on this concept in the classical deterministic approach a global factor of safety against sliding ($F_{s,s}$) is defined as a ratio of the effective unit shear resistance which can be mobilized to the unit shear stress:

$$F_{s,s} = \frac{\sum \tau'}{\sum \bar{G}'} \quad 2.4$$

Where τ' and G' are, respectively, the effective unit shear resistance which can be mobilized and unit shear stress generated on the failure surface. The effective stress (gravitational driving force) (G' , kN/m^2) for an active soil mass of unit width above a failure surface of length L (m) can be given as:

$$G' = W \cdot \sin\alpha$$

2.5

Where, W is the weight of the active mass of unit width above the failure surface length L (m) and α is the angle of inclination of the slip surface to the horizontal. The situation is schematized in Figure 2-3 assuming the active mass is divided in to slices to facilitate the equilibrium analysis.

The expression for $F_{s,s}$ that correspond to the most commonly employed analytical methods is given as either the Swedish Circle (Fellenius) method Eq.(2-6) or as Alan Bishop semi-rigorous solution Eq.(2-7). The difference between these two methods is the assumption made with regard to the interslice geostatic and porewater forces, which are represented by $Q_i, Q_{i+1} \dots, Q_n$ in Figure 2-6, required for static equilibrium. In Fellenius method it is assume that interslice forces are horizontal (normal forces) at either side of a slice having equal magnitude and opposite direction($Q' = Q'_{n+1}$). This means they cancel out each other. This assumption is equivalent to ignoring all (normal and shear) interslice forces.

However, Bishop's method assumes that Q' and Q'_{n+1} are both horizontal forces having different magnitude. Both methods ignore existence of interslice shear forces and satisfy moment equilibrium.

$$F_{s,s} = \frac{\sum_1^m c' \cdot l_n + \tan\phi' \cdot \sum_1^m (W_n \cdot \cos\alpha_n - U_n \cdot l_n)}{\sum_1^n W_n \cdot \sin\alpha_n} \quad 2.6$$

Where W_n and l_n are, respectively, the weight and base length of the slices into which the active mass is subdivided for analysis, α_n is the angle of inclination of the slice base to the horizontal, u_n is the porewater pressure at the slice base and $L = \sum l_n$ is the overall length of the failure surface. Other, variables as defined earlier.

$$F_{s,s} = \frac{\sum_1^m (c' \cdot b_n + (W_n - U_n \cdot b_n) \cdot \tan\phi') \cdot \frac{1}{m_\alpha}}{\sum_1^n W_n \cdot \sin\alpha_n} \quad 2.7$$

In which $m_\alpha = \left(1 + \frac{\tan\alpha_n \cdot \tan\phi'}{F_s}\right) \cdot \cos\alpha_n$

Thus, using either Eq. (2-6) or Eq. (2-7) stability analysis (computation of factor of safety) is applied to all conceivable failure surfaces, and the supposed minimum factor of safety F_{min} is sought. In deterministic design the calculated minimum factor of safety has to always be

compared with the required factor of safety to see if the conditions of design are satisfactory. Table 2.4 gives the commonly used deterministic guidelines on acceptable factor of safety against sliding. In Bishop's method the factor of safety $F_{s, s}$ appears on both side of the equation and iterative solution is required.

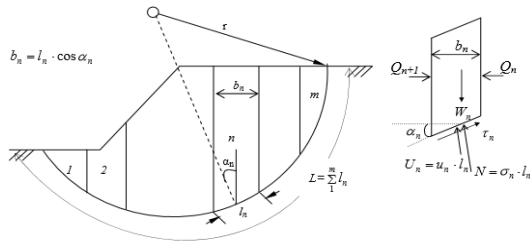


Figure 2-4. Slope stability analysis using analytical method (method of slices) – elements.

For additional reference on Fellenius and Bishop methods the following books and articles could be referred Novak et al. (2003), Bishop (1955), Bishop and Bjerrum (1960), Bishop and Morgenstern (1960), Jansen et al. (1988).

Table 2.4: Deterministic effective stress stability analysis $F_{s, s \text{ min}}$ guidelines after Jansen R. et al. 1988 (values in bracket from Novak et al. 2003 giving different guidelines for $F_{s, s \text{ min}}$)

Design loading condition	Minimum Factor of safety, $F_{s,s \text{ min}}$	
	Downstream slope	Upstream slope
under construction; end of construction	1.25	1.25
with earthquake loading in addition (pseudo static)	1.0 (1.1)	1.0 (1.1)
Steady seepage long-term operational at partial pull, upstream slope	1.5	1.5
with earthquake loading in addition (pseudo static)	1.25	1.25
Rapid drawdown	-	1.25 (1.2)
with earthquake loading in addition (pseudo static)	-	1.0 (1.1)
Seismic loading with 1,2, or 3 above	1.1	1.1

As the reservoir is 90% full, the upstream reservoir condition is not critical, but it is critical during drawdown condition. Table 2.5 below summarizes the loading conditions and corresponding minimum factor of safety, FoS requirements proposed by USACE, 2003.

Table 2.5: Various Load Cases and Minimum Required Factor of Safety for Full Supply Condition (USACE, 2003).

Case	Loading condition	Critical slope	FoS
I	End of construction	Upstream	1.3
		Downstream	1.3
II	Sudden drawdown	Upstream	1.3
III	Steady seepage	Downstream	1.5
IV	Sudden drawdown & steady seepage with earthquake effect	Upstream	1.1
		Downstream	1.1

2.6 Methods of Slope Stability Analysis in GeoStudio Software

Embankment dam stability must be assessed in relation to the changing conditions of loading and seepage régime which develop from construction through first impounding into operational service, including reservoir drawdown (P.Novak, 2004).

Duncan et al, 1987 recommends that evaluation of a slope focus on defining geometry, shear strengths, unit weights, and pore water pressures. The various methods available for slope stability analysis in GeoStudio yield similar results (within $\pm 6\%$), and selection of the method is less important than choosing accurate parameters and adding earthquake effects. Seismic slope stability is evaluated using a “pseudo static” analysis where the failure mass is assumed to be horizontally accelerated by the seismic coefficient, α_h as percentage of gravity, appropriately chosen for the expected seismicity of the site (Duncan et al, 1987). And the following methods are employed in slope stability analysis of natural slope and manmade embankment slope.

2.6.1 Limit Equilibrium Method

Limit equilibrium types of analyses for assessing the stability of earth slopes have been in use in geotechnical engineering for many decades. The idea of discretizing a potential sliding mass into vertical slices was introduced early in the 20th century and is consequently the oldest numerical analysis technique in geotechnical engineering (SLOPE/W, 2007).

Many different solution techniques for the method of slices have been developed over the years. Basically, all are very similar. The differences between the methods are depending on: what equations of statics are included and satisfied and which interslice forces are included and what is the assumed relationship between the interslice shear and normal forces? Figure 2-5 illustrates a typical sliding mass discretized into slices and the possible forces on the slice. Normal and shear forces act on the slice base and on the slice sides.

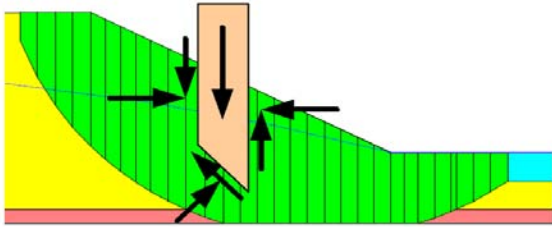


Figure 2.5 Slice discretization and slice forces in a sliding mass

During the next few decades, Fellenius (1936) introduced the Ordinary or Swedish method of slices. In the mid-1950s Janbu (1954) and Bishop (1955) developed advances in the method. The advent of electronic computers in the 1960's made it possible to more readily handle the iterative procedures inherent in the method, which led to mathematically more rigorous formulations such as those developed by Morgenstern and Price (1965) and by Spencer (1967). The introduction of powerful desktop personal computers in the early 1980s made it economically viable to develop commercial software products based on these techniques, and the ready availability today of such software products has led to the routine use of limit equilibrium stability analysis in geotechnical engineering practice. Modern limit equilibrium software such as SLOPE/W is making it possible to handle ever-increasing complexity in the analysis. It is now possible to deal with complex stratigraphy, highly irregular pore-water pressure conditions, a variety of linear and nonlinear shear strength models, virtually any kind of slip surface shape, concentrated loads, and structural reinforcement (SLOPE/W, 2007).

2.6.1.1 Spencer Method

This is a very accurate and recent method which satisfies both equilibrium of forces and moments and it works for any shape of slip surface. The basic assumption used in this method is that the inclinations of the side forces are the same for all the slices (SLOPE/W, 2007).

2.6.1.2 Morgenstern and Price

Morgenstern and Price proposed a method that is similar to Spencer's method, except that the inclination of the interslice resultant force is assumed to vary according to a "portion" of an arbitrary function. This method allows one to specify different types of interslice force function. The interslice functions available in SLOPE/W for use with the Morgenstern-Price (M-P) method are:

- Constant
- Half-sine
- Clipped-sine
- Trapezoidal
- Data-point specified

Selecting the Constant function makes the M-P method identical to the Spencer method (Morgenstern & Price, 1965).

2.6.2 Finite Element Modeling

The Mohr–Coulomb model is used for this analysis. This model involves the following parameters, namely Young's modulus, E , Poisson's ratio, ν , the cohesion, c , the friction angle, ϕ , (Lambe, T. and Whitmen, R. 1969). One way of including a stress-strain relationship in a stability analysis is to first establish the stress distribution in the ground using a finite element analysis and then use these stresses in a stability analysis. This idea has been implemented in SLOPE/W. The ground stresses can be computed using SIGMA/W, and SLOPE/W uses the SIGMA/W stresses to compute safety factors (SLOPE/W, 2007).

2.6.3 Slip Surface Shapes

The importance of the interslice force function depends to a large extent on the amount of contortion the potential sliding mass must undergo to move. The function is not important for some kinds of movement while the function may significantly influence the factor of safety for other kinds of movement. The following examples illustrate this sensitivity.

Circular slip surface

Figure 2-6(a) presents a simple circular slip surface together with the associated FS vs λ plot. In this case the moment equilibrium is completely independent of the interslice shear forces, as indicated by the horizontal moment equilibrium curve. The force equilibrium, however, is dependent on the interslice shear forces. The moment equilibrium is not influenced by the shear forces because the sliding mass as a free body can rotate without any slippage between the slices. However, substantial interslice slippage is necessary for the sliding mass to move laterally. As a consequence, the horizontal force equilibrium is sensitive to interslice shear. Since the moment equilibrium is completely independent of interslice shear, any assumption regarding an interslice force function is irrelevant. The interslice shear can be assumed to be zero, as in the Bishop's Simplified method, and still obtain an acceptable factor of safety, provided the method satisfies moment equilibrium. This is, of course, not true for a method based on satisfying only horizontal force when only horizontal force equilibrium is satisfied for a curved slip surface results in a factor of safety significantly different than when both force and moment equilibrium is satisfied.

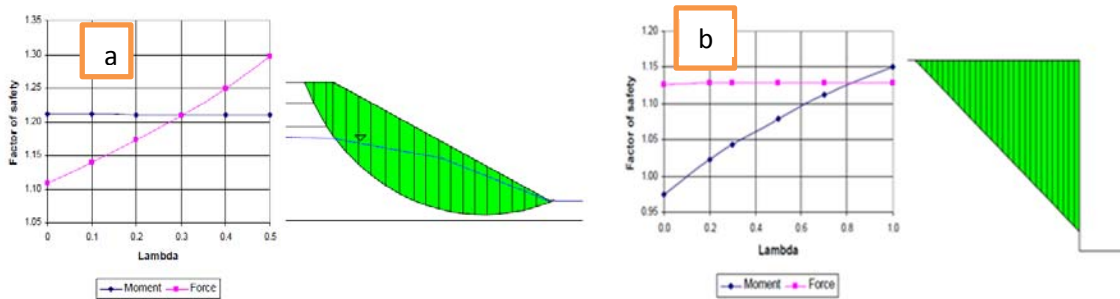


Figure 2-6 a) Conditions for a simple circular slip surface b) Situation for a planar slip surface

The moment equilibrium curve is not always perfectly horizontal for circular slip surfaces. The moment curve in Figure 2-6(a) was obtained from a circular slip surface analysis and it is slightly inclined. Usually, however, the slope of the moment curve is nearly horizontal. This is why the Bishop and Morgenstern-Price factors of safety are often similar for circular slip surfaces (SLOPE/W, 2007).

Planar slip surface

Figure 2-6(b) illustrates a planar slip surface. The moment and force equilibrium curves now have reverse positions from those for a circular slip surface. Now force equilibrium is completely independent of interslice shear, while moment equilibrium is fairly sensitive to the interslice shear. The soil wedge on the planar slip surface can move without any slippage between the slices. Considerable slippage is, however, required for the wedge to rotate.

Composite slip surface

A composite slip surface is one where the slip surface is partly on the arc of a circle and partly on a planar surface, as illustrated in Figure 2-7(a). The planar portion in this example follows a weak layer, a common situation in many stratigraphic settings. In this case, both moment and force equilibrium are influenced by the interslice shear forces. Force equilibrium factors of safety increase, while moment equilibrium factors of safety decrease as the interslice shear forces increase (higher lambda values).

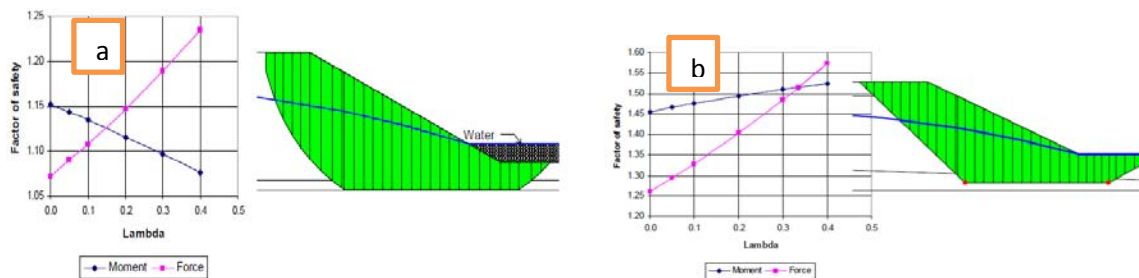


Figure 2-7 a) situation for a typical composite slip surface b) typical situation for a block slip surface

This illustrates that a Bishop's Simplified type of analysis does not always err on the safe side. A more rigorous formulation such as the Morgenstern-Price or Spencer method will give a lower factor of safety than a Bishop Simplified factor of safety. This is not necessarily true for all composite slip surfaces. For some composite slip surfaces, a mathematically more rigorous factor of safety may be higher than the Bishop's Simplified. It is not possible to generalize as to when a more simplified factor of safety will or will not err on the safe side.

Slippage between the slices needs to occur for both moment and force equilibrium for a slip surface of this shape and, consequently, the interslice shear is important for both types of equilibrium.

Block slip surface

Figure 2-7(b) shows a block-type slip surface. As with the previous composite slip surface, the moment and force equilibrium are both influenced by the interslice shear. The force equilibrium is more sensitive to the shear forces than the moment equilibrium, as indicated by the curve gradients in Figure 2-7(b). Once again it is easy to visualize that significant slippage is required between the slices for both horizontal translation and rotation, giving rise to the importance of the shear forces.

2.7 Slope/w

SLOPE/W is the leading slope stability software product for computing the factor of safety of earth and rock slopes. SLOPE/W can effectively analyze both simple and complex problems for a variety of slip surface shapes, pore-water pressure conditions, soil properties, analysis methods and loading conditions (SLOPE/W, 2007).

SLOPE/W uses the theory of limit equilibrium of forces and moments to compute the factor of safety against failure in limit equilibrium methods.

A factor of safety is defined as that factor by which the shear strength of the soil must be reduced in order to bring the mass of soil into a state of limiting equilibrium along a selected slip surface.

For an effective stress analysis, the shear strength is defined as:

$$s = c' + (\sigma - u)\tan\phi' \quad 2.8$$

Where:

s = shear strength,

C' = effective cohesion,

Φ' = effective angle of internal friction,

σ_n = total normal stress, and

u = pore-water pressure.

The limit equilibrium formulation assumes that:

The factor of safety of the cohesive component of strength and the frictional component of strength are equal for all soils involved. The factor of safety is the same for all slices.

Figure 2.8 show all the forces acting on a circular slip surface. The variables are defined as follows:

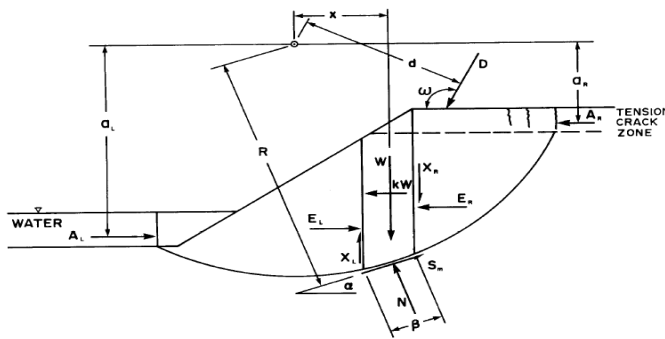


Figure 2.8 Forces acting on a slice through a sliding mass with a circular slip surface

Where: -

W = the total weight of a slice of width b and height h

N = the total normal force on the base of the slice

S_m = the shear force mobilized on the base of each slice.

E = the horizontal interslice normal forces. Subscripts L and R designate the left and right sides of the slice, respectively.

X = the vertical interslice shear forces. Subscripts L and R define the left and right sides of the slice, respectively.

D = an external point load.

kW = the horizontal seismic load applied through the centroid of each slice.

R = the radius for a circular slip surface or the moment arm associated with the mobilized shear force,

S_m = for any shape of slip surface.

f = the perpendicular offset of the normal force from the center of rotation or from the center of moments. It is assumed that f distances on the right side of the center of rotation of a negative slope (i.e., a right-facing slope) are negative and those on the left side of the center of rotation are positive. For positive slopes, the sign convention is reversed.

x = the horizontal distance from the centerline of each slice to the center of rotation or to the center of moments.

e = the vertical distance from the centroid of each slice to the center of rotation or to the center of moments.

d = the perpendicular distance from a point load to the center of rotation or to the center of moments.

h = the vertical distance from the center of the base of each slice to the uppermost line in the geometry (i.e., generally ground surface).

a = the perpendicular distance from the resultant external water force to the center of rotation or to the center of moments. The L and R subscripts designate the left and right sides of the slope, respectively.

A = the resultant external water forces. The L and R subscripts designate the left and right sides of the slope, respectively.

ω = the angle of the point load from the horizontal. This angle is measured counter-clockwise from the positive x-axis.

α = the angle between the tangent to the center of the base of each slice and the horizontal. The sign convention is as follows. When the angle slopes in the same direction as the overall slope of the geometry, α is positive, and vice versa.

The magnitude of the shear force mobilized (S_m) to satisfy conditions of limiting equilibrium is:

$$S_m = \frac{S\beta}{F} = \frac{\beta(c' + (\sigma_n - u)\tan\phi')}{F} \quad 2.9$$

$\delta_n = N/\beta$ = average normal stress at the base of each slice,

F = the factor of safety, and

β = the base length of each slice.

Moment equilibrium factor of safety

Reference can be made to Figure 2.6, for deriving the moment equilibrium factor of safety equation. In each case, the summation of moments for all slices about an axis point can be written as follows:

$$\sum Wx - \sum SmR - \sum Nf + \sum kW_e \pm \sum Dd \pm \sum Aa = 0 \quad 2.10$$

After substituting for S_m and rearranging the terms, the factor of safety with respect to moment equilibrium is:

$$F_m = \frac{\sum(c'\beta R + (N - u\beta)R\tan\phi')}{\sum Wx - \sum Nf + \sum kW_e \pm \sum Dd \pm \sum Aa} \quad 2.11$$

This equation is a nonlinear equation since the normal force, N , is also a function of the factor of safety.

Force equilibrium factor of safety

Again, reference can be made to Figure 3-6, for deriving the force equilibrium factor of safety equation. The summation of forces in the horizontal direction for all slices is:

$$\sum(E_L - E_R) - \sum(N\sin\alpha) + \sum(S_m\cos\alpha) - \sum(kW) + \sum D\cos\omega \pm \sum A = 0 \quad 2.12$$

The term $\sum(EL-ER)$ presents the interslice normal forces and must be zero when summed over the entire sliding mass. After substituting for S_m and rearranging the terms, the factor of safety with respect to horizontal force equilibrium is:

$$F_f = \frac{\sum(c'\beta\cos\alpha + (N-u\beta)\tan\phi'\cos\alpha)}{\sum(N\sin\alpha) + \sum(kW) - \sum D\cos\omega \pm \sum A} \quad 2.13$$

2.8 Rapid Drawdown

Rapid drawdown (RDD) has long been recognized as one of the critical design conditions for the upstream or riverside slope of dams and levees. The rapid drawdown condition occurs when the water level adjacent to a slope or embankment is lowered quickly after a long period of being elevated either at the normal operating level for a dam or in the case of levees, during a prolonged flood. Rapid removal of the supporting water load from the upstream face of the embankment, combined with changes in pore pressure, results in an undrained unloading condition in which total stresses decrease, but shear stresses within the embankment increase (Bishop, A. W. (1954). Sudden or rapid drawdown is typically an important condition controlling the design of the upstream slope in embankment dams. In particular, slides due to rapid drawdown can lead to reduced reservoir capacity and dam failure (Bishop and Bjerrum 1960; Morgenstern 1963; Sherard 1953).

2.9 Pore Water Pressure

Pore water pressure can be defined as pressure experienced by water contained in the pores of earth materials, concrete structures or rock. Via instrumentation associated with large civil engineering structures such as dams, underground tunnels, tall buildings and other mega structures measurement of pore water pressure enables to study detail geotechnical aspects of the structures.

The study of pore pressure has following main purposes:

- Effect of water in pores of soil or rock is to reduce load bearing capacity of soil or rock. Effect is more pronounced with higher pore water pressure leading eventually in some cases to total failure of load bearing capacity of the soil.
- Ground water level and flow pattern determination
- Determine flow pattern of water in embankment & concrete dams and their foundations and to delineate the phreatic line.

Excess pore water pressure is developed in highly compressive, low permeability soils. But this pore water pressure dissipated through time and this might have adverse effect on the stability of

the structures such as dams during and immediately after construction and after rapid drawdown. So it is important to know the magnitude of pore water pressure developed at a certain level after rapid drawdown. Based on the value determined a possible solution will be recommend for the safety of dam and to alleviate problems ([Casagrande,A 1937](#)).

2.10 Seismic dam Slope Analysis

The seismic resistant analysis of an earthdam requires knowledge of seismology and earthquake engineering. Earthquakes are vibrations caused by movement of base rocks along fault surfaces. Most earthquakes occur when the energy stored by elastic deformation in the rocks on both sides of a fault is enough to rupture the rocks or to overcome the friction on an existing fault plane. The deformation is understood as being caused by internal forces such as of convectional, gravitational and magnetic origins.

The energy of the earthquake, generated at the fault is radiated outwards by means of elastic waves. As these waves travel through and along the crust of the earth they shake the earth in all directions with varying degree of intensity and the pattern of oscillation changes by refraction, reflection and superposition of one type of wave on others. Generally, the magnitude of these waves decrease with distance.

The size of an earthquake depends on the amount of energy released. This can be measured by earthquake magnitude. The amount of energy released in turn can be related to the size of the geologic offset, fault parameters and to the consequences of the seismic hazard on people and their environment.

An earthquake can induce failure of a slope that is statically safe. The reason is twofold: The earthquake increases the driving moment, mostly through horizontal shaking; and in some soils it can decrease the shear strength of the soil by increasing the water compression stress through cyclic loading, possibly leading to liquefaction ([Jeanjean, P. 2012](#)).

There are several ways to include earthquake loading in slope stability analysis:

- Pseudostatic method
- Newmark's displacement method
- Post-earthquake stability method

➤ Dynamic finite element method

2.10.1 Pseudo static Method

The pseudo static analysis does not apply where there may be a loss of soil strength (e.g., liquefaction) in the embankment or foundation materials during a seismic event. The pseudo static analysis assumes that the earthquake causes an additional horizontal force in the direction of failure. This force is equal to a seismic coefficient times the weight of the sliding mass. The pseudo static method of analysis is normally applied to those critical failure surfaces determined by the long-term static loading conditions (such as steady-state seepage resulting from normal reservoir pool elevation). The pseudo static method of analysis is not usually applied to short-term to temporary static loading conditions (such as end of construction, flood storage pool), except when this condition is the normal operating case. Where reservoir drawdown occurs on a daily cycle (such as for a pumped storage project) and emergency depletion of reservoir water, earthquake loading in combination with rapid drawdown is recommended by respondents.

During earth quake, as the ground under a dam moves, the dam must also move with it to avoid rupture. This means that the dam has to resist the inertial force caused by the sudden movement of the earth crest.

Figure 2.9 shows, Inertial forces always act opposite to the direction earthquake movement. In stability analysis of embankment dams against earthquake, the direction of the earthquake will be chosen in such a way that it will be unfavourable to the stability.

Inertial Force = Mass of the dam x Earthquake ground acceleration

$$P_e = \frac{W}{g} \cdot \alpha g = \alpha W$$

2.14

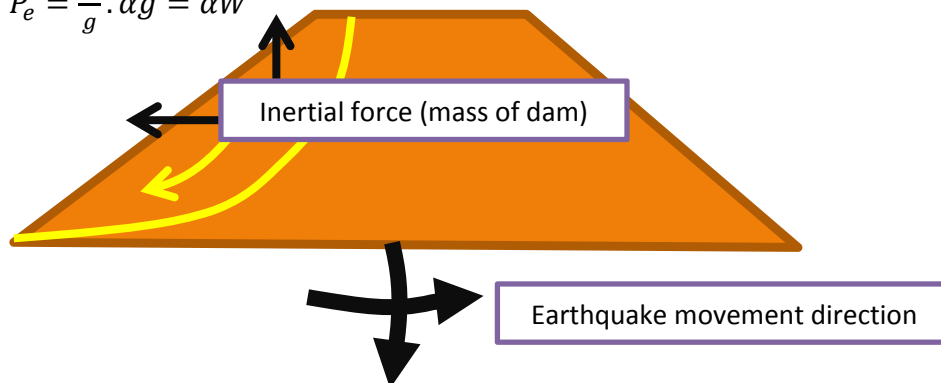


Figure 2.9 Inertial forces and earthquake movement direction (Asie K. lecture note,2016)

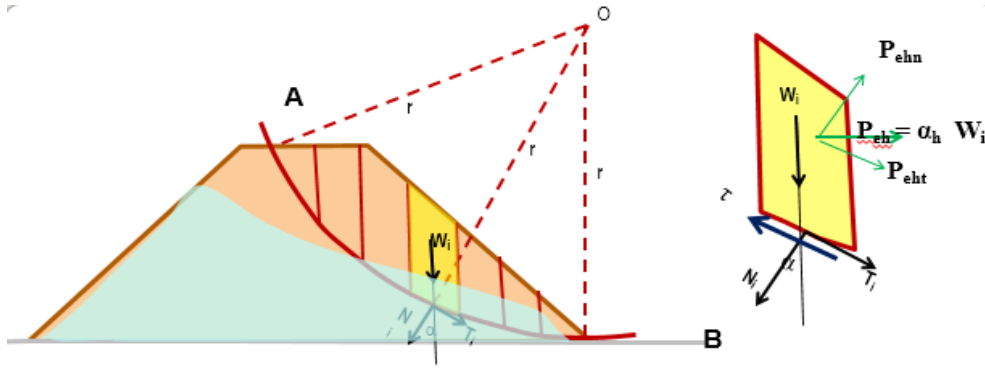


Figure 2.10 Inertial forces due to earthquake movement (Asie K. lecture note,2016)

$$N_i = W_i \cos \alpha$$

$$T_i = W_i \sin \alpha$$

$$P_{eht} = P_{eh} \cos \alpha = \alpha_h W_i \cos \alpha = \alpha_h N_i$$

$$P_{ehn} = P_{eh} \sin \alpha = \alpha_h W_i \sin \alpha = \alpha_h T_i$$

$$\text{Disturbing} = T_i + P_{eht} = T_i + \alpha_h N_i$$

$$\begin{aligned} \text{Resisting} &= c\Delta L + (N_i - P_{ehn} - U\Delta L) \tan \phi \\ &= c\Delta L + (N_i - \alpha_h T_i - U\Delta L) \tan \phi \end{aligned}$$

$$FS = \frac{c\Delta L + (N_i - \alpha_h T_i - U\Delta L) \tan \phi}{T_i + \alpha_h N_i} \quad FS > 1 \quad 2.15$$

2.10.2 Dynamic finite element method

In static loading after assessing the strength of the structure by comparing it with external destabilizing force, the major concern is to evaluate the factor of safety against failure. Failure in soil occurs at a few percent of strain level. So, a static problem deals with a few percent of strain level, which can occur due to compression or consolidation. The strain level is in order of 10^{-3} or greater. In dynamic problems the soil is in motion and the large impact of inertial force due to velocity change is considered. As the duration of time for deformations become shorter the role of inertia becomes larger and larger. In such a cyclic motion even if the strain level is so small, the inertial force will increase in proportion to the square of the cyclic frequency. Due to this fact, up to a strain level of 10^{-6} such consideration must be given for dynamic loading. The other issue differentiating dynamic problem with that of static is the rapidity of load. Problem where the load is applied for more than tens of seconds is cited as static. If the load application time is less than this, the problem is of dynamic type. In addition of the time of application, the

other factor differentiating dynamic and static problem is the loading repetition in dynamic loading. The period of impulse in earthquake is from 0.1-3 seconds.

In static loading since we deal with a strain level of 10^{-3} or greater which is a failure state, the deformation characteristic is not dependent on shear strains. But in dynamic loading, the deformation characteristic is dependent on shear strain. The below table show the relation between strain level and mechanical properties, with expected phenomena to occur.

Earthquake can be designed for maximum credible earthquake (MCE) and Operating Basis Earthquake (OBE). Maximum credible earthquake is the largest or maximum expected conceivable earthquake that appears along a recognized fault. In considering MCE, extensive damages of the dam due to the earthquake are tolerated as long as no catastrophic flooding occurs. Time history data is needed to define the earthquake character. The other design option is design for Operating Basis Earthquake (DBE), which only minor damages are acceptable. It is lower than the MCE. (ICOLD, 1989) To elaborate this in other words, Operating Basis Earthquake is expected to occur within the service life of the project, that is, with a 50% probability of exceedance during the service life. But Maximum Design Earthquake is a minimum of 10% chance of being exceeded in a 100-year period, or a 1000 year return period. Dams with more than 45-meter height and with a reservoir capacity of 120 hecto-meter cubes need dynamic analysis. The rate of seismic hazard is related with site conditions in the below table (ICOLD, 1989)

Table 2.6: Rate of seismic hazard

Rate of seismic hazard	
Condition	Hazard
$PGA < 0.1 \text{ gravity}$	Low
$0.1 \text{ gravity} \leq PGA \leq 0.25 \text{ gravity}$	Medium
$PGA > 0.25 \text{ gravity}$ (but no active fault in 10km radius)	High
$PGA > 0.25 \text{ gravity}$ (with active fault in 10km radius)	Extreme

Dynamic analysis of a dam can follow the below steps.

Step 1: Determine pre-earthquake static stress using a static numerical model of the embankment for initial effective normal stress and shear stress along the potential failure surface. The numerical models are usually based on finite element or finite difference approximations

Step 2: Evaluate the dynamic soil behavior from in-situ and cyclic laboratory tests for input soil properties required in the dynamic analyses.

Step 3: For the numerical model developed in Step 1, determine the dynamic response of the dam or embankment and foundation using a basket of plausible base rock motions. The base rock motions should include appropriate accelerograms representing earthquakes of magnitude and peak acceleration similar to those of the design earthquake from earthquakes recorded in a similar geologic environment. The response of the embankment is determined by dynamic finite element or finite difference modeling, using either equivalent linear or nonlinear procedures.

Step 4: The stress-strain models used in the dynamic analysis should reasonably represent the following aspects of material behavior: (a) material non-linearity, (b) stress and strain dependence, (c) stress-path dependence, (d) inherent anisotropy, and (e) strain rate dependence. Calibration of the stress-strain model should ideally be based on testing of undisturbed samples.

Step 5: Evaluate embankment deformations on the basis of strain potential for the individual elements, which corresponds to the strain that would be experienced if the element were not constrained by surrounding soil.

Step 6: Calculate total embankment deformation on the basis of gravity loads and softened material properties to determine whether they are within the acceptable limits.

2.11 Empirical review

Mandali Dam in Iraq (2013)

In the journal in entitled “Slope Stability Analysis under Rapid Drawdown Condition and Seismic Loads of Earth Dam” Traditional limit equilibrium methods and a finite element software, SLIDE V.6.0 computer program was utilized in the slope stability analysis.

Excess pore pressure result refers to changes in pore pressure within a soil due to rapidly drawdown of pounded water in upstream side conditions (undrained loading). Materials with low permeability such as clays, may exhibit this behavior. With the so-called "B-bar" method, the change in pore pressure is assumed to be directly proportional to the change in vertical stress.

The Mandali Dam is one of an earth fill dams in Iraq, which had been designed by Directorate General of Dam and Reservoirs. Mandali dam with a central core total length of the dam is about (1316 m) and its maximum height is about (14m). The shell, which is composed mainly of poorly graded gravel with high percentage of coarse gravel, and the central core, the investigation and laboratory testing show clay the available materials at site as a construction material for core.

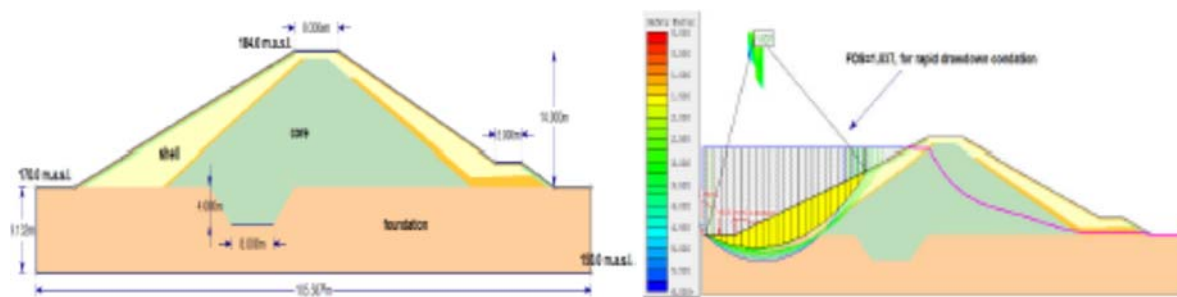


Figure 2.11 Mandali dam

The slope stability against landslide risk is represented by safety factor (SOF), which is determined using Morgenstern-Price Method. The slope stability in the rapid drawdown was examined. In a rapid drawdown of water level, deformation and crack occurred in the dam model at the upstream slope. The failure process in the rapid drawdown of water level was begun with movement of soil particles in the surface of upstream slope model. In this analysis it is found that the factor of safety of upstream decrease when rapid drawdown condition and seismic load effect and the upstream slope is still stable during rapid drawdown, and the minimum value obtained

for FOS is about 1.254 during rapid drawdown and seismic load coefficient 0.07 (Saleh I. Khassaf, 2013).

Al-Wand Dam (2017)

In the journal entitled “Flow and stability of Al-Wand earth dam during rapid drawdown of water in reservoir” In this study, the finite element method is used to study seepage through the body of an earthfill dam. For this purpose, the software Geostudio 2007 is used through its subprograms SEEP/W and SLOPE/W. The water levels on the upstream and downstream sides, the properties of materials and boundary conditions of the dam were input variables and the water flux, exist gradient, and pore water pressure were the target outputs

Al-Wand Dam is an earth dam with clayey core located at 3 km south-east Khanakeen - Dayala at a distance of 6 km from Iraq-Iran borders. Al-Wand dam stores the water coming from the western mountains of Iran through the Wand River. The embankment dam length is 2.8 km, and the area of the reservoir is 3204 km² some of the storage lies in the Iranian lands.

Geostudio 2007 software is utilized in this dam analysis and the dam section is analysed for different conditions of rapid drawdown. The reservoir is assumed to be emptied within 11 days, 3 days and 1 day. The reservoirs period of evacuation has been chosen based on many cases which are:

The period of reservoir emptying of 11 days is the designed period.

The period of reservoir emptying of 3 days is the theoretical assumption for emergencies.

The period of reservoir emptying of 1 day is the theoretical assumption for emergencies.

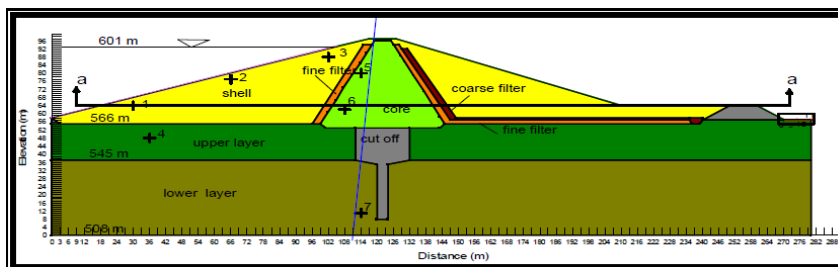


Figure 2.12. Typical section of Al-Wand dam with the material details.

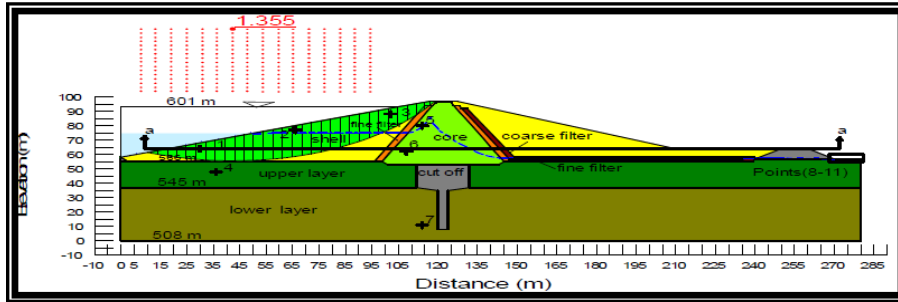


Figure 2.13. The minimum factor of safety and slip surface in Al-Wand dam (at the time of 6 days) during rapid drawdown for a period of reservoir emptying of 11 days using Bishop's method of slices.

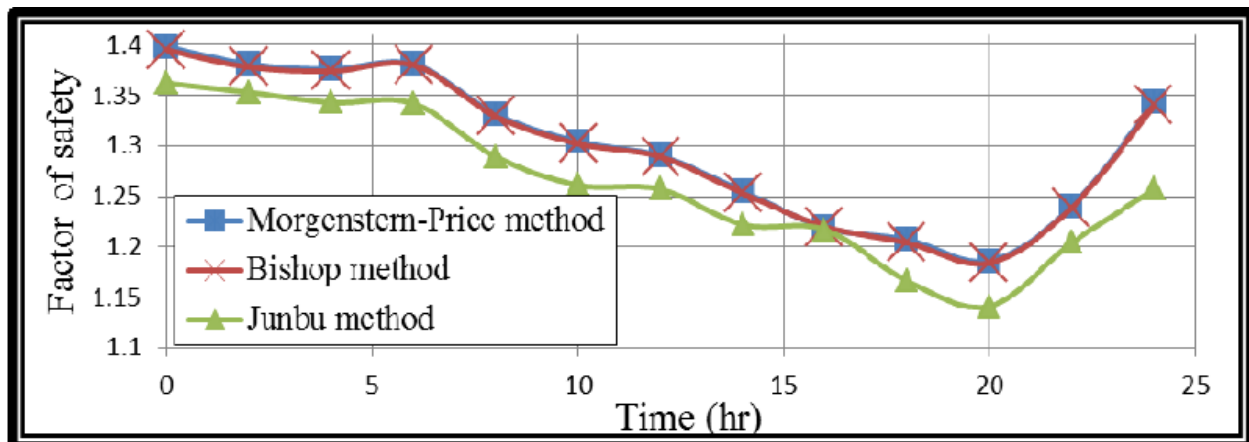


Figure 2.14 Values of a factor of safety during rapid drawdown for a period of reservoir emptying of 1 day in Al-Wand dam.

Figure 2.14 shows that the factor of safety against sliding of the dam slopes decreases slightly within the short period after the start of rapid draw down of water in the reservoir, then starts to increase (Mohammed Y. and Hasan A, 2017).

GEO-SLOPE International Ltd, (Rapid Drawdown)

One way of computing the changes in pore-pressures resulting from the drawdown is to do a SEEP/W analysis. Another way is to do a fully coupled stress/pore-pressure analysis using SIGMA/W. The results from these two types of analyses are presented and compared here.

The embankment used in analysis has a height of 10 m with 2h:1v side slopes and sits on 10 m of foundation soil. The reservoir depth is 9 m as shown in figure below.

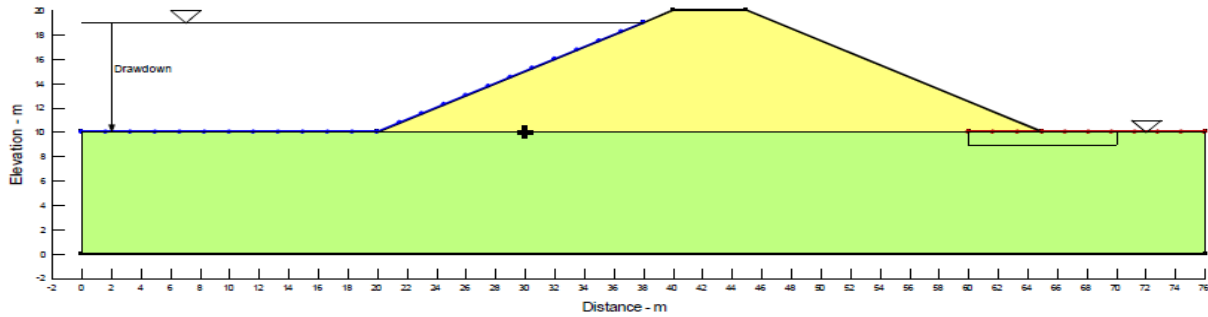


Figure 2.15 dam cross section for rapid drawdown analysis.

The embankment soil and foundation soil are, in essence, treated as being one and the same for this illustrative example. The soil has a saturated hydraulic conductivity K_{sat} of 0.1 m/day (about 1×10^{-4} cm/sec). The E-modulus is 5000 kPa and Poisson's ratio ν is 0.334 (1/3). The equivalent $m\nu$ is 0.0002/kPa.

The resulting behavior of the SEEP/W-alone analysis and a fully coupled SIGMA/W analysis is very similar. The pore-pressures at Point + for these analyses are compared in Figure 10. Initially, the pore-pressures from the coupled analysis are slightly lower than from the SEEP/W-alone analysis. This is due to the rebound associated with the unloading. The tendency for the volumetric expansion is offset by a greater decrease in the pore-water pressure.

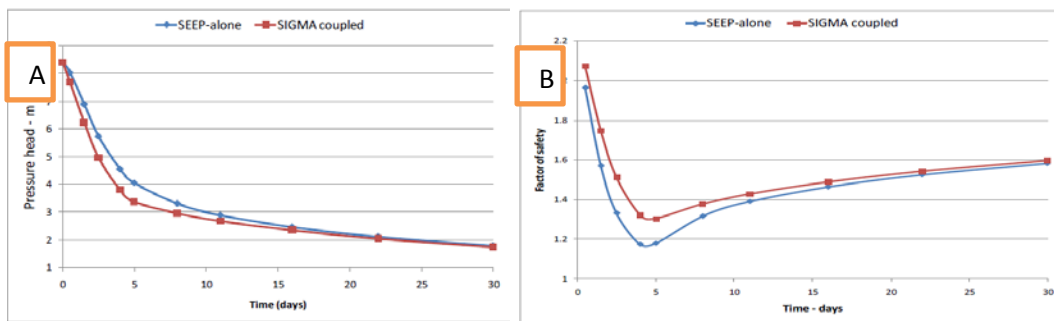


Figure 2.16 A) Comparison of pore pressure B) Comparison of FoS

The lower pore-pressure from the coupled analysis is reflected in the variation in the factors of safety with time as shown in Figure 2.16. The minimum factor of safety for from the coupled analysis is 1.266 while the minimum from the SEEP/W-alone analysis is 1.115. The minimum factor of safety tends to occur just before the completion of the reservoir drawdown as illustrated in figure 2.18B.

3. MATERIALS AND METHODS

3.1 Description of Study Area

3.1.1 Location

The Tendaho dam and irrigation development project is found in the Lower Awash valley in the Afar Regional State in the North Eastern part of Ethiopia. Dam site is located at 600Km from Addis Ababa. Geographically, the project command area is situated between latitude $11^{\circ} 20'$ to $11^{\circ} 50'$ N and Longitude $40^{\circ} 55'$ to 41° E. as shown in the following figure [3-1]. It lies on both banks of river Awash between the proposed Dam near Tendaho and the confluence of river Awash with *Gamari* and *Afambo* lakes. Tendaho dam and reservoir are located in Zone-one of Mille Woreda whereas, Irrigation command is located between Tendaho dam and the delta region downstream of Assaita town, almost up to the outfall of the river Awash into Lake Abbe; that is in the same Zone-one, in Dubti, Afambo and Assaita Woredas.

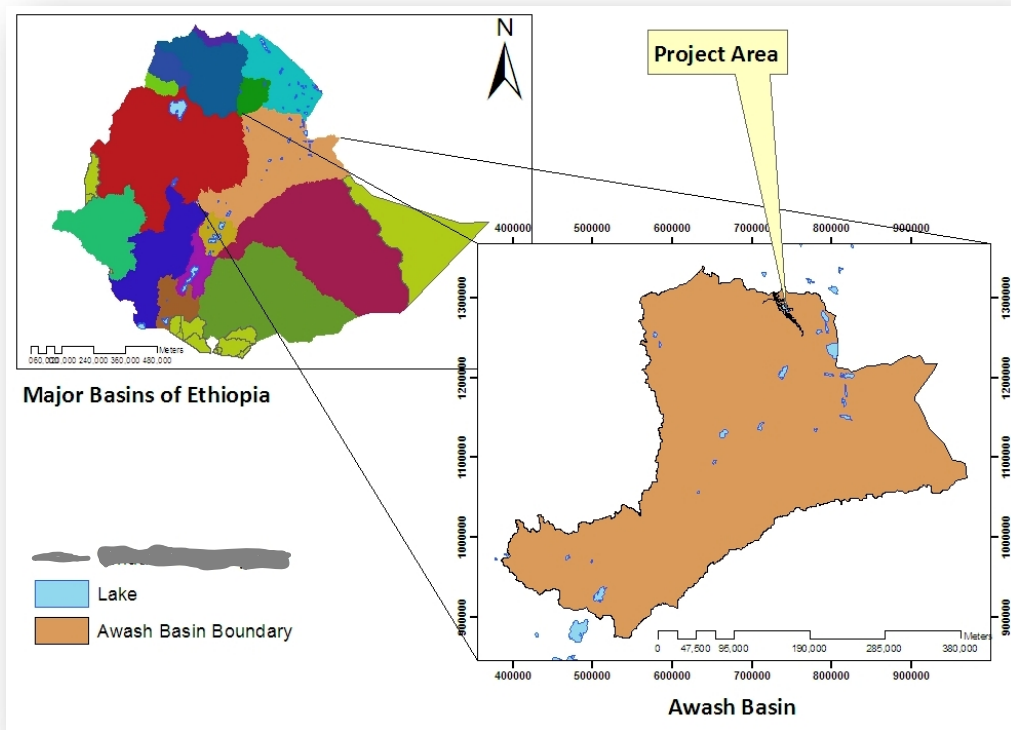


Figure 3-1 Location map of study area (WWDSE, 2013)

3.1.2 Climate

Tendaho dam area is a low land and a very hot area located in the arid zone of the country. Temperature and rainfall recordings are available only at one location, at Dubti. Accordingly, the mean maximum temperature recorded at Dubti ranges from 32.1⁰C - 42.1⁰C and mean minimum temperature as 15.5-24.9⁰C. The hottest months are from March to October and the coldest months from November to February. Mean monthly rainfall at the area (recorded at Dubti) ranges from 3.9-57.7mm. March, April, July and August receive more rainfall [WWDSE, 2005].

3.1.3 Geology of the Dam Area

The Tendaho Dam site is located within an area known as the ‘Tendaho’ which forms the Centre of the Afar triangle, a low lying area of land, where the East African, the Red sea and the Gulf of Eden Rift systems converge.

Figure 3.2 shows that this area is filled by various types of sedimentary deposits ranging from clay to gravel, volcanic tuffs, and hot spring deposits. The Pleistocene age sediments in the area consist of marine and lacustrine clays, silts, sandstones, siltstones, mudstones and conglomerates.

The bedrocks underlying the sedimentary rocks are Pleistocene age flood basalts belonging to the Afar group of the Ethiopian volcanic series [WWDSE, 2005].

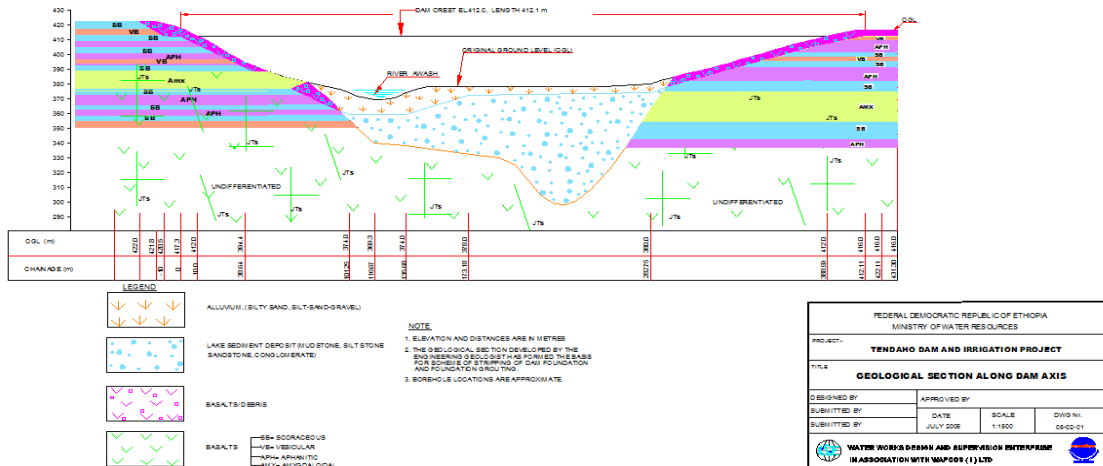


Figure 3.2 geological sections along tendaho dam axis (WWDSE, 2005)

3.2 Material Sources and Properties

The geotechnical study report (July 2005) for the Tendaho dam and irrigation project states that sixteen material sources were identified as possible potential areas. Out of these, 14 were

investigated and sampled, and the remaining two sources were identified as potential rock fill areas. Out of the 16 material source areas, three areas are private areas that supply sand and building stone for construction works in the locality. Three locations are selected as potential sources for the core material (Area 2, Area 5, and Area 9). The laboratory tests on samples collected from these areas indicate the available material for the core of the dam is a highly plastic clay (CH) soil.

The materials being used to construct the core are blended clays and for more material properties look appendix 7B. The blending was done by mixing clay soils with sandy gravel materials (Fig 3.4). Yet, there is no any study conducted on the effects of drawdown speed under static and earthquake loading condition of Tendaho dam. In spite of the fact that, Tendaho dam is taken as a case study here, the useful findings of this thesis can be used as guidelines in other dam design and operation.

Figure 3.3, scheme, the dam section shall comprise 7 different zones with material description as below:

Zone 1	Impervious core	Clay blended with sandy gravel
Zone 2 A	Upstream shell	Sandy Gravel Silt, < 5%
Zone 2 B	Upstream & Downstream shell	Sandy Gravel
Zone 3A	Transition zone	Fine sand –filter criteria not required
Zone 3B	Transition Filter	Fine sand–filter criteria required
Zone 4 Coarse Filter	Coarse sand, pebble, gravel up to 75mm size	
Zone 5	Dumped Rock Riprap	Max. size 1000 mm
		40–50 % > 800 mm
		50-60 % > 300 – 800 mm
		0-10% >300 mm
		Sand & rock dust < 5%

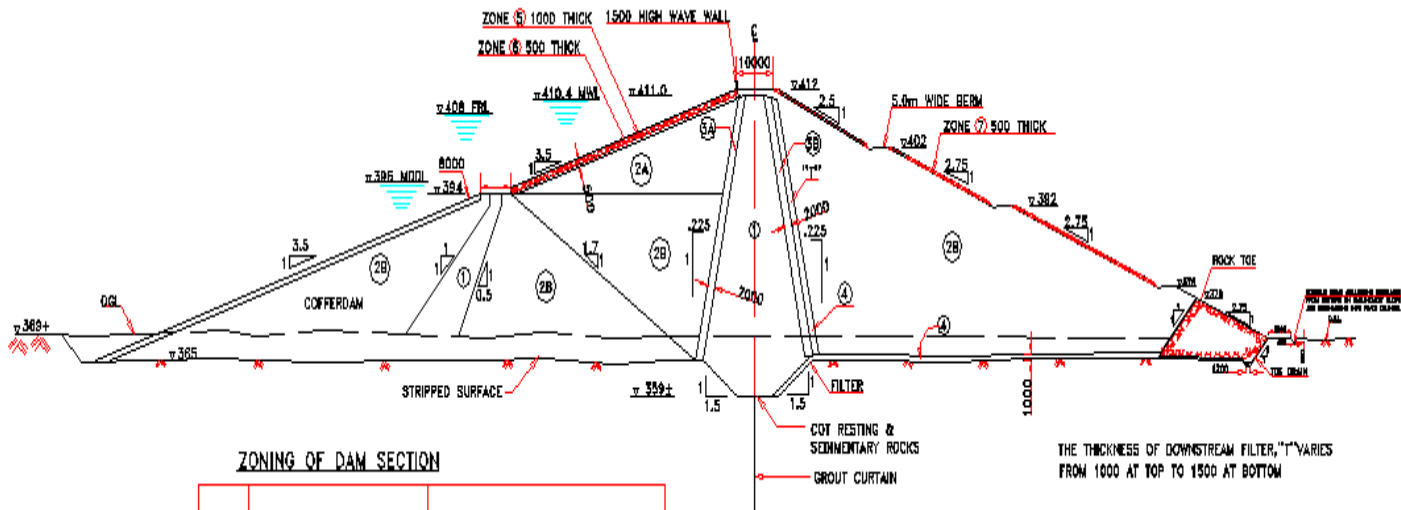
Zone 6 Blanket below U/S Riprap

Crushed rock or natural gravel, graded from

4.75 – 80 mm.

Zone 7 Hand Placed Rock Rip rap

flat or stratified rock fragments



ZONING OF DAM SECTION

ZONE	DESIGNATION	MATERIAL DESCRIPTION
①	IMPERVIOUS CORE	BLENDED SOIL CLAY & SANDY GRAVEL BY EQUAL WEIGHTS
2A	UPSTREAM SHELL	SANDY GRAVEL SILT < 6%
2B	DOWNSTREAM SHELL	SANDY GRAVEL
3A	TRANSITION ZONE	FINE SAND – FILER CRITERIA NOT REQUIRED
3B	TRANSITION FILTER	FINE SAND – FILER CRITERIA REQUIRED
4	COARSE FILTER	COARSE SAND, PEBBLE & GRAVEL UP TO 75 SIZE AND SILT < 5%
5	DUMPED ROCK RIPRAP	MAX. SIZE 1000 MM 40-50% > 800 MM 50-60% > 300-800 MM 0-10% > 300 MM SAND & ROCK DUST < 5%
6	BLANKET BELOW U/S RIPRAP	CRUSHED ROCK OR NATURAL GRAVEL, GRADED FROM 4.75-80
7	HAND PLACED ROCK RIPRAP	FLAT OR STRATIFIED ROCK FRAGMENTS

NOTES :-

- Elevations are in meters and all dimension in millimetres unless specified otherwise
- Topography of valley does not give rise to maximum section, as shown in the drawing. The Section is meant to illustrate Scheme of zoning and to be used for Stability analyses. For section close to maximum section, refer drawing No. 05-02-07
- The stripped level below shell zone is tentative. The excavation depth will be so limited that insitu unit weight of soil matches with target compacted unit weight in this zone.
- For details near dam crest, wave wall, and Rock toe, refer to drawing No. 05-02-08
- Upstream face of the cofferdam is provided with 800 thick layer of rock fragments available as waste material at rock quarry/brushing plant.

Figure 3.3 Geometry and scheme of zoning of Tendaho Dam (from WWDSE, 2005b).

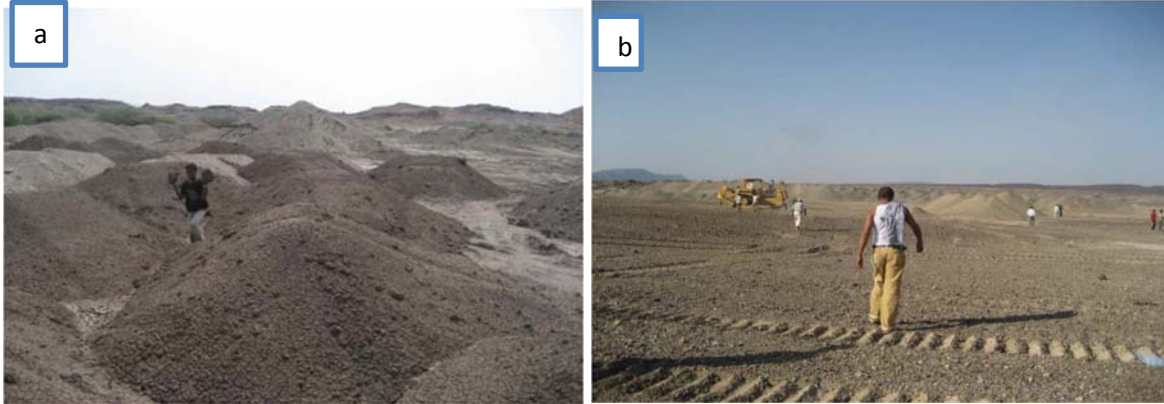


Figure 3.4: Material site: a) borrow area for clay core, and b) for sandy gravel shell.

Important dam Elevation and features

✚ Name of River	Awash
✚ Type of Dam	Earth dam with impervious clay core
✚ Top of Embankment	El. 413.5m
✚ Top of U/S Cofferdam	El. 395 m
✚ Crest Width	10 meters
✚ U/S Slope	3.5: 1
✚ D/S Slopes	2.5: 1 & 2.75: 1
✚ General Riverbed	El. 369.5m
✚ Deepest foundation	El. 359.0m
✚ Height above riverbed	44 m
✚ Height above deepest foundation	54.5m

Reservoir

❖ Maximum water level	El. 410.4m
❖ Full Retention level	El. 408 m
❖ Minimum Draw Down Level	El. 396 m
❖ Live storage at zero year	1416 Mm ³
❖ Live storage at 25 years	1100 Mm ³

3.3 Data Collection

The following data is used in this thesis work

- Material properties of dam

Table 3.1 Main Material laboratory test result of tendaho dam (WWDSE, 2005).

Zone	Sp. Gravity	Unit Weight γ (kN/m ³)	Permeability K (cm/s)	C' (kpa)	ϕ' Degree
Core	2.72	16	2.5×10^{-6}	7	25
Shell 2A	2.70	18.5	5×10^{-3}	0	37/35
Shell 2B	2.70	18.5	10^{-4}	0	35/33
Filter 3	2.70	18.0	10^{-3}	0	35
filter 4	2.70	18.0	10^{-2}	0	34

Table 3.2 material properties from liquefaction analysis of Tendaho earth-fill dam (Hadush and messele, 2006)

Zone of dam	K2max	K_G	Poisson's Ratio ν	Young's modulus E(MPa)
Core	50	11000	0.4	75.432
Shell 2A	90	19800	0.3	150.1
Shell 2B	90	19800	0.3	150.1
Filter 3	70	15400	0.3	113.26
Filter 4	70	15400	0.3	113.26

Where: $E=2G(1+\nu)$, but $G=K_G(\delta_m')^{0.5}$ and $K_G=220 \cdot K2max$

$K2max$ =soil modulus coefficient

K_G = dimensionless soil modulus

C= cohesion, ϕ' = angle of internal friction, γ =Unit Weight

k = Permeability, E = Young's Modulus,

ν = Poison's Ratio G=shear modulus' δ_m' =mean effective stress

Young's modulus of each zone of the dam is defined in function of depth and shear modulus parameter of the soil in geostudio software. For more information about material properties, refer APENDECE 7A.

- Construction drawing (figure 3.3)
- Reservoir water level (figure 3.3)
- Reservoir operation plan and records
- Geologic data
- Seismic data
- Study area background

3.3.1 Primary Data

The primary data was collected from ECDSWC professional teams for cross checking of secondary data which are collected from ECDSWC, ECWC and MoWIE.

- ✚ Material properties of dam (interview material laboratory technician)
- ✚ Construction drawing ((interview Tendaho dam project RE and PM)
- ✚ Reservoir water level and dam design approach (interview headwork and hydropower design team)
- ✚ Drawdown recorded data from dam site



Figure3.5: Primary data collection at Tendaho dam site

3.3.2 Secondary Data

Secondary is collected from Ethiopia construction design and supervision works corporation (ECDSWC), Ethiopian Construction works Corporation (ECWC) and from Ministry of Water, Irrigation and Electricity (MoWIE).

- ✚ Material properties and geometry of dam, Geological data, and Seismic data are collected from Ethiopia construction design and supervision works corporation (ECDSWC).
- ✚ Construction drawing from Ethiopian Construction Works Corporation (ECWC).
- ✚ Reservoir under operation drawdown record and Study area background from ECDSWC and Ministry of Water, Irrigation and Electricity (MoWIE).

3.4 Modeling and Data Analyzing Tools

In this study GeoStudio 2007 and 2012 software, which can effectively analyze simple to complex problems for a variety of slip surface shapes, pore water pressure conditions, soil properties, analysis methods and loading conditions, is employed to develop pore pressure curve and factor of safety curve under different drawdown speed and loading condition.

The diagram below shows the summery of software employed for modeling and data analyzing.

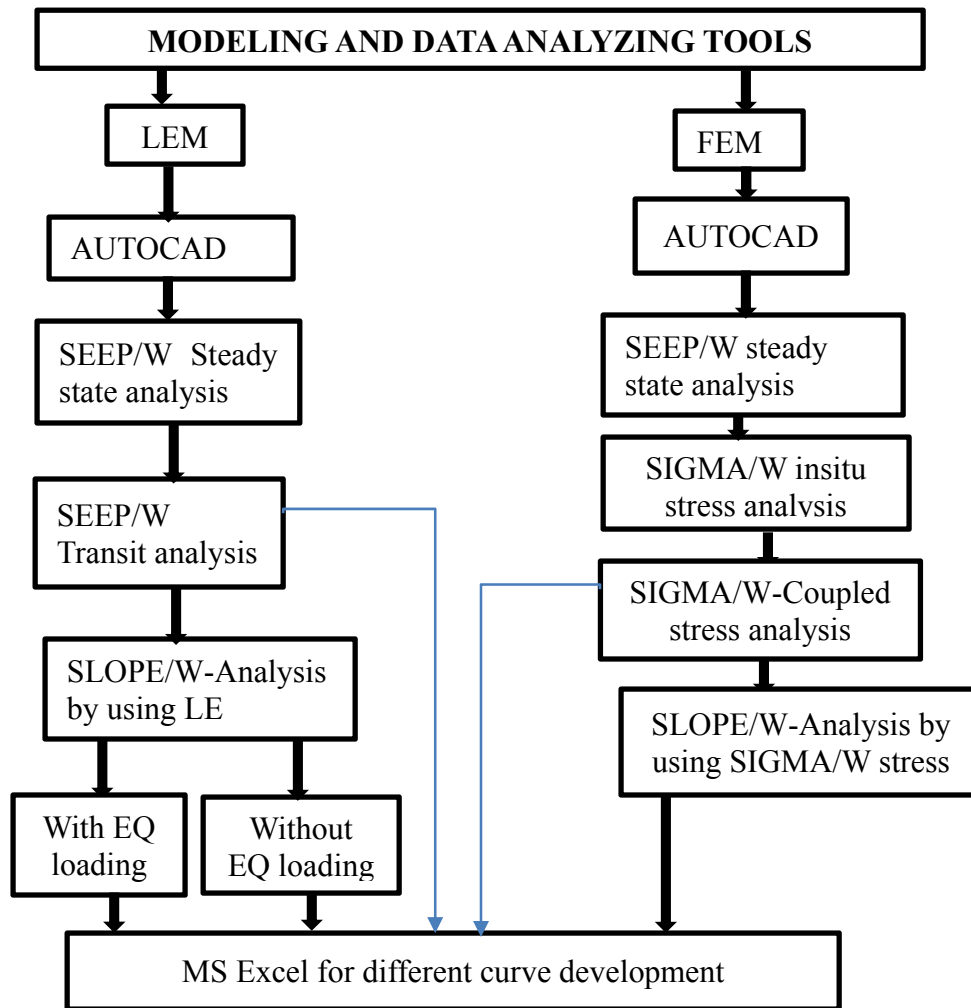


Figure 3-6 summary of modeling and analyzing approaches.

3.4.1 Limit Equilibrium Modeling and Analyzing Method

A limit equilibrium analysis is carried out using GeoStudio software for the slope stability of the earth fill dam slope. The geometry is created and adjusted in AutoCAD 2007 software and imported into the Seep/W sub program for pore water development that is used as input in slope/w slope stability analysis. slope/w is used to analysis slope stability of dam by employing different types of analysis methods.

Slope/W program analysis type used could be: - Morgenstern-Price, spencer, Ordinary, Bishop, Janbu and others. The results and output of seep/w and slope/W is imported to Microsoft excel 2016 for purpose pore pressure curve and FoS curve development.

Method in GeoStudio

The Ordinary, or Fellenius method was the first method developed. The method ignored all interslice forces and satisfied only moment equilibrium. Adopting these simplified assumptions made it possible to compute a factor of safety using hand calculations, which was important since there were no computers available.

Later Bishop (1955) devised a scheme that included interslice normal forces, but ignored the interslice shear forces. Again, Bishop's Simplified method satisfies only moment equilibrium. It is interest and significance with this method is the fact that by including the normal interslice forces, the factor of safety equation became nonlinear and an iterative procedure was required to calculate the factor of safety. The Janbu's Simplified method is similar to the Bishop's Simplified method in that it includes the normal interslice forces and ignores the interslice shear forces. The difference between the Bishop's Simplified and Janbu's Simplified methods is that the Janbu's Simplified method satisfies only horizontal force equilibrium, as opposed to moment equilibrium. Later, computers made it possible to more readily handle the iterative procedures inherent in the limit equilibrium method, and this lead to mathematically more rigorous formulations which include all interslice forces and satisfy all equations of statics. Two such methods are the Morgenstern-Price and Spencer methods.

Table 3-3 lists the methods available in SLOPE/W and indicates what equations of statics are satisfied for each of the methods. Table 3-3 gives a summary of the interslice forces included and the assumed relationships between the interslice shear and normal forces. Further details about all the methods are presented in literature review parts.

Table 3-3 Equations of Statics Satisfied (GEO-SLOPE International Ltd, 2007)

Method	Moment Equilibrium	Force Equilibrium
Ordinary or Fellenius	Yes	No
Bishop's Simplified	Yes	No
Janbu's Simplified	No	Yes
Spencer	Yes	Yes
Morgenstern-Price	Yes	Yes
Corps of Engineers – 1	No	Yes
Corps of Engineers – 2	No	Yes

Lowe-Karafiath	No	Yes
Janbu Generalized	Yes (by slice)	Yes
Sarma – vertical slices	Yes	Yes

Table 3-4 Interslice force characteristics and relationships (GEO-SLOPE International Ltd,2007)

Method	Interslice Normal (E)	Interslice Shear (X)	Inclination of X/E Resultant, and X-E Relationship
Ordinary or Fellenius	No	No	No interslice forces
Bishop's Simplified	Yes	No	Horizontal
Janbu's Simplified	Yes	No	Horizontal
Spencer	Yes	Yes	Constant
Morgenstern-Price	Yes	Yes	Variable; user function
Corps of Engineers 1	Yes	Yes	Inclination of a line from crest to
Corps of Engineers 2	Yes	Yes	Inclination of ground surface at top of slice
Lowe-Karafiath	Yes	Yes	Average of ground surface and slice base inclination
Janbu Generalized	Yes	Yes	Applied line of thrust and moment equilibrium of slice
Sarma – vertical slices	Yes	Yes	$X = C + E \tan \phi$

In this study case Morgenstern-Price method is employed, since it satisfies the following conditions

- ✚ Considers both shear and normal interslice forces,
- ✚ Satisfies both moment and force equilibrium, and
- ✚ Allows for a variety of user-selected interslice force function.

Slip surface

After the material input and pore pressure assign, a slip surface would be defined. The analyses would be performed for failure models namely the circular failure model. There are several methods for defining the slip surface for the circular failure but the entry and exit method was selected. One of the problems with the other methods is how to visualize the extents or the range

of the trial slip surface. This difficulty is solved by the entry and exit method because it specifies the location where the trial slip surfaces should enter the ground surface and where they should exit.

Inherent in limit equilibrium stability analyses is the requirement to analyze many trial slip surfaces and find the slip surface that gives the lowest factor of safety. Included in this trial approach is the form of the slip surface; that is, whether it is circular, piece-wise linear or some combination of curved and linear segments. SLOPE/W has a variety of options for specifying trial slip surfaces. In our study case circular slip surface is defined in entry and exit defining approach.

The position of the critical slip surface is affected by the soil strength properties. The position of the critical slip surface for a purely frictional soil ($c = 0$) is radically different than for a soil assigned an undrained strength ($\phi = 0$). This complicates the situation, because it means that in order to find the position of the critical slip surface, it is necessary to accurately define the soil properties in terms of effective strength parameters.

3.4.2 Steady State Seepage

To compute the pore pressure developed and the phreatic line which is used as input for both the transient and in-situ stress analysis of Tendaho dam. The steady state seepage analysis at full reservoir water level was first computed by the Seep/W component of the Geo-Studio 2007 software developed by the GEO-SLOPE International Ltd, in 2007. Seep/W uses Darcy's law. The steady state analysis of Seep/W assumes that the water inflow is equal to the water outflow. But, during the analysis of rapid drawdown stability, transient seepage and coupled sigma analysis, in which the inflow is not equal to outflow, is used.

The material model used in the seep/W component is saturated/unsaturated for all the materials. In unsaturated soil, the difference between the air and the water pressure, the matric suction varies the volume of water stored in the soil. To account for this the sample function in the software are used by inserting the saturated water content for the materials. Saturated water content is almost equal to the porosity of the soil. Hydraulic conductivity of materials is also defined with respect to the matric suction. Having the boundary condition of the static water pressure up to the full reservoir level in the upstream side and zero flux boundary in downstream side, zero pressure water is expected at the rock toe of the dam.

3.4.3 Slope/W

By using slope/w slope stability analysis focus on defining geometry, shear strengths, unit weights, and pore water pressures. And assigning the define soil strength parameter and pore pressure condition to the dam geometry in GeoStudio software is major points in slope/w modeling.

- ✚ Geometry: - description of the stratigraphy and shapes of potential slip surfaces.
- ✚ Soil strength: - parameters used to describe the soil (material) strength.
- ✚ Pore-water pressure: -means of defining the pore-water pressure conditions.

4.4.4 Finite Element Modeling and Analyzing Method

A finite element analysis consists of two steps. The first step is to model the problem, while the second step is to formulate and solve the associated finite element equations. Modeling involves designing the mesh, defining the material properties, choosing the appropriate constitutive soil model, and defining the boundary conditions. SIGMA/W can formulate and solve the finite element equations.

One way of including a stress-strain relationship in a stability analysis is to first establish the stress distribution in the ground using a finite element analysis and then use these stresses in a stability analysis. This idea has been implemented in geostudio 2007 software sup programs as described in next sentence. The ground stresses can be computed using SIGMA/W, and SLOPE/W uses the SIGMA/W stresses to compute safety factors. The basic information obtained from a finite element stress analysis is σ_x , σ_y and τ_{xy} within each element. The finite element-computed stresses can be imported into a conventional limit equilibrium analysis. The stresses σ_x , σ_y and τ_{xy} are known within each element, and from this information the normal and mobilized shear stresses can be computed at the base mid-point of each slice. Once the mobilized and resisting shear forces are available for each slice, the forces can be integrated over the length of the slip surface to determine a stability factor.

Initial in-situ stresses

Inherent to almost all SIGMA/W analyses is the wish to start from the existing state of stress in the ground; that is, the state of stress in the ground before we as engineers come along apply some load, place some fill or perhaps take away some soil to create an excavation.

Establishing the insitu stress state is analogous to doing a centrifuge test. We build the model first and then apply gravity after the fact. In a finite element analysis gravity is applied through

the material self-weight. The specified soil unit weight times the element volume of the element forms the self-weight. The element weight is converted into downward nodal forces which in turn lead to the stresses in the elements. SIGMA/W has a special analysis type called ‘Insitu’ for this part of a project. For an Insitu analysis, SIGMA/W uses the unit weight and Poisson’s ratio specified for each soil. All other stiffness related parameters are ignored. Poisson’s ratio ν is used to control the K_o conditions. K_o is the ratio of horizontal to vertical stress in the ground. For a 2D analysis, the relationship between K_o and Poisson’s ratio is,

$$K_o = \frac{\nu}{1-\nu} \quad 3.7$$

Since ν cannot be greater than 0.5, K_o cannot be greater than 1.0. Actually, for numerical reasons ν cannot be greater than 0.495 in SIGMA/W and therefore the maximum K_o is just less than 1.0 (about 0.98).

Coupled Stress-Pore Pressure Analysis

SIGMA/W is formulated to solve soil consolidation problems using a fully coupled or any of several un-coupled options. A fully coupled analysis requires that both the stress-deformation and seepage dissipation equations be solved simultaneously.

With the coupled analysis, it is no longer necessary to have SEEP/W as well as SIGMA/W. All hydraulic properties and boundary conditions can be developed and applied from within SIGMA/W. When coupled, three equations are created for each node in the finite element mesh. Two are equilibrium (displacement) equations and the third is a continuity (flow) equation. Solving all three equations simultaneously gives both displacement and pore-water pressure changes.

Of perhaps more use in many real situations is the un-coupled consolidation formulation in SIGMA/W. In this analysis, the seepage analysis is solved independently of the volume change analysis. The incremental change in pore water pressures from the seepage solutions are used at each load step in the stress deformation calculation in order to determine the change in effective stresses. With the un-coupled analysis, the changes in pore-water pressures can be obtained from any other SIGMA/W, SEEP/W, VADOSE/W or QUAKE/W analysis and for any two or multiple time steps in those analyses.

In a coupled consolidation analysis, both equilibrium and flow equations are solved simultaneously. In SIGMA/W, the finite element equilibrium equations are formulated using the

principle of virtual work, which states that for a system in equilibrium, the total internal virtual work is equal to the external virtual work. In the simple case when only external point loads $\{F\}$ are applied, the virtual work equation can be written as:

$$\int \{\varepsilon^*\}^T \{\Delta\sigma\} dV = \int \{\delta^*\}^T \{F\} dV \quad 3.8$$

where:

$\{\delta^*\}$ = virtual displacements,

$\{\varepsilon^*\}$ = virtual strains, and

$\{\sigma\}$ = internal stresses.

The flow equation can similarly be formulated for finite element analysis using the principle of virtual work in terms of pore-water pressure and volumetric strains. If virtual pore-water pressures, u_w^* , are applied to the Flow Equation and integrated over the volume, the following virtual work equation can be obtained.

$$\int U_w^* \left[\frac{K_x}{Y_w} \frac{\partial U_w^*}{\partial X^2} + \frac{K_y}{Y_w} \frac{\partial U_w^*}{\partial Y^2} + \frac{\partial \theta_w}{\partial t} \right] dV = 0 \quad 3.9$$

A coupled consolidation analysis for saturated/unsaturated soils is thus formulated using incremental displacement and incremental pore-water pressure as field variables.

In summary, the coupled equations for finite element analysis are rewritten in the following form.

$$[K]\{\Delta\delta\} + [Ld]\{\Delta uw\} = \{\Delta F\} \text{ and}$$

$$\beta [L_f]\{\Delta\delta\} - \left(\frac{\Delta t}{Y_w} [K_f] + \omega [M_N] \right) \{\Delta U_w\} = \Delta t \left(\{Q\} \Big|_t + \Delta t + \frac{1}{Y_w} [K_f]\{U_w\} \Big|_t \right)$$

$$\text{Where: } [K] = \sum [B]^T [D] [B]$$

$$[L_d] = \sum [B]^T [D] \{m_H\} (N)$$

$$\{m_H\} = \left(\frac{1}{H} \frac{1}{H} \frac{1}{H} \ 0 \right)$$

$$[K_f] = \sum [B]^T [K_w] [B]$$

$$[M_N] = \sum [N]^T [N]$$

$$[L_f] = \sum (N)^T \{m\} [B]$$

Finite element computed stresses in a limit equilibrium framework

The finite element computed stresses can be imported into a conventional limit equilibrium analysis. The stresses σ_x , σ_y , and τ_{xy} are known within each element, and from this information the normal and mobilized shear stresses can be computed at the base midpoint of each slice. The procedure is as follows:

1. The known σ_x , σ_y , and τ_{xy} at the Gauss numerical integration point in each element are projected to the nodes and then averaged at each node. With the σ_x , σ_y , and τ_{xy} known at the nodes, the same stresses can be computed at any other point within the element.
2. For slice 1, find the element that encompasses the x - y coordinate at the base mid-point of the slice.
3. Compute σ_x , σ_y , and τ_{xy} at the midpoint of the slice base.
4. The inclination (α) of the base of the slice is known from the limit equilibrium discretization.
5. Compute the slice base normal and shear stress using ordinary Mohr circle techniques.
6. Compute the available shear strength for the computed normal stress.
7. Multiply the mobilized shear and available strength by the length of the slice base to convert stress into forces.
8. Repeat the process for each slice in succession up to slice number n .

Once the mobilized and resisting shear forces are available for each slice, the forces can be integrated over the length of the slip surface to determine a stability factor.

The stability factor is defined as

$$F.S. = \frac{\sum S_r}{\sum S_m} \quad 3.10$$

Where: - S_r is the total available shear resistance and S_m is the total mobilized shear along the entire length of the slip surface.

4.4.5 Pseudo Static Seismic Parameters determination

The pseudo-static approach has a number of attractive features. The analysis is relatively simple, straightforward and its similarity to the static limit equilibrium analysis routinely conducted by geotechnical engineers makes its computations easy to understand and perform. It produces a scalar index of stability (the factor of safety) that is analogous to that produced by static stability analyses. It must always be recognized, however, that the accuracy of the pseudo-static approach

is governed by the accuracy with which the simple pseudo-static inertia forces represent the complex dynamic inertial forces that actually exists in an earthquake. Difficulty in assignment of appropriate pseudo static coefficients and in interpretation of pseudo static factors of safety, coupled with the development of more realistic methods of analysis, have reduced the use of pseudo-static approach for seismic slope stability analysis purposes.

In order to analyze the stability of Tendaho earth dam during an earthquake, the additional horizontal and vertical loads under pseudo static analysis are represented by appropriate seismic coefficient to give the design acceleration as a fraction of the acceleration due to gravity. The design values of horizontal seismic coefficient α_h can be computed either by seismic coefficient method or by response spectrum method as following section.

1. Seismic coefficient Method

In seismic coefficient method the design value of horizontal seismic coefficient α_h is computed by the following expression:

$$\alpha_h = \beta I \alpha_o \quad 3.8$$

Where: β = a coefficient depending upon the soil foundation system

I = a factor depending upon the importance of the structure, and

α_o = basic horizontal seismic coefficient applicable for that area.

IS: 1893 specifies that value of ' β ' for dams be taken as 1.0 and the value of ' I ' for all types of dams be taken as 3.0.

The Tendaho dam Site is considered to be equivalent of lying somewhere in between zone IV and Zone V identified by IS:1893. The values of basic horizontal seismic coefficient for zone IV and zone V are 0.05 and 0.08 respectively. Value of α_o for Tendaho dam site may be taken as 0.06 (WWDSE, 2005).

Accordingly,

$$\begin{aligned} \alpha_h &= 1.0 \times 3.0 \times 0.06 \\ &= 0.18 \end{aligned}$$

2. Response Spectrum Method:

In response spectrum method, the design value of horizontal seismic coefficient is computed by using following expression:

$$\alpha_h = \beta I F_o S_a/g \quad 3.9$$

Where: β = a coefficient depending upon the soil formation system

I = a factor depending upon the importance of the structure.

F_o = Seismic zone factor for average acceleration spectra

S_a / g = average acceleration coefficient for appropriate natural period and damping of the structure.

The values of β and I are 1.0 and 3.0 respectively. Value of F_o for zones IV and V are 0.40 and 0.25 respectively. Value of F_o for Tendaho dam site can thus be taken as 0.30.

' S_a/g ' is dependent on fundamental period of the structure, T which is determined by the formula:

$$T = 2.9 H_t \sqrt{\frac{\rho}{G}} \quad 3.10$$

Where: T = fundamental period of the earth dam in s,

H_t = height of the dam above toe of the slopes

ρ = mass density of the shell material, and

G = modulus of rigidity of the shell material

The Quantity $\sqrt{\frac{G}{\rho}}$ is the shear wave velocity through the material of the dam.

The shear wave velocity may be determined in the field by block vibration tests, wave propagation tests or by vertical dynamic plate load tests. All the three kinds of tests were conducted on nearly similar material at Tehri Dam Project in India. Based on the results of these tests, the shear wave velocity through sandy gravel material used in Tendaho dam has been considered as 250 m/s (WWDSE, 2005).

For Tendaho dam, $H_t = 42.0$ m

Hence, $T = 2.9 \times 42/250$
 $= 0.49$ seconds

As per IS: 1893, value of S_a/g corresponding to T equal to 0.49 seconds and 10% dumping is 0.135

Hence, $\alpha_h = 1.0 \times 3.0 \times 0.30 \times 0.135 = 0.12$

Guided by the above section 1 & 2 value of α_h for pseudo static analysis of Tendaho Dam shall be taken as 0.18. The vertical seismic coefficient shall be taken as half of the horizontal seismic coefficient, as recommended by IS: 1893 ([WWDSE, 2005](#)).

The above determined seismic coefficient parameter was assigned to the modeled dam section in GeoStudio software.

4 RESULTS AND DISCUSSIONS

4.1 General

In this study, Slope stability analysis under different drawdown speed and loading condition was successfully carried out with the use of two dimensional models GeoStudio 2007 and 2012 software for both limit equilibrium and finite element methods. Material properties are assigned to the model such as the soil strength parameters (cohesion, angle of internal friction and unit weight of soil), soil permeability characters, Poisson's ratio and modules of elasticity. Also, the shape of the critical slip surface of the upstream slope of the dam is analyzed using circular failure surface and assigned by enter and exit methods. The seismic loading has been represented by horizontal and vertical seismic coefficients of 0.18 and 0.09 respectively, as described under materials and methods chapter. The Minimum desired values of factor of safety under various loading conditions, specified by Indian Standard are as per Table 4.1 and the factors of safety computed are compared with the minimum factor of safety specified by the code.

Table 4.1- Minimum Desired Values of Factors of Safety for Various Loading Conditions (IS, 1891)

Case No.	Loading condition	Critical Slope	Minimum Factor of Safety
I	Construction condition with or without partial pool	U/S & D/S	1.0
II	Sudden draw down with tail water at maximum	U/S	1.3
III	Steady seepage of Dam with reservoir full	D/S	1.5
IV	Steady seepage and rapid drawdown with seismic loading	D/S U/S	1.0 1.0

4.2 Dam Geometry Modeling Result

The geometry of dam modeling is shown in Figure 4.1. The embankment has a height of 54.5 m above deep foundation, with 3.5: 1 u/s and 2.5: 1 & 2.75: 1 d/s slopes and the reservoir water depth is 39 m above river bed at FRL. On the downstream rock toe is a granular under-drain which keeps the water table at the tail water elevation for a distance of 24.5 m under the embankment toe (the actual granular layer is not required to achieve this effect; the desired effect can be achieved with a specified boundary condition). The assigned boundary conditions are total head boundary for upstream slope, zero flux boundaries for downstream slope and zero pressure boundary at rock toe.

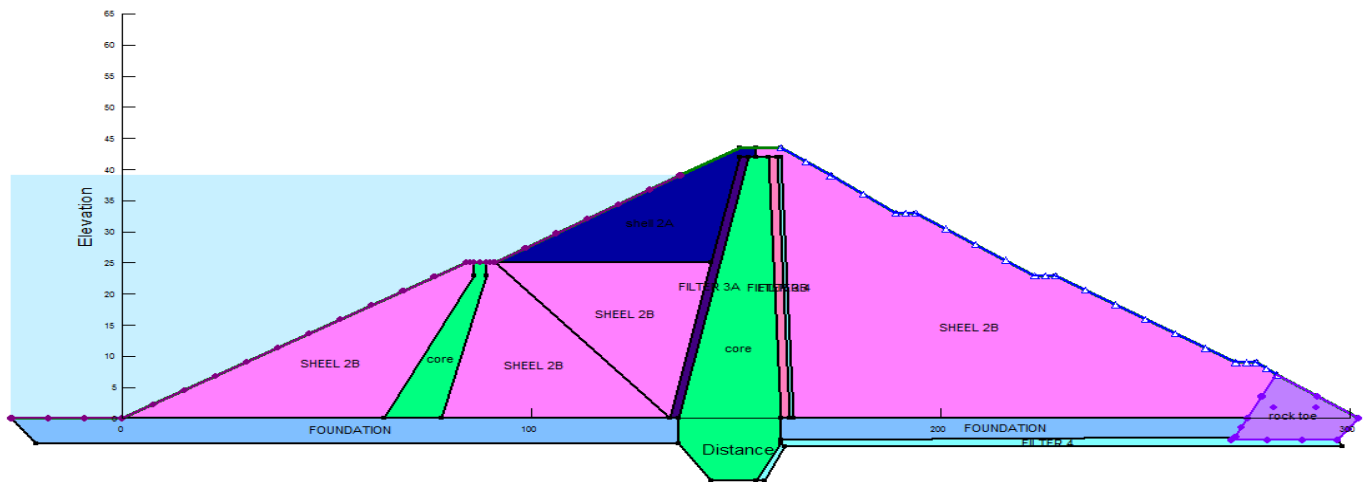


Figure 4.1 material and geometry of tendaho dam

4.3 Long-Term Steady-State Conditions

The first step is to establish the long-term steady-state conditions using a SEEP/W analysis and the pore pressure developed is used as input for both LEM and FEM methods. Figure 4.2 Shows the long-term pore pressure head (H) contours and flux quantity through core of embankment.

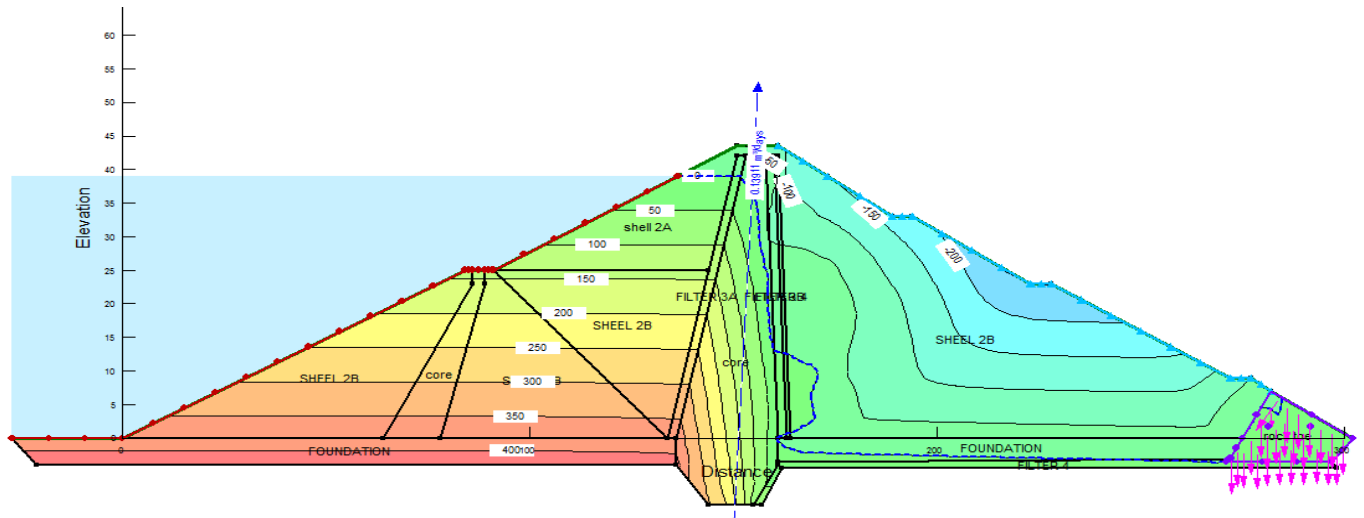


Figure 4.2 Long-term steady-state seep conditions at FRL and pore pressure contour

4.4 Limit Equilibrium Method of Analysis

In limit equilibrium analysis the next step to long-term steady-state conditions establishment is complete a transient SEEP/W analysis to investigate the changes in pore-pressure with time during and after the drawdown of the reservoir. It is assumed that the reservoir will be drained over a period of twenty-seven (20) days. This is modeled with the time-dependent boundary condition shown in Figure 4.3.

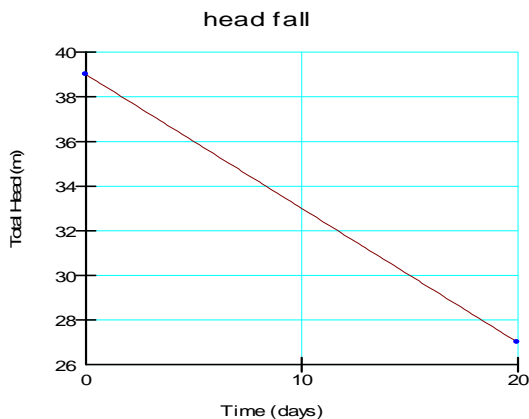


Figure 4.3 Reservoir elevations with time during drawdown

The process is modeled for 100 days after the reservoir has been removed using exponentially spaced time steps. The previous “Parent” steady-state conditions become the initial or starting conditions for the transient drawdown analysis.

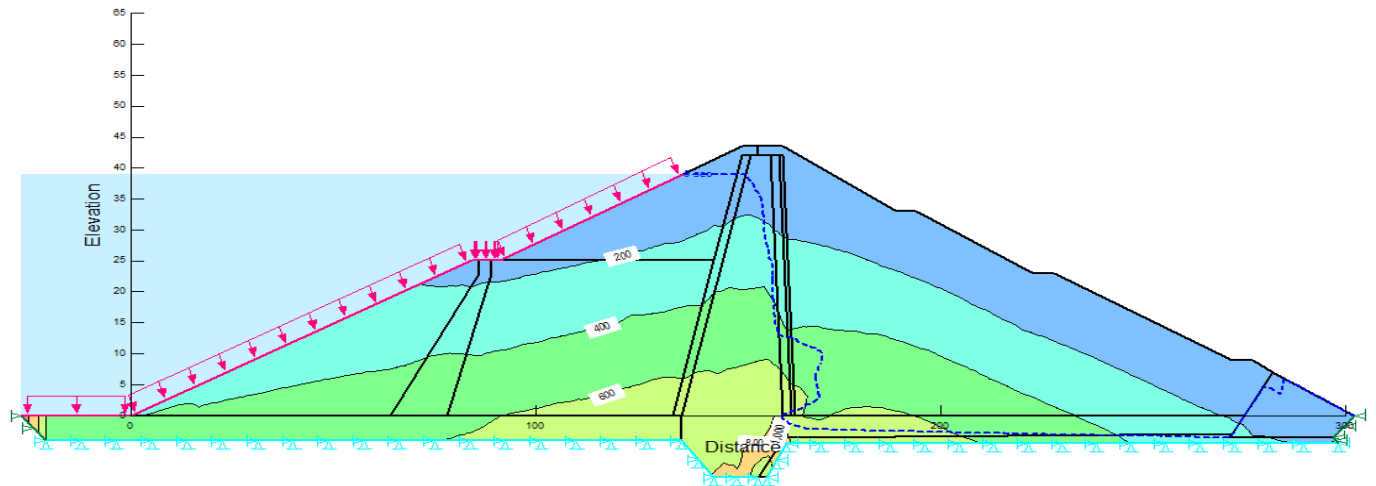


Figure 4.5 Representing insitu fluid-pressure boundary condition the reservoir weight and pore pressure contour

Now that the long-term steady-state and insitu conditions have been established, a couple stress- pore- pressure type of analysis can be completed, which simulates the removal of the reservoir.

Removing the reservoir is like removing a weight from the upstream face of the structure. This can be done with a fluid pressure type of boundary function (Figure 4.6). Recall that the reservoir is being drawdown over a period of 20 days. This is like applying an uplift force which represents the unloading. The uplift force per day is $(18-39)/20 = -1.05$ m /day. Due to the incremental formulation in SIGMA/W, the surface pressure change is the current elevation minus the previous elevation. Since the current elevation is lower than the previous elevation it is a negative fluid pressure, or a negative normal stress.

To simulate the effects two boundary function need to be applied on the upstream face of the dam and the ground surface under the reservoir. These are the stress-strain fluid pressure boundary function and the hydraulic boundary function representing the changing pore-pressures conditions as shown Figure 4.6.

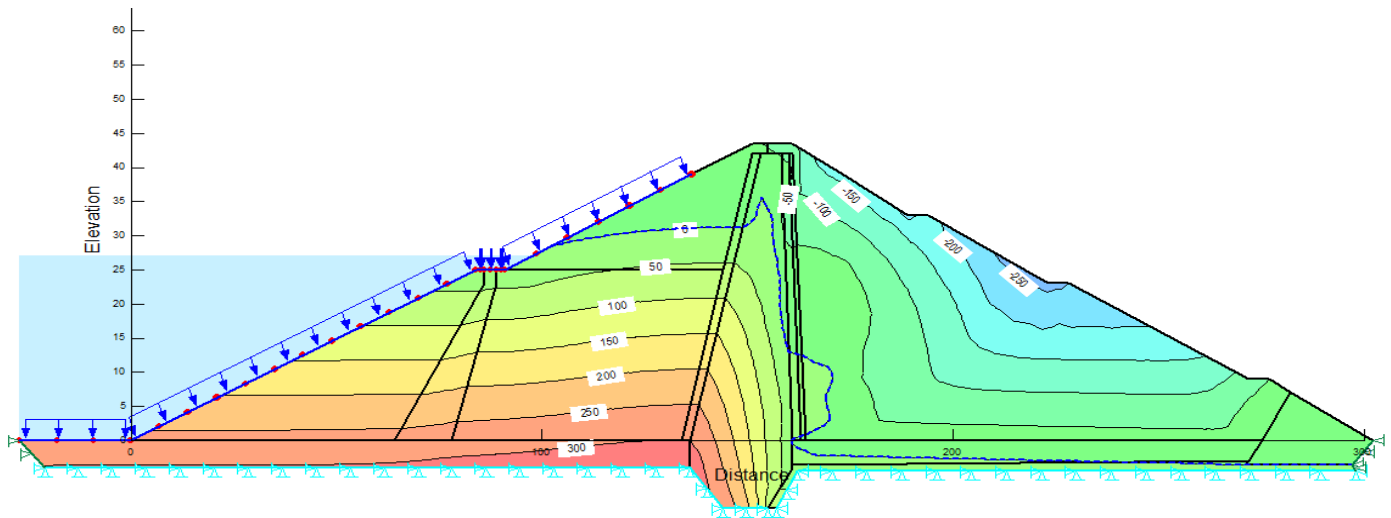


Figure 4.6 Representing Fluid boundary functions, hydraulic boundary function and changing pore-pressures contour after 20 days' drawdown

4.6 Discussions of major results

Leaving apart for the moment the issue of the transition from saturated to unsaturated conditions which takes place during drawdown, there are two fundamental mechanisms controlling the resulting pore water pressure: the change in pore pressure induced by boundary changes in stress and the new flow regime generated. Both of them require a coupled analysis for a proper interpretation and consistency of results. In particular, pure flow models are unable to consider the initial changes in pore pressure associated with stress unloading. The intensity of pore

pressure changes induced by a stress modification is controlled by the soil mechanical constitutive equation. In a simplified situation, under elastic hypothesis for the soil skeleton, the pore pressure depends on the ratio of soil bulk stiffness and water compression modulus. In most situations, this ratio is small and the influence of soil effective stiffness is negligible. This implies a maximum response of the saturated material to stress changes. Without this coupling, the initial pore pressures do not change during fast unloading. Also, permeability and soil stiffness controls coupled flow.

Generally, the resulting behavior of the SEEP/W-alone analysis and a fully coupled SIGMA/W analysis is very similar. The pore-pressures at Point (84, 0) in u/s of the dam analyses are compared in figure 4.7 and 4.8. Initially, The SEEP and SIGMA analyses produce nearly identical pore pressure results. At later times the pore-pressures from the coupled analysis are slightly lower than from the SEEP/W-alone analysis. This is due to the rebound associated with the unloading. The tendency for the volumetric expansion is offset by a greater decrease in the pore-water pressure.

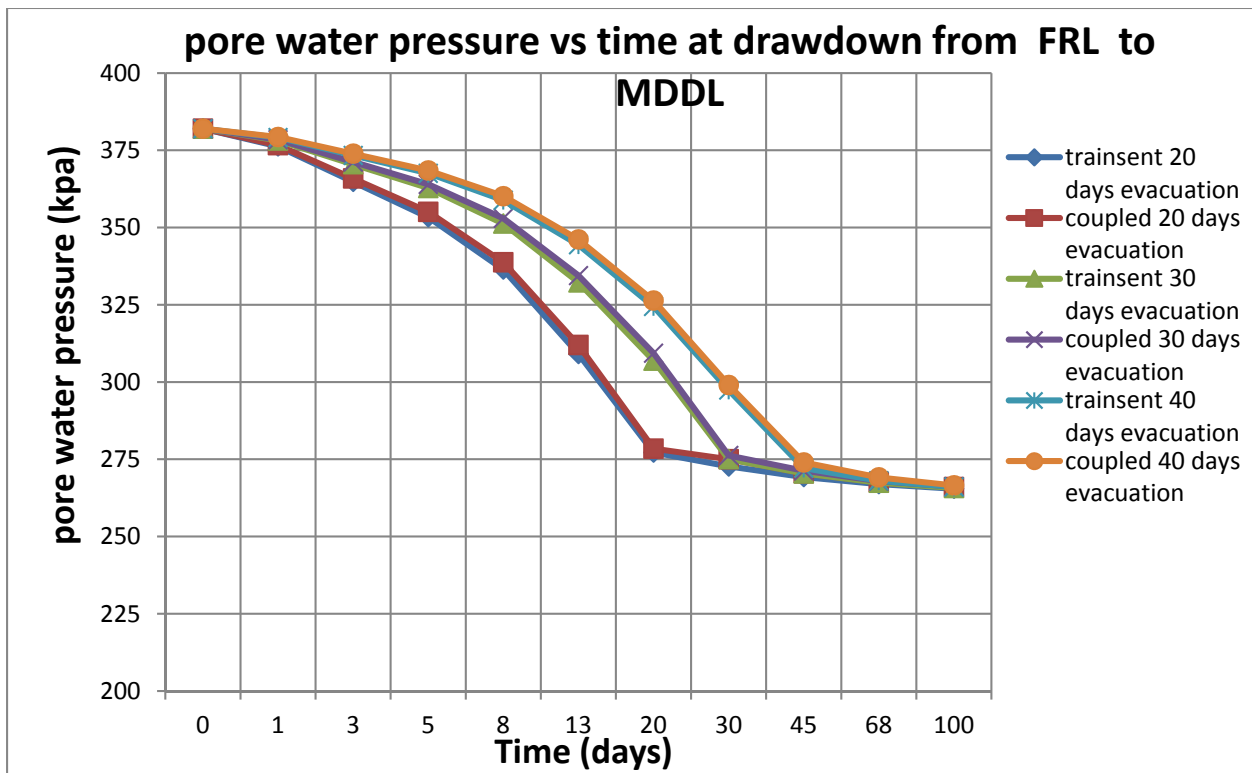


Figure 4.7 Comparison of pore pressures at Point coordinate (84, 0) in u/s from the two types of analyses, various evacuation period and water level fall from FRL to MDDL.

Also, when the reservoir is rapidly evacuated and drawn down, pore water pressures in the dam body are reduced in two ways. There is a slower dissipation of pore pressure due to drainage, and there is an immediate elastic effect due to the removal of the total or partial water load.

Figure 4.7 and 4.8 shows the variation of pore water pressure with time after the start of a drawdown in the reservoir at points (84, 0). It can be seen that the pore water pressure at all points decreases linearly with time.

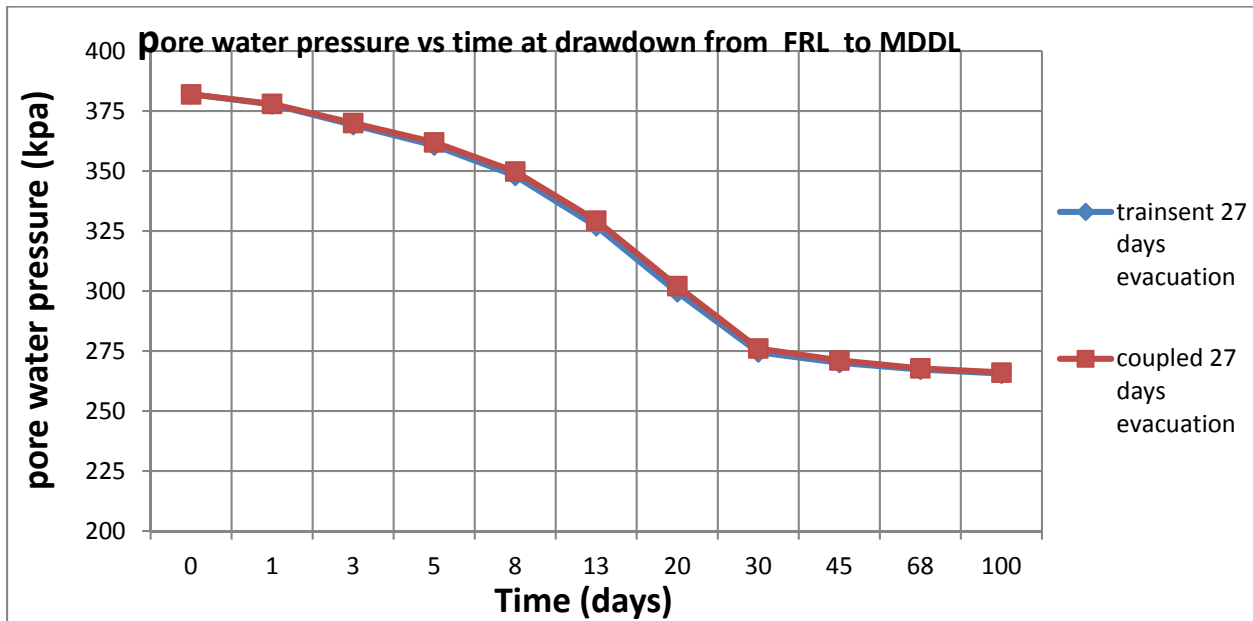


Figure 4.8 Comparison of pore pressures at Point in u/s (84, 0) from the two types of analyses, 27 days' evacuation and water level fall from FRL to MDDL

However, the lower pore-pressure from the coupled analysis is do not reflected direct in the variation in the factors of safety with time and factors of safety computed by limit equilibrium methods is slightly greater than factors of safety computed by finite element methods as shown in Figures 4.9, 4.10, 4.11 below. This indicates that factor of safety in finite element analysis is more influence by unloading effect of reservoir water than pore pressure developed. And also the below graphs show that the value of factor of safety of upstream slope decrease when rapid drawdown condition and seismic load effect.

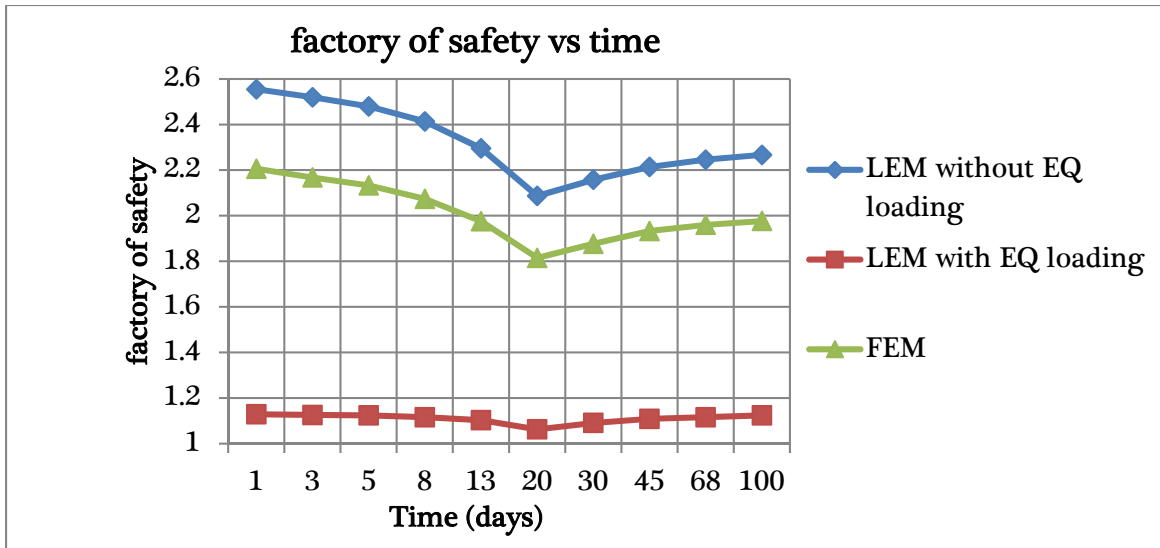


Figure 4.9 Comparison of factors of safety from the three types of analyses, 20 days' evacuation periods and water level fall from FRL to MDDL.

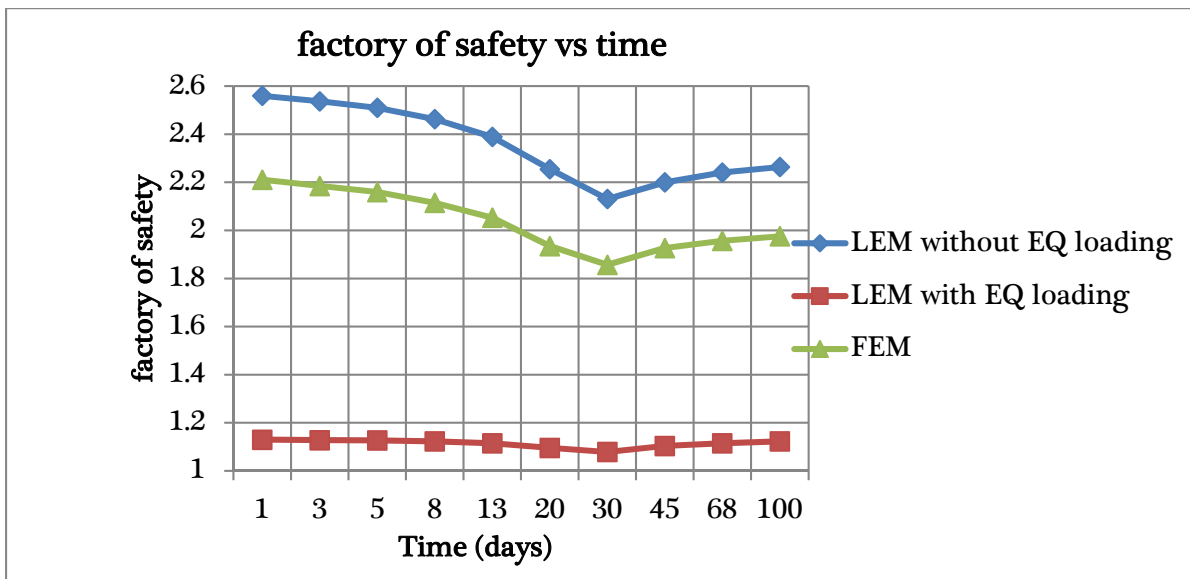


Figure 4.10 Comparison of factors of safety from the three types of analyses, 27 days' evacuation and water level fall from FRL to MDDL

Also, during rapid drawdown the saturated weight of the slope produces the shearing stresses while the shearing resistance is decreased considerably because of the development of the pore water pressures which do not dissipate rapidly.

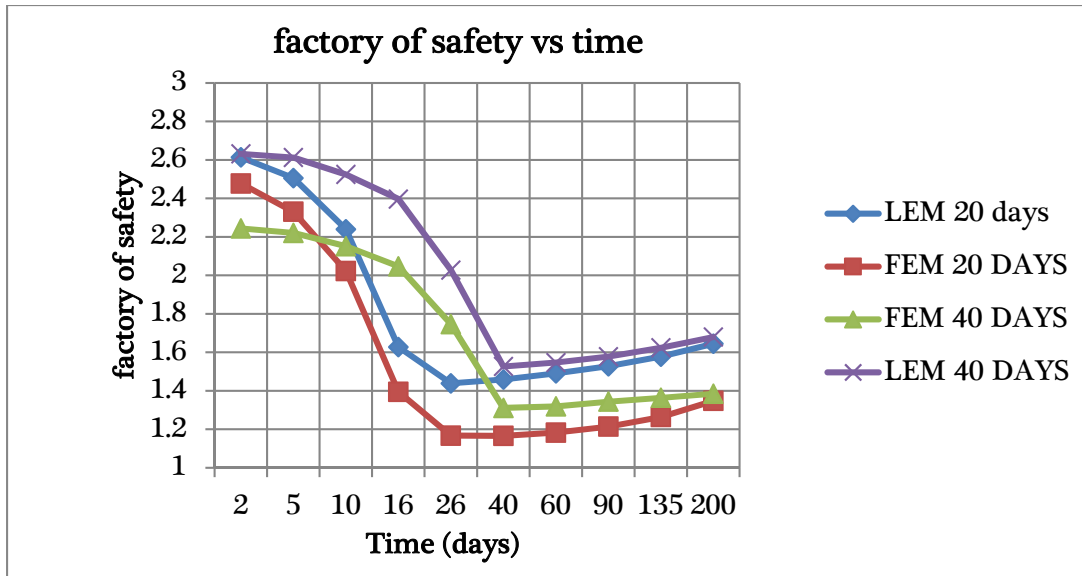


Figure 4.11 Comparison of factors of safety from two types of analyses, three types of evacuation periods constant water level fall from 408m to 387m (21m).

Figure 4.9, 4.10, 4.11, 4.12 show that the value of factor of safety of upstream slope decrease before drawdown period and increases slightly after drawdown period. Since, during rapid drawdown the stabilizing effect of the water on the upstream face is lost, but the pore-water pressures within the embankment may remain high. As a result, the stability of the upstream face of the dam can be much reduced. The dissipation of pore-water pressure in the embankment is largely influenced by the permeability and the storage characteristic of the embankment materials. Highly permeable materials drain quickly during rapid drawdown, but low permeability materials take a long time to drain.

Figure 4.11 traces the variation of the factor of safety with time. It can be noticed that the factor of safety decreases slightly during the first evacuation time after starting of reservoir emptying, then starts to increase rapidly. This is caused by dissipation of excess pore water pressure with time which leads to increase the effective stresses in the soil and hence increase its shear strength.

In tendaho dam case the designer is tried to provided drain materials in upstream slope for dissipation of pore pressure, but in this study result the critical drawdown levels and periods are founded and graphically display in Figure 4.11. Also, Figure 4.11 shows that factor of safety increases as evacuation periods of reservoir stored water increases.

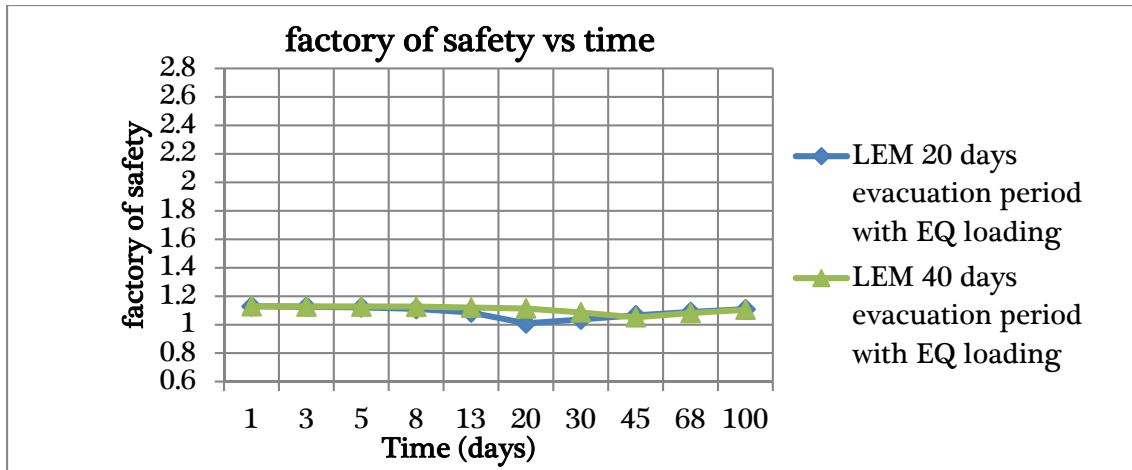


Figure 4.12 Comparison of factors of safety for effect of earthquake is considered, two evacuation periods constant water level fall from 408m to 394m (13m).

The minimum factor of safety tends to occur just before the completion of the reservoir drawdown periods as illustrated in the above Figures.

Seismic load (0.18g) in horizontal direction and (0.09g) in vertical direction is assigned to upstream slope side with drawdown loading condition and from above figure 4.12 indicates that during drawdown of reservoir stored water and earthquake force is assigned to the model the minimum drawdown level is not less than 394m and evacuation period is not less than 40 days. Figure 4.12 shows that the value of factor of safety of upstream decrease when rapid drawdown condition and seismic load effects.

In Table 4.1 below minimum factor of safety of different critical drawdown speed and drawdown level with earthquake loading and without earthquake loading is listed for comparison of methods used for analysis of upstream slope.

In this study the stability of slopes under drawdown conditions are usually analyzed considering two limiting conditions, namely slow and rapid drawdown. In the slow drawdown situation, the water level within the slope is assumed to equalize the reservoir level at any time. In the case of rapid drawdown, which represents the most critical condition, it is assumed that the pore water pressure within the embankment continues to reflect the original water level. The lag of the phreatic line depends on factors such as permeability of soils, drawdown rate and slope gradient.

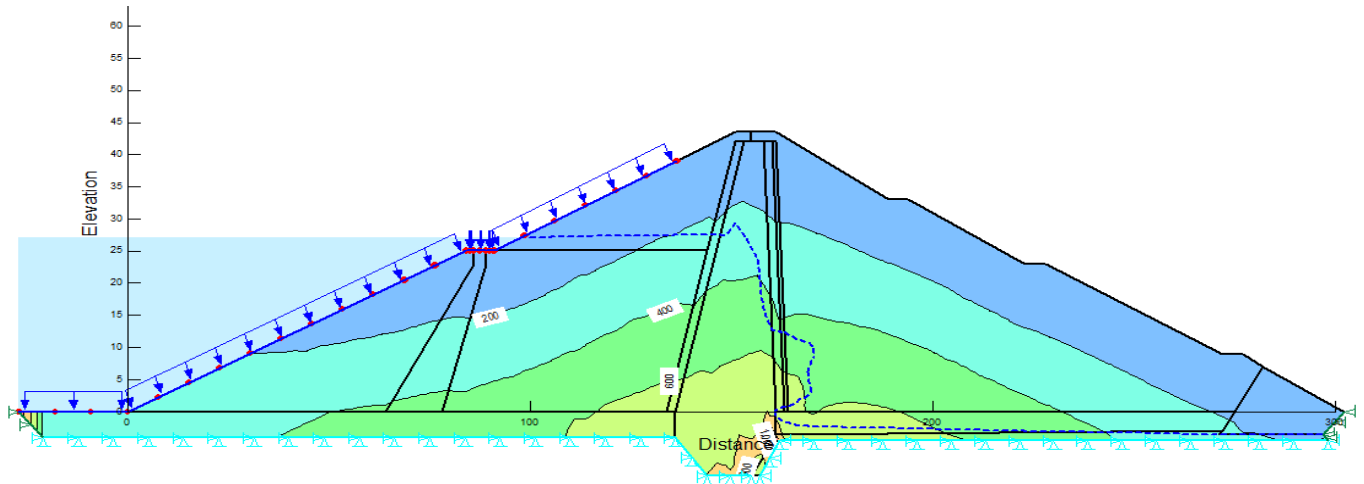


Figure 4.13 Couple analysis capability deformation analysis, represents y-total stress contour variation and seep Conditions after 20 days start of the drawdown

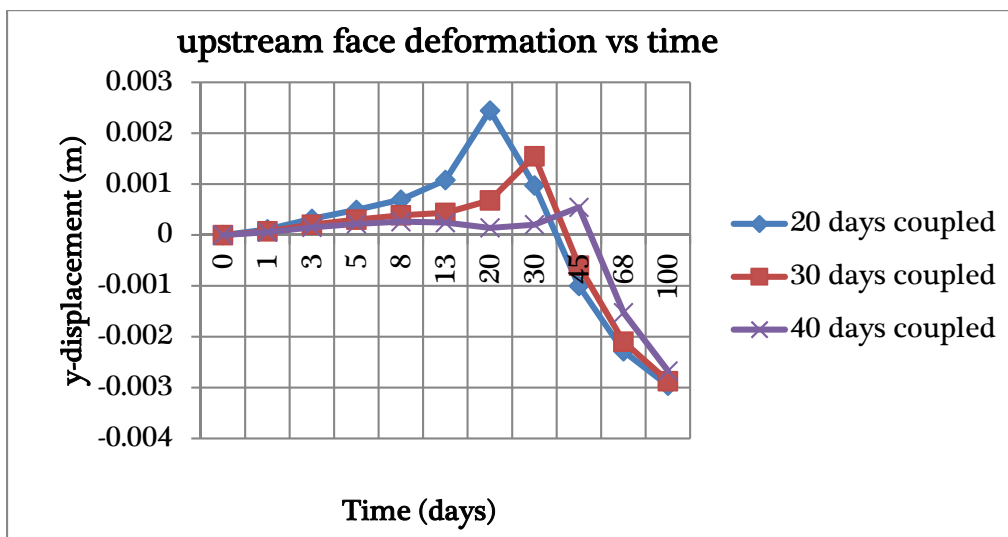


Figure 4.14 Couple analysis capability deformation analysis, at drawdown from FRL to MDDL with various evacuation days

Figure 4.13 and Figure 4.14 demonstrates that using SIGMA/W in coupled analysis have special capability of perform stress and deformation analyses, that is used in serviceability design, Serviceability can tell you how a soil will move towards an unstable state (e.g. going excessively plastic), but it does not tell you, or quantify for you, what that state of instability is. Serviceability deals with obtaining confidence that a design will function as intended.

However, limit equilibrium method is based purely on the principles of statics and says nothing about displacement; it is not always possible to obtain realistic stress distributions. However, Figure 4.14 show that sigma/W coupled analysis capability of deformation analysis and display stress concentration areas.

According to slope/w 2007 manual, soil mass may undergo deformation as a result of changes in external loading called settlement, and/or due to own weight of a compressible soil and changes in drainage conditions called consolidation.

Figure 4.14 results indicate that the deformations at various evacuation periods is in allowable limit and as evacuation period increases deformation decreases due to upstream internal pore pressure loading conditions. The y-displacement up to certain time increases and decreases after certain time due to rebounding and lifting properties of soil under external and internal unloading.

According to Novak et al (2003), the most significant soil deformation usually involves volume changes arising from alterations in the geometric configuration of the soil particles assemblage, e.g. loosely packed arrangement of soil particles will on loading adopt a more compact and denser structure. Such change occurs almost immediately on load application where the soil structure is relatively coarse, as with sands. In saturated clay soils, however, volume changes and settlement due to external loading will take place slowly through complex hydrodynamic process known as consolidation.

The excess pore-pressures may cause some over-stressing which in turn can lead to some permanent deformations. This situation may happen where there is an increase in pore-pressures while the total stress remains constant like in the case of infiltration of water into the ground.

Table 4.1 summary of minimum factor safety at different drawdown level and evacuation periods

Methods of analysis		Factory of safety for different evacuation periods and reservoir water level fall													
		Water fall FRL(408m) to MDDL(396m)					Water fall FRL(408) to 387m				Water fall FRL(408) to 394m				
		Evacuation periods in day					Evacuation periods in day				Evacuation periods in day				
		20	25	27	30	40	20	25	30	40	20	25	30	40	
LEM	Without EQ loading	2.07*	2.14	2.17	2.19	2.21	1.42	1.46	1.48*	1.51	1.92	1.94	1.98	2.02	
	With EQ loading	1.06*	1.08	1.08	1.09	1.1	0.84	0.86	0.86	0.88	1.01*	1.01	1.03	1.05	
FEM		1.82*	1.85	1.88	1.89	1.91	1.26	1.29	1.31*	1.34	1.67	1.69	1.72	1.78	

*critical factor of safety

Table 4.1 It is seen that the derived factors of safety at different drawdown level and evacuation periods are higher than the allowable values, except certain critical points. In addition, Table 4.1 illustrates that factor of safety values is more sensitive to the fall of reservoir water level than evacuation period decrease.

According to WWDSE dam section 3.5: 1 u/s and 2.5: 1 & 2.75: 1 d/s slopes stability analysis under rapid drawdown condition the minimum factor of safety is 1.35. And the idea employed in this analysis is described in the following paragraph.

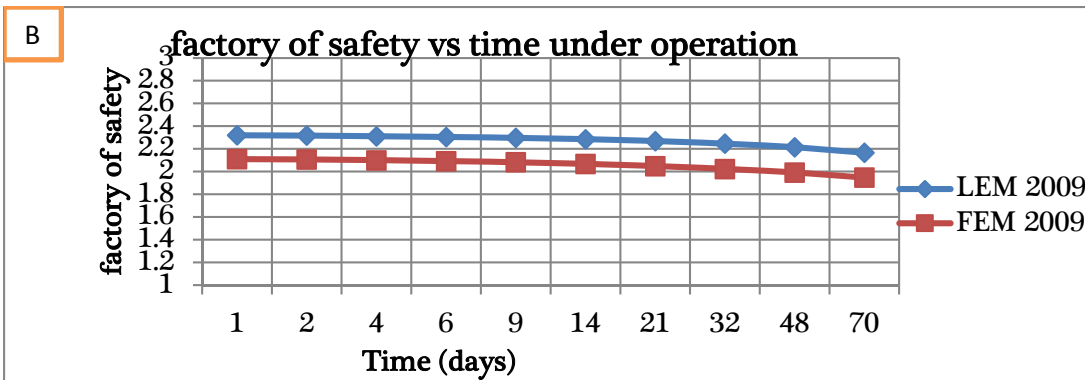
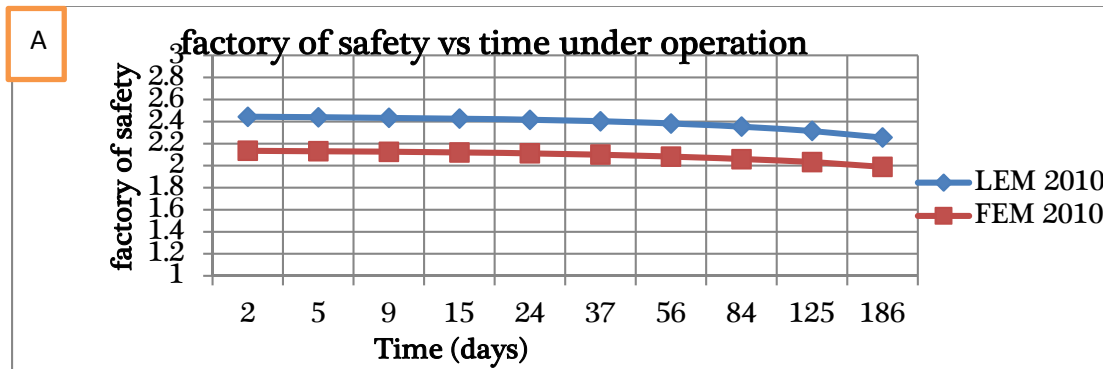
“For the stability of upstream slope under sudden draw down condition the derived factor of safety is dependent upon the rate of reservoir drawdown and the rate of dissipation of pore water pressures. In case of Tendaho Dam, the draw down has been considered to be taking place from FRL to MDDL, by flow passing over spillway and through irrigation outlet. The discharging capacity of irrigation outlet being limited, the draw down below spillway crest level of 400.0 to MDDL of 396.0 m will be slow” (WWDSE, 2007). However, in Table 4.1 minimum factor of safety during reservoir drawdown from FRL to MDDL is 1.88 and 1.72 by using LEM and FEM respectively

The variation of minimum factor of safety between WWDSE and this study is perhaps due to version of GeoStudio employed, methods of data analysis, way of modeling, individual judgements and others criterions.

4.7 Under Operation Drawdown Situation of Tendaho Dam

The drawdown recorded data of Tendaho dam reservoir under operation demonstrates that water level falling takes longer periods and emergency depletion of water level is not required till now as shown in APPEDICES 7E.

Consequently, the upstream slope is safe for all years' reservoir drawdown recorded and the critical drawdown is modeled in GeoStudio's software and Figure 4.15 below shows under operation FoS.



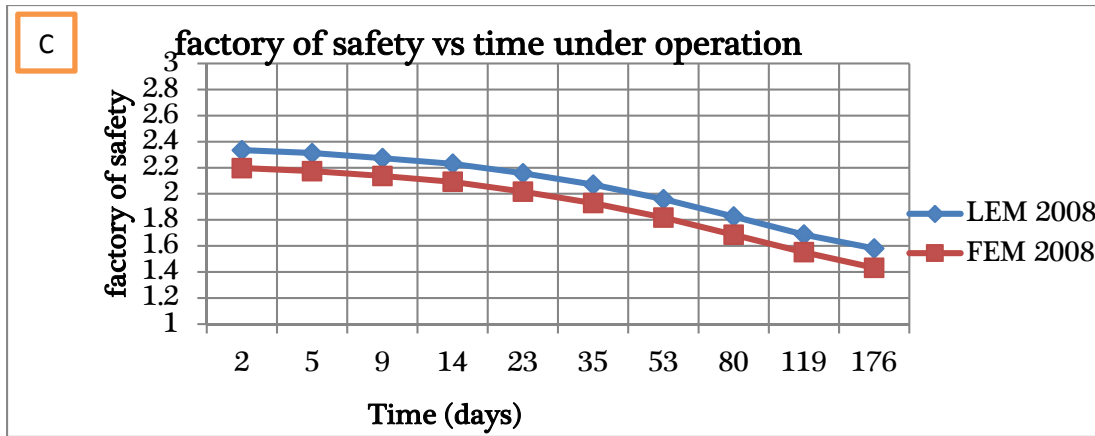


Figure 4.15 Comparison of factors of safety for two types of analyses, drawdown under reservoir operation of A)2010 B)2009 C)2008 E.C years

The critical drawdown condition under operation is analyzed and it indicates that upstream of Tendaho dam is safe and minimum factor of safety is 1.42 it occurs in year of 2008 E.C during reservoir water is dried and inflow of awash river to reservoir is gradually decline.

4.8 Reservoir Evacuation Rating Curve

Reservoir evacuation **rating curve** is a graph of discharge versus reservoir water elevation for a given size of intake and spillway capacity. In all cases of tendaho reservoir evacuation the irrigation intake invert elevation is set at 388m for ease of flow directly from the reservoir using an approach channel and the spillway crest is set at 400m above RBL. Figure 4.17 shows the reservoir elevation-discharge relationship through one 5.0 m diameter tunnel intake and center of intake is set at 391m elevation from bottom bed level. The discharge is calculated under the condition that the entrance provides full tunnel flows for the case that the water depth above the invert is greater than 2.5m. It is assumed also the tunnel discharges freely at the outlet end, USBR (1961), (this assumption could be maintained during reservoir water discharge, otherwise if the outflowing jet is supported, the discharge capacity of the intake tunnel will be reduced).

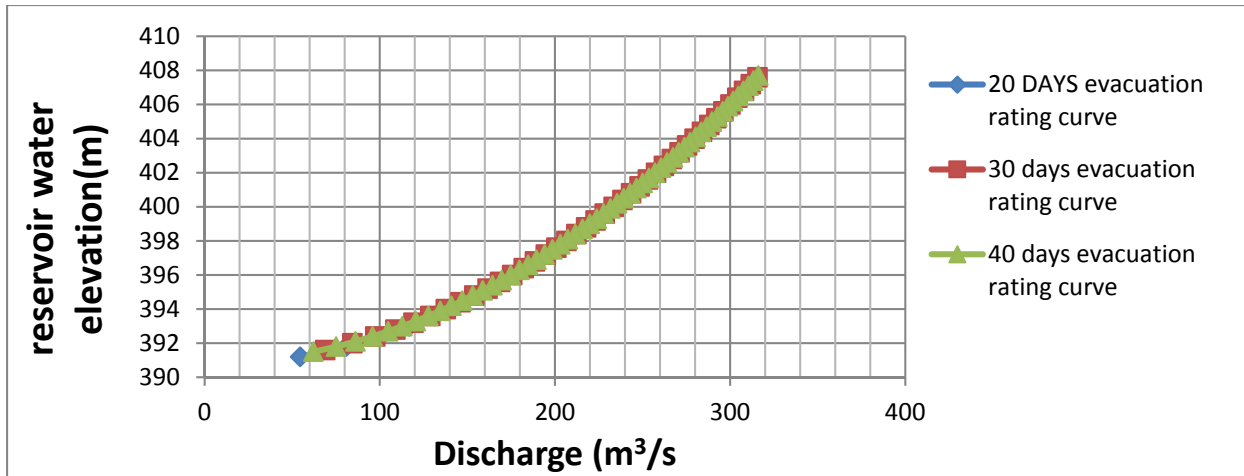


Figure 4.16 Comparison of evacuation rating curve for drawdown from FRL to MDDL.

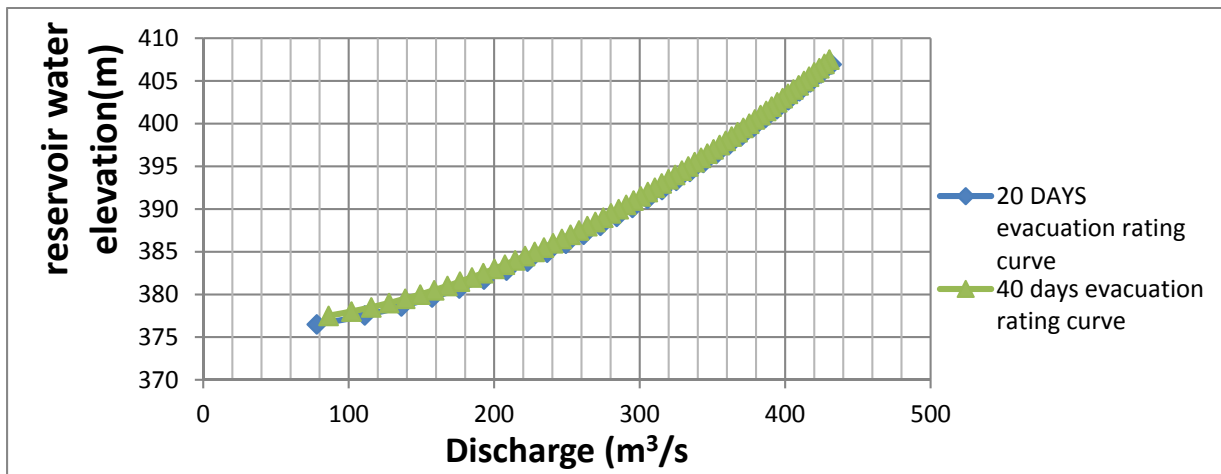


Figure 4.17 Comparison of evacuation rating curve for drawdown from FRL to 387m.

Figure 4.16 and 4.17 indicates that as reservoir water elevation increases the discharge through irrigation outlet and spillway increases. During emergency drawdown the depletion of reservoir up to El 400.0 would be affected by allowing the flow over the spillway crest in addition to the release through Irrigation Outlet. The depletion of reservoir below El 400.0 would be achieved solely by release through the intake structure & irrigation outlet /sluice. Hence, discharge below El 400.0 should be less than or equal to capacity of intake is considered to be adequate for emergency evacuation of reservoir.

5. CONCLUSION AND RECOMMENDATIONS

5.1 Conclusion

Earthen dam slope instability is a major concern for Tendaho earth dam where failures might cause catastrophic destruction on the surrounding area. The failures might be triggered by internal or external factors that cause imbalance to dam material self-weight. An internal triggering factor is the factor that causes failure due to internal changes, such as increasing pore water pressure and or imbalanced forces developed due to external load. In this thesis the effect of drawdown speed with different loading condition was modeled and analyzed in GeoStudio software and critical drawdown level and evacuation periods are demonstrated graphically.

From the result and discussion of the study the following firm conclusions are found for the methods used and critical drawdown level with various evacuation periods.

Pore-water pressures in an initially submerged slope and later subjected to drawdown depend on rate of water level lowering, evacuation periods and boundary conditions. Also, there are two fundamental mechanisms controlling the resulting pore water pressure: the change in pore pressure induced by boundary changes in stress and the new flow regime generated. During different drawdown speed, the pore water pressure at all points within the dam body decreases linearly which indicates that steady state flow takes place.

The stability of the upstream slope for earth dam increasing when storage of reservoir level and evacuation periods increases for both methods employed in the study. The tendaho dam upstream slope may be exposed to the collapse in the case of drawdown of reservoir water level and evacuation periods beyond the critical points indicated in result of this paper.

The analyses presented in this paper show that the minimum drawdown level reservoir water of Tendaho dam is FRL (408m) to 387m within the recommended evacuation periods. The minimum factor of safety at this level is 1.46 and 1.29 by using LEM and FEM, respectively and minimum evacuation period at this level is 20 days.

It is also found that the factor of safety of upstream slope decrease when drawdown condition and seismic load effect and the upstream slope is still stable during different drawdown speed and reservoir water level fall from FRL to MDDL, and the minimum value of FoS obtained is

about 1.012 during 20 days' drawdown period and seismic load coefficient 0.18g horizontal and 0.09 vertical direction. However, during earth quake force was applied to the model the drawdown level and evacuation period is not less than 394m and 40 days, respectively.

From the result of the study FEM analysis seems to be slightly conservative than LEM and consider additionally deformation parameter.

It is concluded that Drawdown situation of tendaho dam under reservoir operation have not affect on upstream slope of the dam and it indicates that emergency depletion of reservoir water is not required till now.

Specifically, the analysis performed in the study is first step towards establish safe operational practices in the Tendaho dam reservoir water level in order to avoid the upstream slope sliding during rapid drawdown condition in the future.

5.2 Recommendations

In order to detect problems before damage occurs monitoring is very important. Hence, it is strongly recommended for preparation of a dam monitoring and surveillance program to monitor the performance of various aspects of the dam visually and using monitoring equipment's and report to the responsible body at least on a monthly basis.

Continuous monitoring of the piezometers in conjunction with reservoir water level and seismic record are considered very essential for further validating the present understanding about the pore water pressure developed in shell and core materials that affects upstream slope stability of tendaho dam.

As design document is referred Tendaho dam drawdown analysis is considered only from FRL to MDDL. But, it doesn't consider the effect of emergence depletion of water level below MDDL. Hence, it is recommended referring critical drawdown level of the study result and working with emergency warning system.

Tendaho dam is located in an area where seismicity is very active. There is also a vulnerability of the dam due to leakage or other hydrological condition such as flooding. For such dam establishing early warning mechanisms to prevent or minimize loss of life to downstream communities and property damages such as farms, factories etc. that may arise due to potential

hazards that faces the dam. Accordingly, detail early warning system coupled with detail surveillance be established in the project area in line with the result of the proposed dam break analysis.

The present study has been conducted under the constraints of time, resources and financial support, therefore the results and the recommendations made through this study must be considered as indicative only. More elaborate systematic studies would be required before coming to any final decisions.

The present study was done by considering earthquake effect pseudo static methods but it is conservative methods. Hence, the later research should be employ dynamic analysis method of earthquake effect in order to get more realistic response and economical dam cross-section.

6. REFERENCES

1. ARORA, K.R. (1996), Irrigation, Water Power and Water Resources Engineering, New Delhi,
2. Ahmad Asnaashari, D. M. (2014). DAM BREACH INUNDATION ANALYSIS USING HEC-RAS AND GIS.
3. Bishop, A.W. and Bjerrum, L. (1960). "The Relevance of the Triaxial Test to the Solution of Stability Problems." Proceedings of the ASCE Research Conference on the Shear Strength of Cohesive Soils, Boulder, CO, 437-501.
4. Bishop, A. W. (1954). "The use of pore-pressure coefficients in practice," Geotechnique, 4(4), 148-152.
5. Bulletin 99, I., 1995. Dam failure statistical analysis. In: Paris: s.n.
6. Casagrande, A., "Seepage Through Dams" Contribution to Soil Mechanics, Boston Society of Civil Engineers, Boston, 1937.
7. Department of the Army, U.S. Army Corps of Engineers, 2003. Washington, DC 20314-1000, "Slope Stability Manual", No. 1110-2-1902.
8. CDA 2014 Annual Conference. Banff, Alberta: CANADIAN DAM ASSOCIATION.
9. D.Nikolovski, Georing MK, Skopje, (2011). "Comparison of constitutive laws for soil materials on earth dams."
10. Duncan, J. M., Byrne, P., Wong, K. S., and Babry, P., (1980)." Strength, Stress-Strain and Bulk Modulus Parameters for Finite Element Analyses of Stresses and Movements in Soil Masses", Report No: UCB/GT/80-01, University of California, Berkeley.
11. (ETCOLD), E. C. O. L. D., 2014. ETHIOPIAN DAM SAFETY GUIDELINE. s.l.: s.n.
12. Fredlund M., Lu H., and Feng T.: Combined Seepage and Slope Stability Analysis of Rapid Drawdown Scenarios for Levee Design, Geo-Frontiers 2011, ASCE, pp. 1595-1604.
13. Fredlund Murray and Feng Tiequn, (2011), "Combined Seepage and Slope Stability Analysis of Rapid Drawdown Scenarios for Levees Design", Soil Vision System Ltd, Saskatoon, 640 Broadway Ave, Suite 202, 57N, SK, Canada
14. GEO-SLOPE International Ltd, Calgary, Alberta, Canada www.geo-slope.com SIGMA/W Example File: Rapid drawdown.doc (pdf) (gsz)
15. Gorden, J. E. (1978). Structures or Why Things do not Fall Down. Penguin Books.

16. Höeg, K. (1993). Asphaltic concrete cores for embankment dams, Stikka Press, Oslo, Norway.
17. Hadush and Messele H., (2010) “earthquake induced liquefaction analysis of tendaho earth-fill dam”, Journal of EEA, Vol. 27, 2010
18. ICOLD (1995). “Dam failure statistical analysis.” Bulletin 99, ICOLD, Paris. 1974, 83, 98
19. Jean-Louis Briaud. (2013) Geotechnical Engineering: Unsaturated and Saturated Soils Published by John Wiley & Sons, Inc., Hoboken, New Jersey Published simultaneously in Canada
20. Lambe, T. and Whitman, R. (1969). Soil Mechanics. New York: John Wiley and Sons Inc.
21. Mohammed Y. and Hasan A. (2017) “Flow and stability of Al-Wand earth dam during rapid drawdown of water in reservoir” Acta Montanistica Slovaca Volume 22 (2017), number 1, 43-57.
22. Morgenstern, N., & Price, V. (1965). The Analysis of the Stability of General Slip Surfaces. Geotechnique, Vol. 15 (No. 1), pp. 77-93.
23. Murthy, G. S. R., Murty, K. G., Raghupathy, G.: Designing of Earth Dams Optimally, 40th Anniversary Volume of IAPQR Transactions, 2013, pp. 91-126.
24. Negede, Abate Kassa (2009). “Probabilistic Safety Analysis of Dams (tendaho dam).” Doctor of Engineering (Dr.-Ing.). Dissertation, Technische University Dresden, Germany, The Germany.
25. Novak, P. , Moffat, A. I. B., Nalluri, C. and Narayanan, R. (2003). “Hydraulic structures.” Taylor and Francies Group, London.
26. Saleh I. Khassaf, (2013) “Slope Stability Analysis under Rapid Drawdown Condition and Seismic Loads of Earth Dam”, International Journal of Innovative Research in Science, Engineering and Technology (An ISO 3297: 2007 Certified Organization) Vol. 2, Issue 12, December 2013, ISSN: 2319-8753
27. SLOPE/W, 2007. Stability modeling with SLOPE/W 2007 Version. s.l.:Geo-Slope international ltd,.
28. Small Dam, D., 2011. SMALL DAMS Design, Surveillance and Rehabilitation. s.l.:s.n
29. Spencer, E. 1967. A Method of Analysis of Embankments assuming Parallel Interslice Forces. Geotechnique, Vol 17 (1), pp. 11-26.

30. Tran X. Tho, (2008) “Stability Problems of an Earth Fill Dam in Rapid Drawdown Condition”, Grant Project, No.1/9066/02
31. USBR, 2001. US Bureau of Reclamation, Embankment dams static stability analysis, DS-13(4)-6, 2011.
32. Water Works Design and Supervision Enterprise in Association with Water and Power Consultancy Services Ltd (2007), “Tendaho Dam and Irrigation Project”, Final Main Design Report, Addis Ababa
33. WWDSE (Ethiopian Water Works Design and Supervision Enterprise) (2005). “Geology of Tendaho Dam.”, WWDSE, Addis Ababa.
34. WWDSE (2005a). “Hydrology of Tendaho Dam.”, WWDSE, Addis Ababa.
35. WWDSE (2005b). “Dam and appurtenant works tendaho dam.” WWDSE, Addis Ababa.
36. Zomorodian, A., Abodollahzadeh, S. M.: Effect of Horizontal Drains on Upstream Slope Stability during Rapid Drawdown Condition, International Journal of Geology, 2010, Issue 4, Volume 4, pp. 85

7. APPENDICES

A. Tendaho Dam main features

1. Important elevations and lengths:

✚ Crest length	412m
✚ Crest width	10m
✚ Dam height above deepest foundation	54.5 m
✚ Dam height from toe	47 m
✚ Volume of fill material	$1.37 \cdot 10^6$
✚ Reservoir capacity	$1.86 \cdot 10^9$
✚ Water surface area at FRL	1,700 km ²
✚ Top of parapet wall elevation	413.5 m a.m.s.l
✚ Dam crest elevation	412 m a.m.s.l
✚ Core crest elevation	411 m a.m.s.l
✚ Maximum water level (MWL)	410.4 m a.m.s.l
✚ Maximum retention level (FRL)	408 m a.m.s.l
✚ Minimum drawdown level (MDDL)	396 m a.m.s.l
✚ River bed level (OGL)	369 m a.m.s.l
✚ Dam toe elevation	365 m a.m.s.l (after stripping 4m from OGL)
✚ Core bottom elevation	359 m a.m.s.l
✚ Spillway crest level	400 m a.m.s.l
✚ Irrigation intake centerline elevation	391 m a.m.s.l
✚ Upstream slope	3.5:1
✚ Downstream slope	2.5:1 and 2.75:1

Table 7.1: Dam component elevations in relative terms from dam toe elevation (WWDSE,2005).

Dam component	absolute elevation (m)	relative elevation (m) a.m.s.l
Wave wall (parapet wall)	412.5	47.5
Dam crest	412	47
Core crest	411	46
MWL	410.4	45.4
FRL	408	43
MDDL	396	31
OGL	369	4
Dam toe	365	0
Core bottom elevation	359	-6

2. Spillway information:

✚ Crest length	37.5 m
✚ Type	Ogee type
✚ Crest level	400 a.m .s.l
✚ Design discharge	1900 m ³ /s

3. Diversion Tunnel:

✚ Design discharge	331 m ³ /s
✚ Tunnel length	247.36 m
✚ Tunnel diameter-	6 m
✚ Approach channel length	320.44 m
✚ Out let channel length	357.04 m

4. Intake tower

✚ Discharging capacity	78m ³ /s
✚ Irrigation command area	60,000 ha (600 km ²)
✚ Irrigation outlet diameter	6.0 m
✚ centerline elevation	391 m a.m.s.l

5. Main canal

✚ Length	65.0 km
✚ Discharging capacity	78.0 m ³ /s
✚ Bed width	22. 65 m
✚ Water depth	2.55 m

6. Sugar factory

✚ Factory capacity	26,000 tones cane per day
✚ Sugar cane production	7.02 x10 ⁶ tones per year
✚ Max. period of operation per year	270 days

3. Selected Tendaho dam core and shell material properties (Negede, A., Dissertation,2009)

Quarry location	Dam zone	grain size distribution			shear strength		MDD (gm/cm ³)	OMC (%)	Permeability (cm/s)
		Gravel (%)	Sand (%)	Fines (%)	c'(kN/m)	φ'(degrees)			
Area1	shell		1.2	98.8					
Area1	shell	40.7-42.2	55.06-58.4	0.4-2.6					
Area1	shell	75.1	23.6	1.3			1.33		5.21E-03
Area1	shell	9.7	90.1	0.2			1.77		
Area1	shell		97.7	2.3					
Area1	shell	64	31.4	4.6	4	44			3.16E-03
Area1	shell	47.7	52.3		12	41			2.30E-03
Area1	shell	56.1	43.9		4	44			4.60E-03
Area1	shell	62	37	1					
Area1	shell	57	42	1	3	35	1.832	21.25	1.28E-02
Area3	shell		99.8	0.2	19	38			
Area3	shell	27	73		5	46			2.30E-02
Area3	shell	31.3	68.7		14	45			9.50E-03
Area3	shell	37.6	62.4		8	44			1.50E-03
Area3	shell	51.1	48.9		2	48			2.80E-03
Area3	shell	1.7	98.1	0.2					
Area3	shell	18.2	81.5	0.3	12	40			
Area3	shell	35.6	64.4						
Area3	shell				2.5	42			1.01E-03
Area3	shell				4	42			6.31E-02
Area7	shell	41.4	58.6				2.31		
Area7	shell	42.8	55.6	1.8			2.26		
Area7	shell	45.8	53.1	1.1			1.9		
Area7	shell	41.9	56.9	1.2			2		
Area7	shell	51.1	45.1	3.8					
Area7	shell	46.3	53.1	0.6					
Area7	shell				17	40			
Area7	shell				12.4	42			
Area7	shell				16	40	2.087	3	
Area7	shell	70	29	1	4	41	2.168	10.5	4.29E-03
Area7	shell	25	68	7			2.27	8	1.06E-02
Area11	shell	49	51		18	40			
Area11	shell	45.7	54.3		31	40			
Area11	shell	64.5	35.5		4	43	1.33	30.79	5.92E-04

Area11	shell	42.7	57.3		2	45	1.77	15.29	2.84E-03
Area11	shell	69.4	30.6		4	45	1.78	14.25	5.54E-03
Area11	shell	50.1	49.9		5	46	2.255	7.25	4.09E-03
Area11+11A	shell	65	30	5	6	38	1.934	7	3.18E-03
Area 11	shell	0	0.85	99.15					
Area 11A	shell	36.19	59.77	4.04					
Area 2	core		2.3	97.7					
Area 2	core		1	99			1.4	30.43	3.70E-09
Area 2	core		17	83	37	35	1.53	22.25	1.07E-05
Area 2	core		1.1	98.9	2	21	1.25	31.5	1.45E-05
Area 2	core	14	85.5	0.5	66	21			1.50E-05
Area 5	core		33.6	66.4	24	20			
Area 5	core		27.2	72.8	11	18	1.7	19.3	3.7E-09
Area 5	core		14.4	85.6	33	15	1.82	12.4	
Area 5	core		4	96	64	31	1.43	25.25	
Area 5	core		9	91	64	18	1.38	33	3.9E-09
Area 5	core		3.6	96.4	64	31	1.43	28.5	1.44E-06
Area 5 (blended)	core		3	97	4	33	1.623	15.18	4.18E-06
Area 5	core	5			6	31	1.537	23.63	1.37E-06
Area 5	core				95	17	1.757	18	1.23E-06
Area 5	core	18	20	62	20	19	1.72	18.3	2.20E-08
Area 6	core	1.4	94.5	4.1					
Area 6	core		93.4	6.6			1.83	16.4	2.48E-08
Area 6	core		59	41	32	30			1.07E-07
Area 9	core		4.3	95.7			1.4	34	2.33E-09
Area 9	core		2.9	97.1	26	4			
Area 9	core		12.1	87.9	21	28.6	1.4	29.6	1.45E-07
Area 9	core		10.3	89.7			1.49	27.5	
Area 9	core		6.6	93.4			1.35	33.5	1.23E-08

**C. Tendaho Dam elevation storage-area relationship at year 0, 25 and 50
(WWDSE hydrology report, 2005a)**

Water surface elevation (m a.m.s.l)	Year zero years (10^6 m ³)	After 25 years (10^6 m ³)	After 50 years (10^6 m ³)
384	21	0.0	0
390	125	28.8	0
391	149	36.5	0
392	186	55.1	0
393	237	87.5	1.9
394	297	126.8	9.1
395	366	174.3	22.4
396	444	228.7	41.1
397	528	288.7	63.4
398	617	353.4	88.7
399	713	422.4	116.8
400	815	497.5	149.4
401	924	578.9	187.1
402	1040	665.8	229.1
403	1161	758.3	276
404	1289	856.8	328.3
405	1422	959.8	385.4
406	1561	1070.1	450.7
407	1708	1190.2	528.7
408	1860	1329.6	604.9
409	2017	1464	642
410	2181	1600	717
411	2351	1742	795
412	2528	1891	877

D. GeoStudio different scenarios analysis outputs

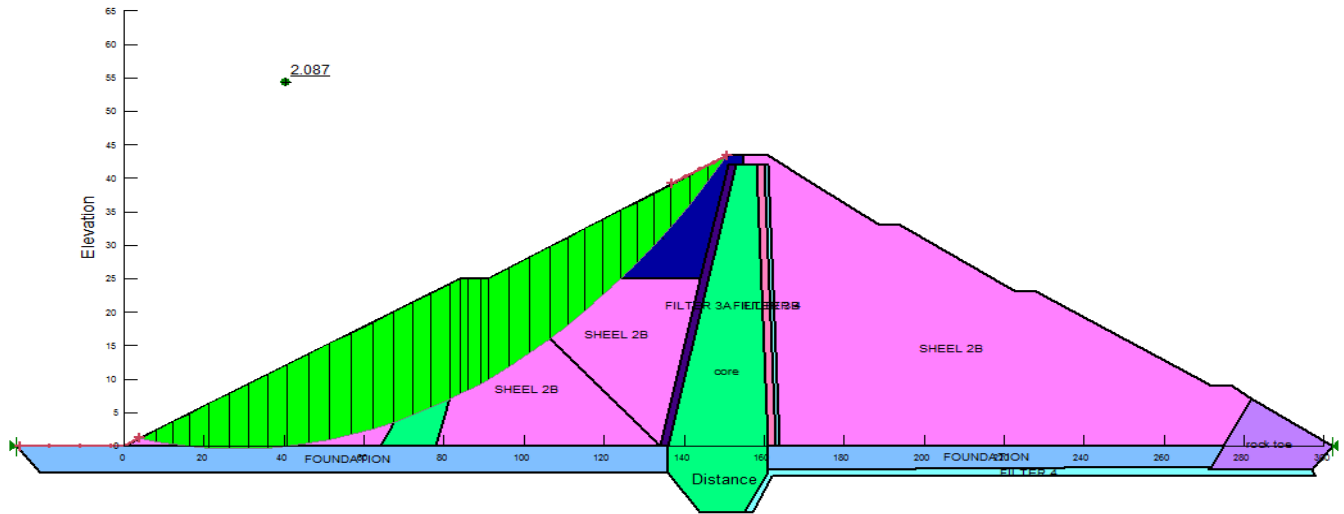
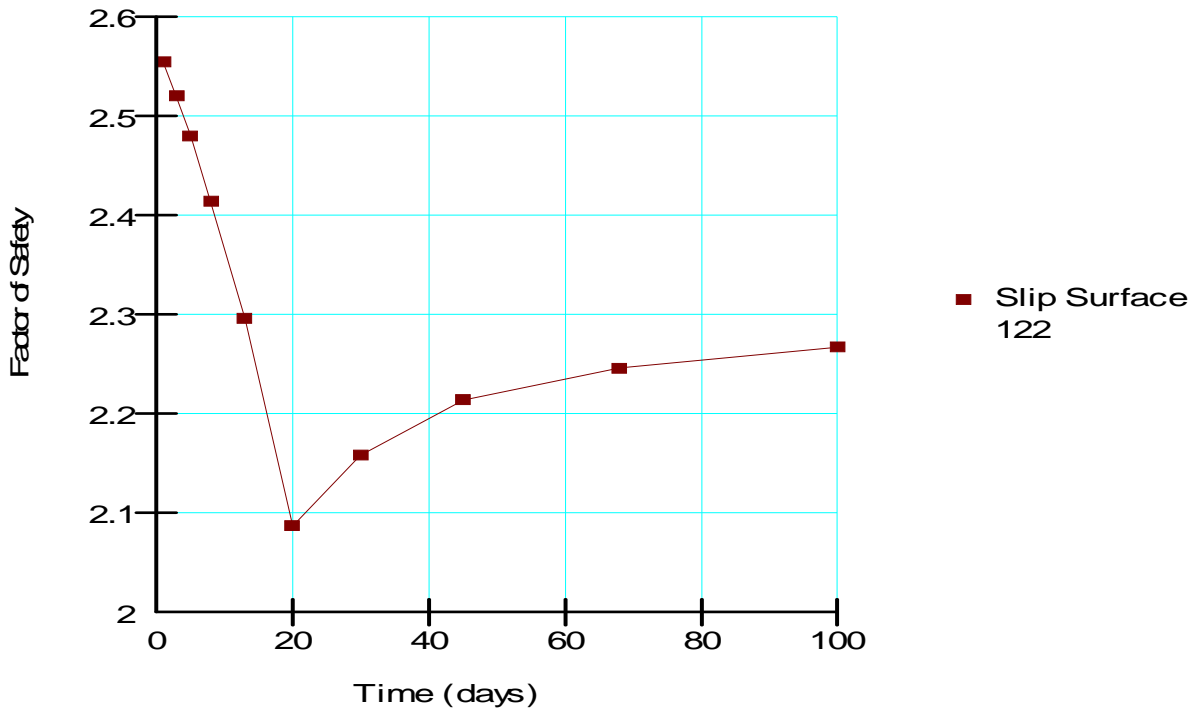


Figure 7.1 Minimum factor of safety for LEM Without EQ loading condition, 20 days' evacuation periods and water level fall from FRL to MDDL

Factor of Safety vs Time



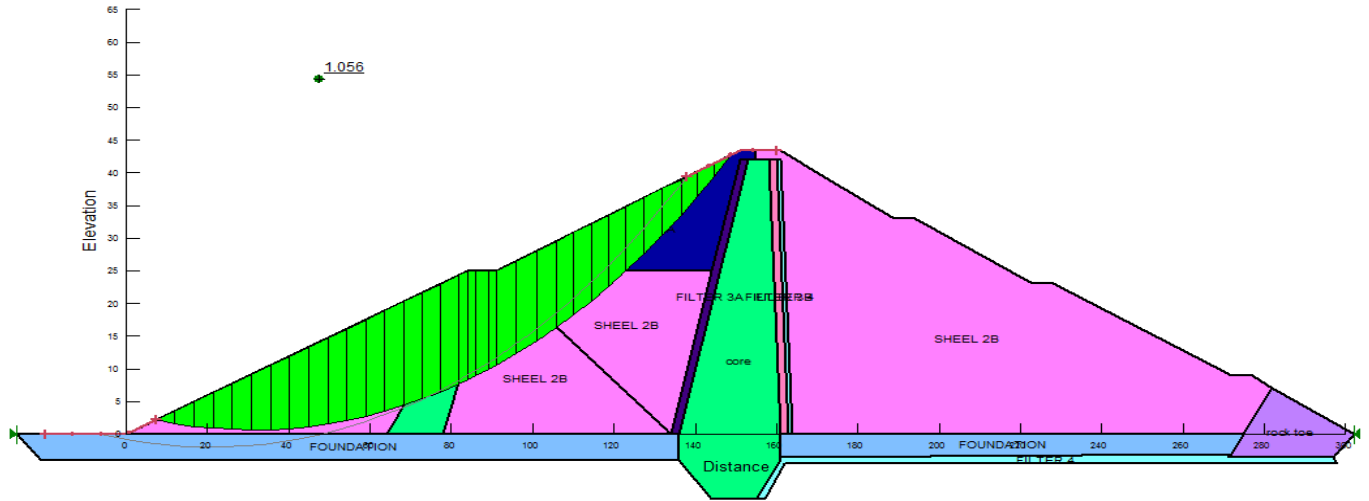
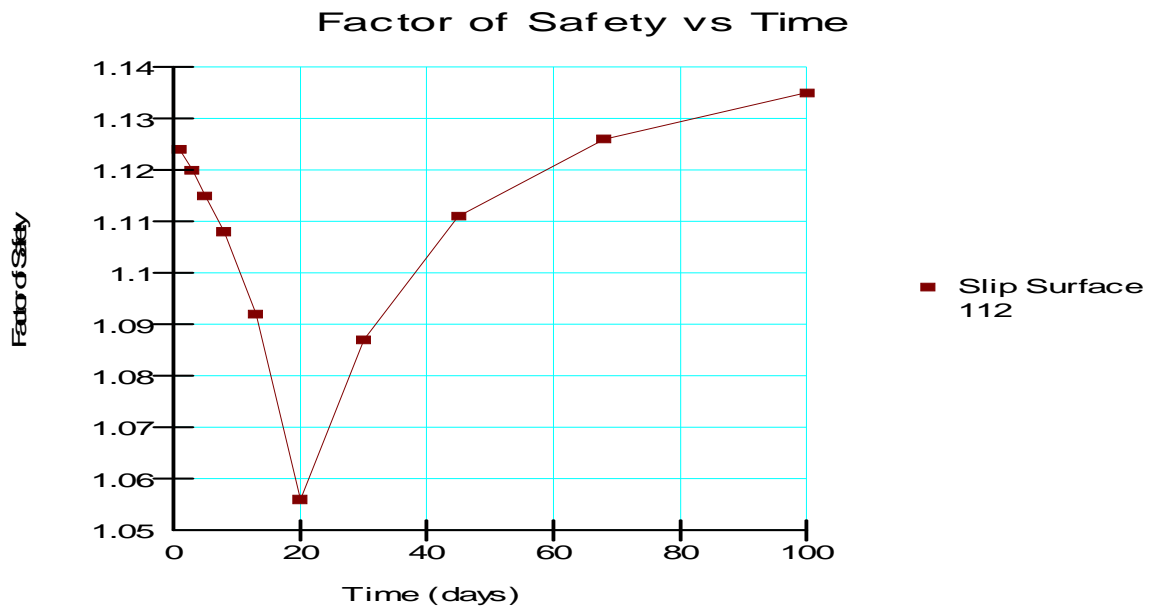


Figure 7.2 Minimum factor of safety for LEM with EQ loading condition, 20 days' evacuation periods and water level fall from FRL to MDDL



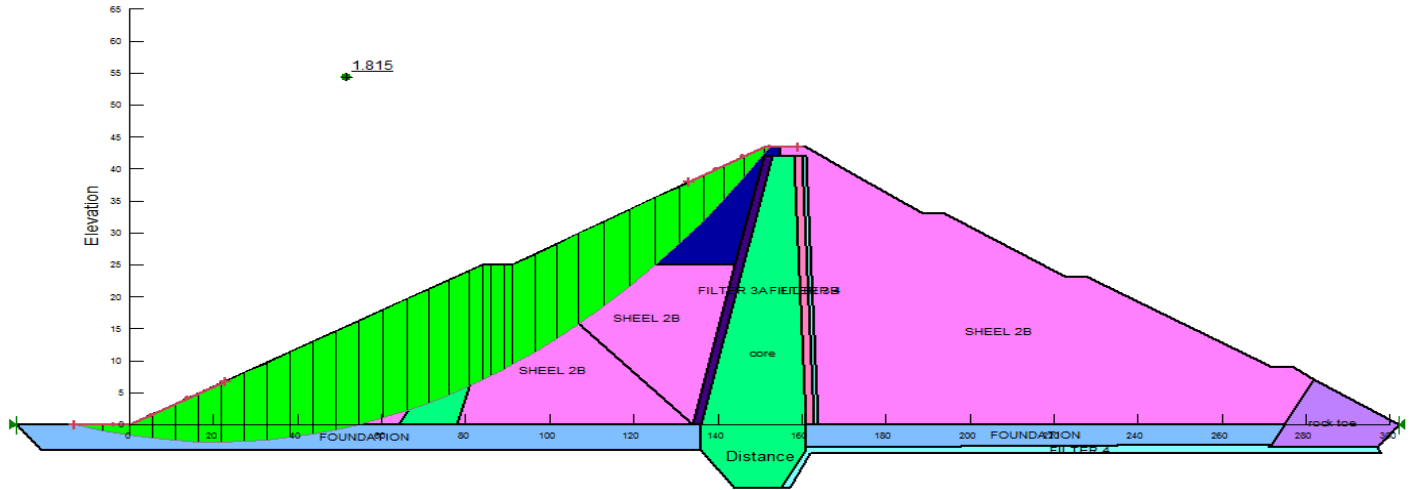
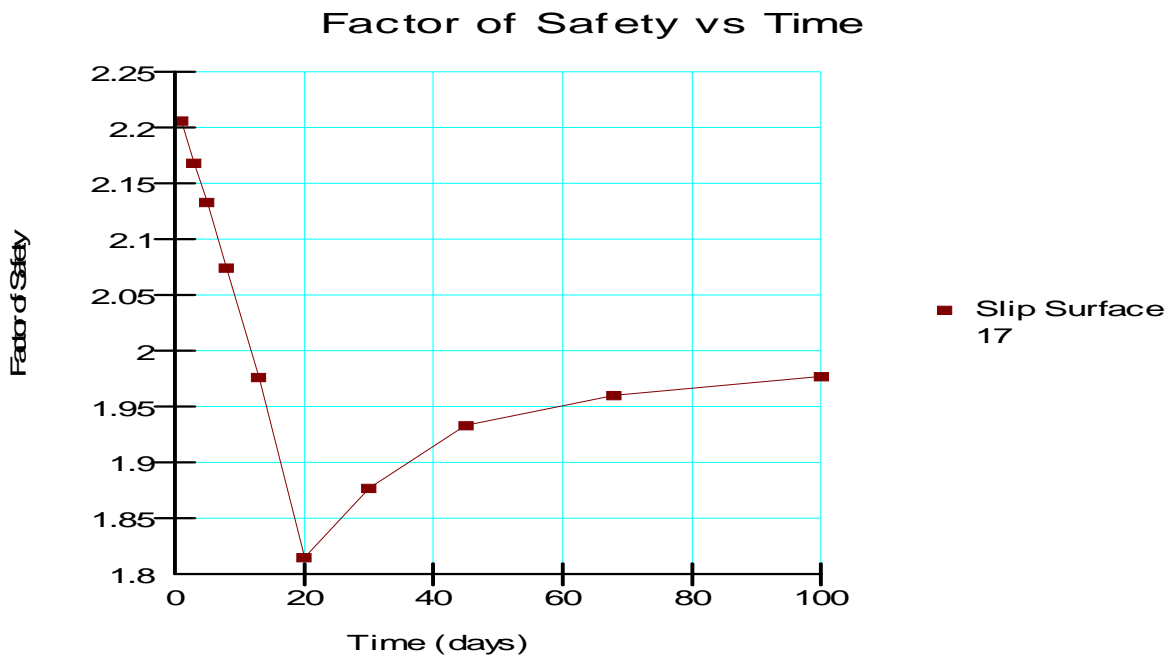


Figure 7.3 Minimum factor of safety for FEM, 20 days' evacuation periods and water level fall from FRL to MDDL



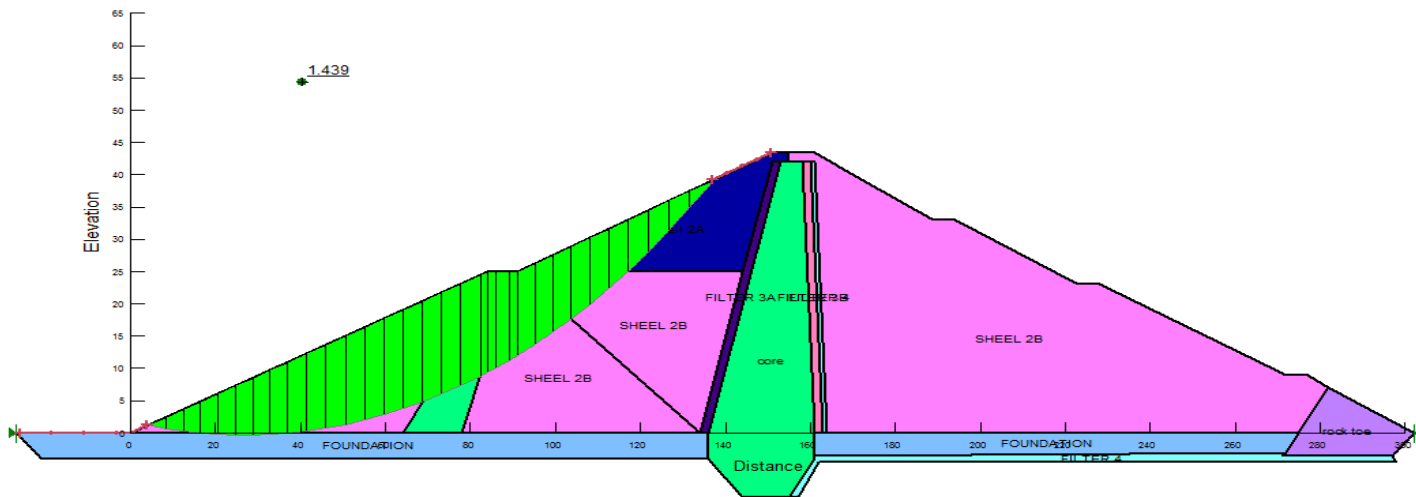
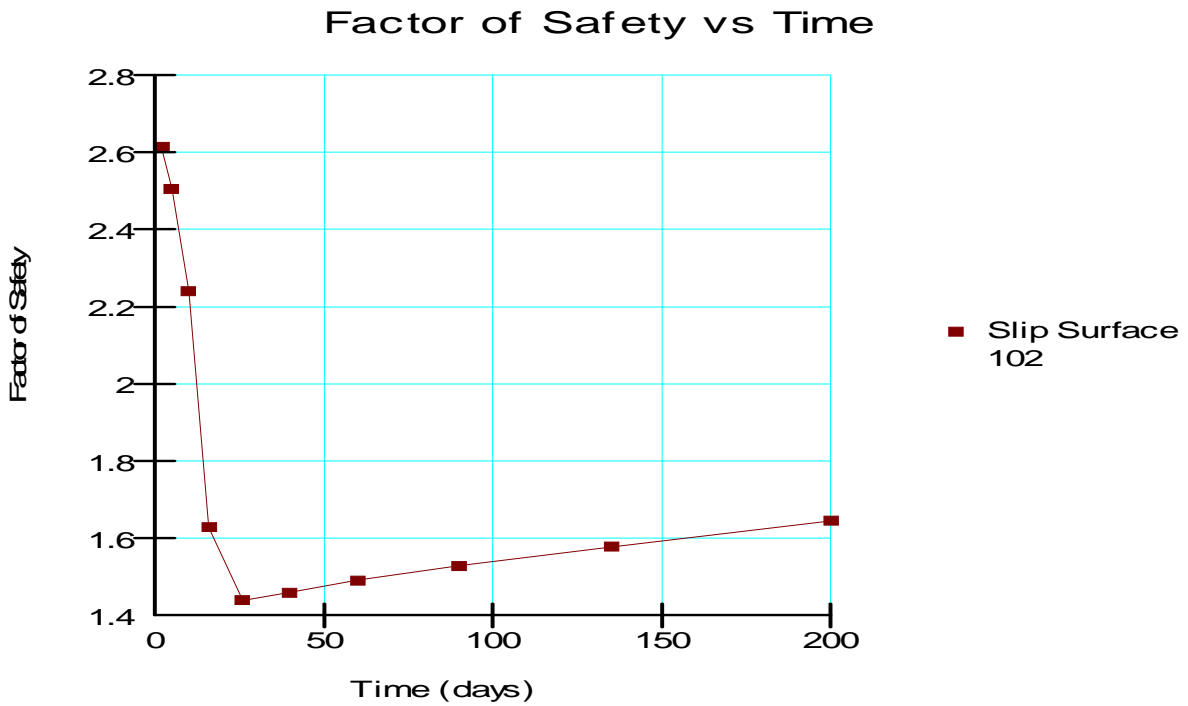


Figure 7.7 Minimum stability conditions for 20 DAYS LEM and water level fall from FRL to 387m elevation



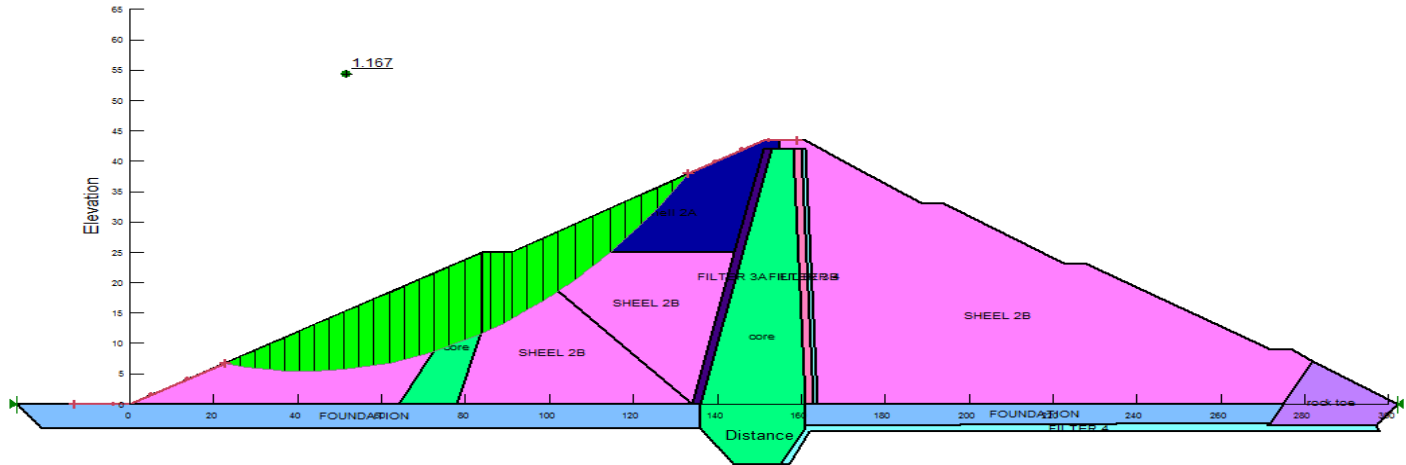
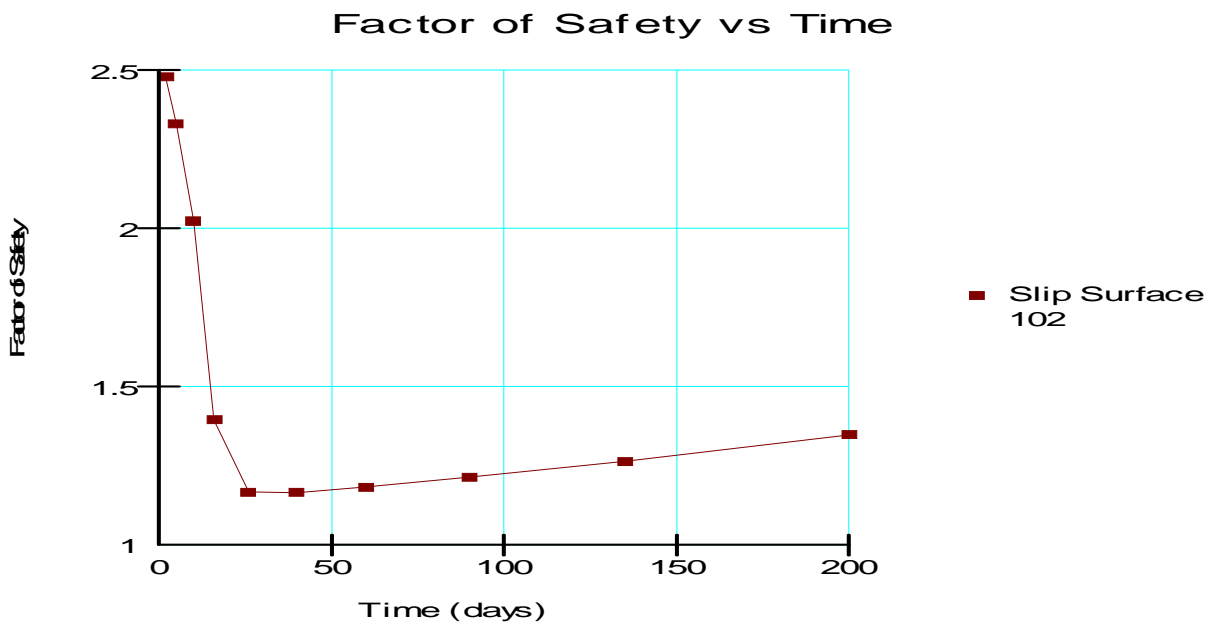


Figure 7.8 Minimum stability conditions for 20 DAYS FEM and water level fall from FRL to 387m elevation



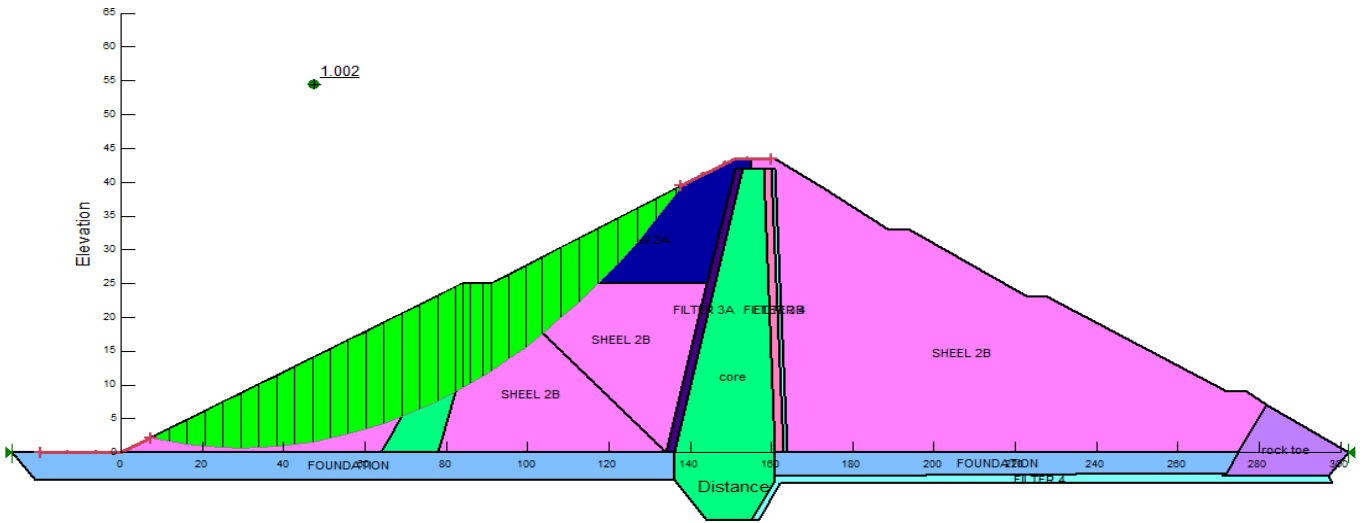
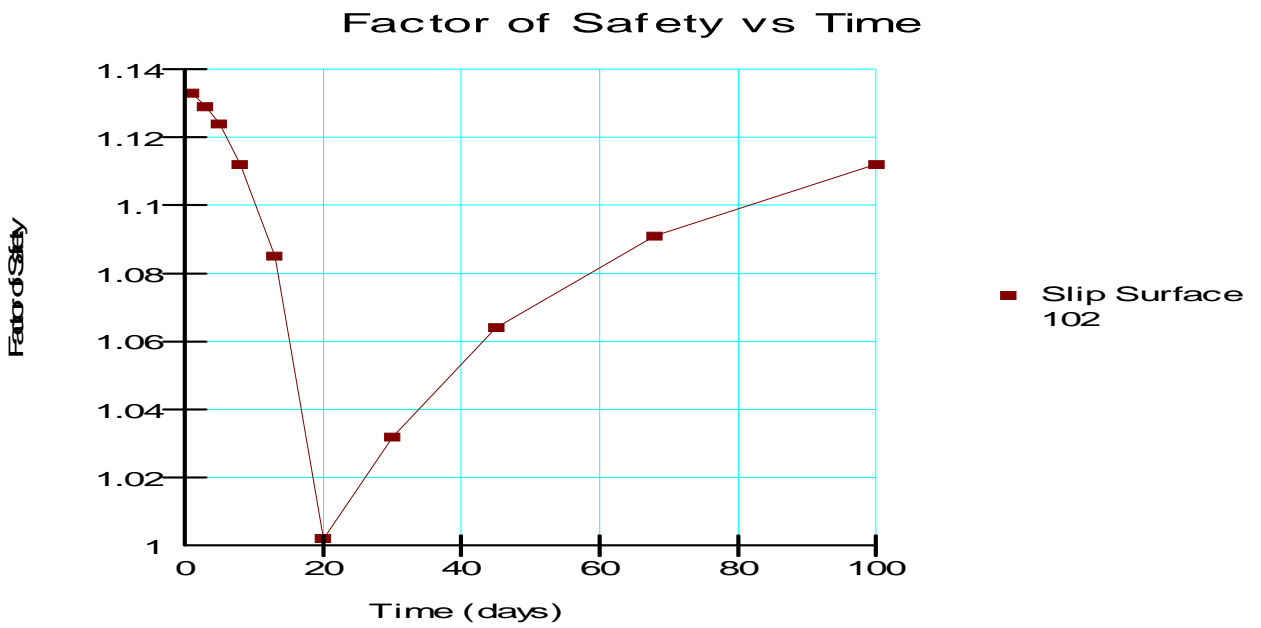


Figure 7.13 Minimum stability conditions for 20 DAYS LEM with EQ loading condition and water level fall from FRL to 394m water level.



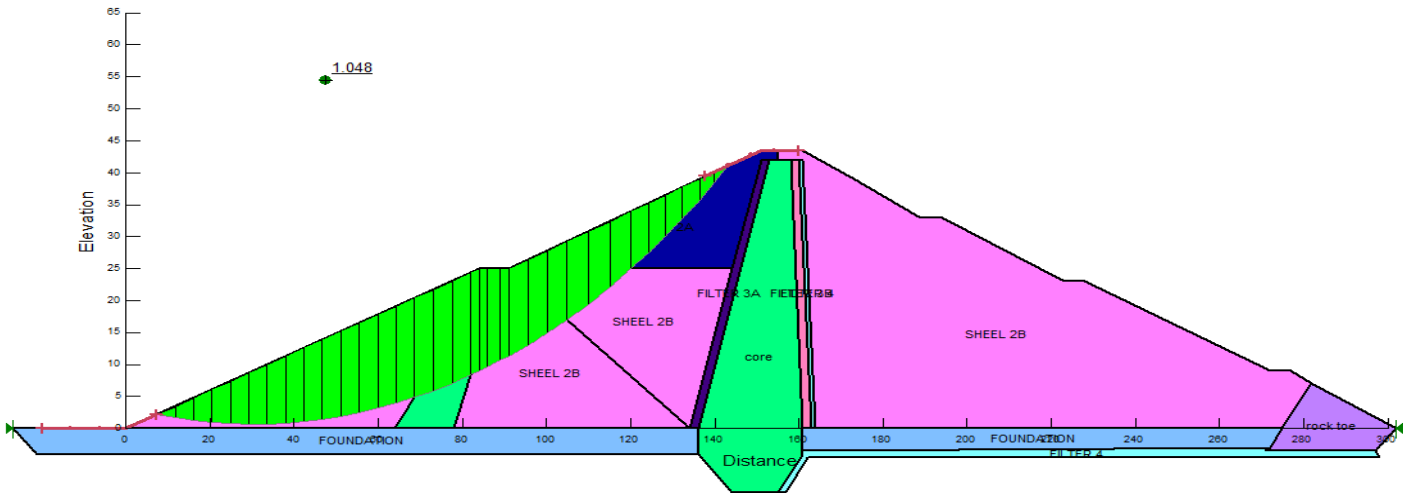
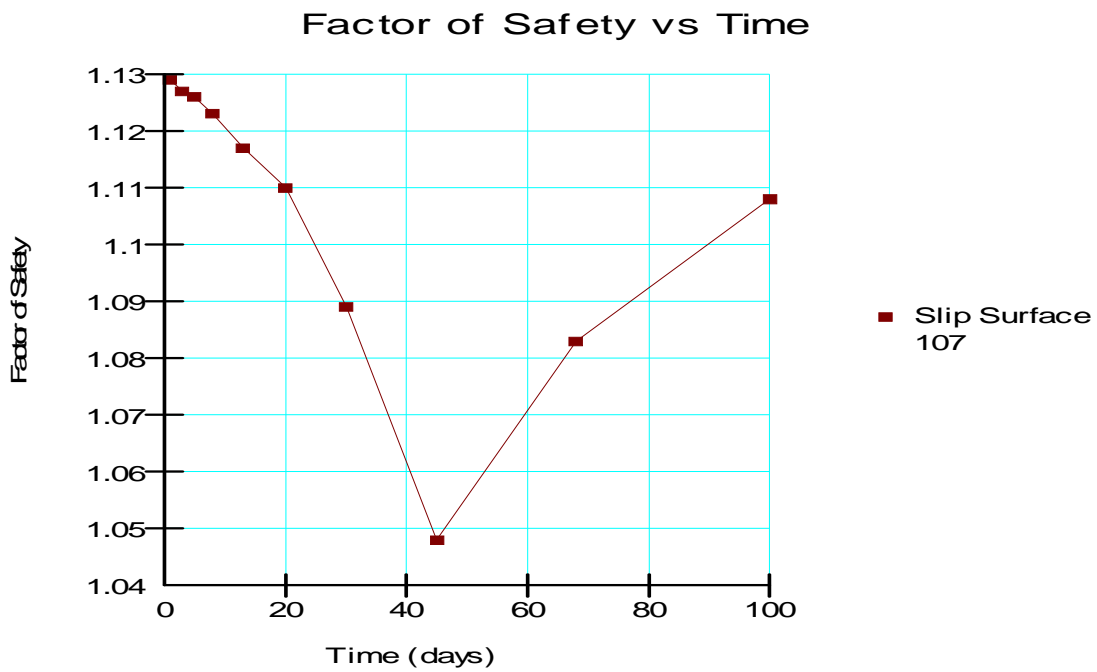


Figure 7.14 Minimum stability conditions for 40 DAYS LEM with EQ loading condition and water level fall from FRL to 394m water elevation.



E. Tendaho dam critical drawdown records under operation situation

Year (E.C)	Date of water level changed	Water level in(m)	Duration of water level changing in (days)	Change in water level in(m)
2010	14/02/10	402.4	186	6.43
	22/08/10	395.97		
2009	11/09/09	397.68	70	3.68
	29/11/09	394.00		
2008	14/01/08	394.55	176	18.2
	12/07/08	376.35		
2007	11/01/07	402.85	311	14
	30/11/07	388.85		
2006	09/02/06	401.93	148	4.91
	19/07/06	397.02		